

Exponential-to-polynomial scaling of measurement overhead in circuit knitting via quantum tomography

Hiroyuki Harada,^{1,*} Kaito Wada,¹ Naoki Yamamoto,^{2,3} and Suguru Endo^{4,5,†}

¹*Graduate School of Science and Technology, Keio University,
Hiyoshi 3-14-1, Kohoku, Yokohama 223-8522, Japan*

²*Department of Applied Physics and Physico-Informatics,
Keio University, Hiyoshi 3-14-1, Kohoku, Yokohama 223-8522, Japan*

³*Quantum Computing Center, Keio University, Hiyoshi 3-14-1, Kohoku, Yokohama 223-8522, Japan*

⁴*NTT Computer and Data Science Laboratories, NTT Inc., Musashino 180-8585, Japan*

⁵*NTT Research Center for Theoretical Quantum Information,
NTT Inc. 3-1 Morinosato Wakanomiya, Atsugi, Kanagawa, 243-0198, Japan*

(Dated: December 23, 2025)

Circuit knitting is a family of techniques that enables large quantum computations on limited-size quantum devices by decomposing a target circuit into smaller subcircuits. However, it typically incurs a measurement overhead exponential in the number of cut locations, and it remains open whether this scaling is fundamentally unavoidable. In conventional circuit-cutting approaches based on the quasiprobability decomposition (QPD), for example, rescaling factors lead to an exponential dependence on the number of cuts. In this work, we show that such an exponential scaling is not universal: it can be circumvented for tree-structured quantum circuits via concatenated quantum tomography protocols. We first consider estimating the expectation value of an observable within additive error ϵ for a tree-structured circuit with tree depth 1 (two layers), maximum branching factor R , and bond dimension at most d on each edge. Our approach uses quantum tomography to construct, for each cut edge, a local decomposition that eliminates the rescaling factors in conventional QPD, instead introducing a controllable bias set by the tomography sample size. After cutting R edges, we show that $\mathcal{O}(d^3 R^3 \ln(dR)/\epsilon^2)$ total measurements suffice, including tomography cost. Next, we extend the tree-depth-1 case to general trees of depth $L \geq 2$, and give an algorithm whose total measurement cost $\tilde{\mathcal{O}}(d^3 K^5/\epsilon^2)$ scales polynomially with the number of cuts for complete R -ary trees. Finally, we perform an information-theoretic analysis to show that, in a comparable tree-depth-1 setting, conventional QPD-based wire-cutting methods require at least $\Omega((d+1)^R/\epsilon^2)$ measurements. This exponential separation highlights the significance of tomography-based construction for reducing measurement overhead in hybrid quantum-classical computations.

I. INTRODUCTION

A. Background

Quantum computing has emerged as a promising paradigm capable of addressing computational problems that are intractable for classical computers [1, 2]. The anticipated applications span a wide range of domains, including quantum chemistry [3, 4], materials science [5, 6], machine learning [7–10], and even finance [11, 12]. Despite these prospects and the rapid progress in quantum hardware and algorithms, near-term quantum processors remain severely constrained by physical noise and engineering limitations, which restrict usable qubit resources, connectivity, coherence times, and gate performance. In particular, limited qubit resources are expected to persist into the early stages of fault-tolerant quantum computing, because quantum error correction will introduce substantial overhead in the number of physical qubits per logical qubit.

To overcome the hardware limitations of near-term de-

vices, a number of divide-and-conquer approaches, collectively referred to as *circuit knitting*, have been developed [13–17]. In general, these methods decompose a quantum computational task into multiple smaller subcircuits that fit on limited quantum hardware, and then reconstruct the original result via classical post-processing [18]. Among them, quantum circuit cutting methods have been actively explored, which can be implemented via wire cutting [14, 19–23] and gate cutting [23–28]. These cutting methods are formulated within the quasiprobability simulation framework [29–31]: replacing an identity channel (i.e., a wire) or an entangling gate with randomly sampled local operations, together with multiplication of the circuit output by a possibly negative weight. By employing the quasiprobabilistic replacement, circuit cutting enables the emulation of larger quantum circuits beyond the available qubit capacity. Recent experiments have also demonstrated the practical benefit of circuit knitting on several platforms, such as alleviating the effects of noise [32, 33] and relaxing connectivity constraints [34].

Despite their appeal, existing divide-and-conquer approaches typically face a fundamental bottleneck: the number of measurements required to achieve a desired accuracy increases exponentially as the computation is decomposed into more pieces. A representative example

* hiro.041o_i7@keio.jp

† suguru.endou@ntt.com

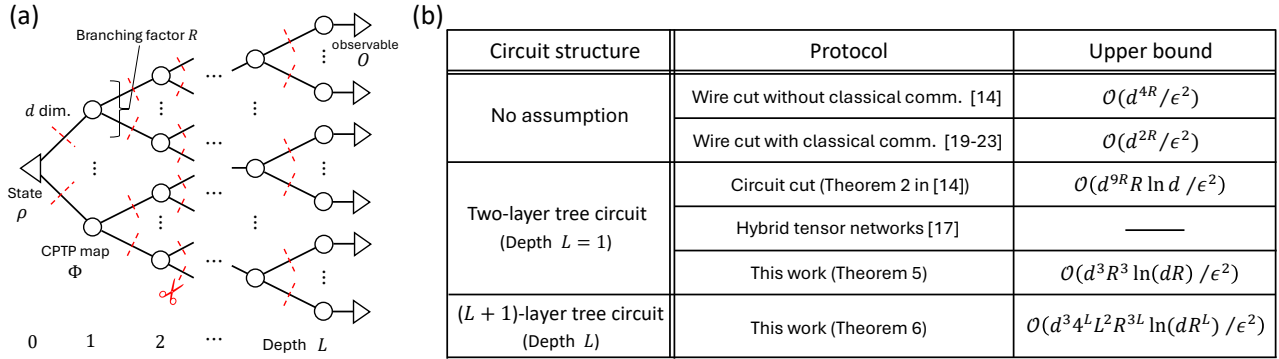


FIG. 1. (a) Schematic representation of tree-structured quantum circuits considered in our analysis, characterized by a maximum branching factor R , maximum depth L , and maximum bond dimension d . Each node represents either a quantum state, an observable with operator norm bounded by 1, or a quantum channel. Each edge denotes an identity channel of dimension at most d . (b) Comparison of the number of measurements required by existing circuit-knitting methods to achieve an accuracy ϵ with high probability. In the “No assumption” setting, we consider a general quantum circuit without structural assumptions, and a d -dimensional wire cut is applied at R locations. The bound is estimated via Hoeffding’s inequality, as in standard circuit-cutting analyses. The “Two-layer tree circuit” and “ $(L + 1)$ -layer tree circuit” settings consider situations where we cut the tree-structured circuits in (a), with depth 1 and L , respectively, along the red dashed edges.

is quantum circuit cutting. Because conventional wire cutting and gate cutting rely on quasiprobability simulation, the reconstruction step introduces rescaling factors in the estimator, which in turn amplify statistical fluctuations. Concretely, let $\gamma \geq 1$ denote the rescaling factor and K the number of cut locations. Then, when estimating the expectation value of a product observable with operator norm bounded by 1 within additive error ϵ , the conventional cutting scheme typically uses the bound that it suffices to take $\mathcal{O}(\gamma^{2K}/\epsilon^2)$ measurements, as implied by Hoeffding’s inequality.

This exponential scaling has motivated extensive efforts to reduce the measurement overhead of circuit cutting. Most prior work focuses on two main directions: reducing the number of cut locations K via classical optimization [35–37], and reducing the rescaling factor γ by developing improved quasiprobability decompositions. For example, in the context of wire cutting, letting d denote the dimension of the wire, the original midcircuit Pauli measurement schemes have $\gamma = d^2$ [14], whereas subsequent works reduce it to $2d - 1$ by allowing the use of local operations and classical communication (LOCC) [19–23]. Nevertheless, because existing cutting methods are built on quasiprobability decompositions, γ is subject to fundamental lower bounds for both wire and gate cutting: for wire cutting, $\gamma = 2d - 1$ is proven to be optimal when LOCC is allowed [20, 38]. Moreover, while there are other circuit-knitting protocols, such as hybrid tensor network methods [17, 39–41], Deep-VQE [16, 42], and entanglement forging [15, 43], the scaling of the resources for the required accuracy and simulated system size is unclear. Fig. 1 shows a comparison of the upper bounds on the number of measurements for relevant circuit-knitting methods.

Then, the natural question arises: *Is it really impos-*

sible to avoid the exponential sampling-overhead scaling in the number of cuts, even in any situation in circuit knitting? Actually, several prior works have implicitly explored the possibility of avoiding exponential scaling in the number of cuts, from a computational complexity-theoretic viewpoint [44] and through algorithmic design [14, 45, 46]. However, even for restricted graph families, it has remained open whether this can be achieved without significantly relaxing the device requirements typically assumed in circuit knitting [14].

B. Overview of results

These fundamental questions motivate our work. In this study, we propose a new quantum algorithm for estimating expectation values of observables in tree-structured quantum states, which, crucially, achieves polynomial scaling in the number of circuit cuts. As in standard circuit-knitting settings, our approach assumes access only to local quantum devices that can simulate the subsystem corresponding to each node of the tree (Fig. 2(a)). Our main contributions are summarized below.

- **Rescaling-free wire cut.** We first show that, for wires located at positions where a quantum circuit can be partitioned into two parts (i.e., the clustered subsystem on the later-time side is closed), there exists a *rescaling-free wire cut*, i.e., a wire cut that introduces neither rescaling factors nor additional bias. However, constructing such an ideal wire cut requires access to a perfect classical description of Heisenberg-evolved observables on the clustered subsystem, which is typically inaccessible. Therefore, we show that if this approximate classical de-

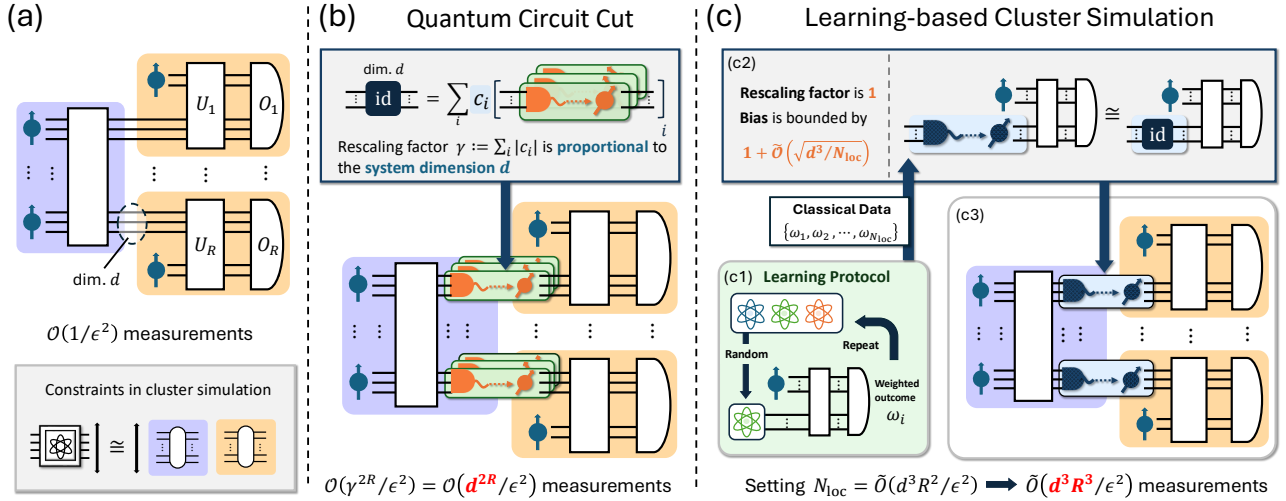


FIG. 2. (a) An example of a quantum circuit for simulating a clustered quantum system. (b) Conventional circuit-cutting protocol that uses a measure-and-prepare channel to decompose the identity channel for a clustered quantum system. Due to the rescaling factor in the quasi-probability decomposition, the sampling overhead scales exponentially with the number of clustered systems. (c) Our learning-based cluster simulation. (c1) By randomly choosing the input states, we can estimate the Heisenberg-evolved observable with the weighted measurement outcome. (c2) Using the learned information about the observable, we perform circuit cutting with bounded bias and no rescaling. (c3) We apply the procedure in (c2) to multiple clustered systems.

scription is available, with its error bounded in the operator norm, we can construct an approximate *rescaling-free wire cut* that introduces no rescaling and incurs only a bounded bias (Sec. III).

- **Randomized learning of observables.** To control the error of the approximate rescaling-free wire cut, we introduce a quantum tomography protocol for Heisenberg-evolved observables under unknown quantum channels (Fig. 2(c1)). This learning protocol enables us to reveal the trade-off between the number of measurements required in quantum tomography and the resulting bias of the approximate wire cut (Fig. 2(c2)); see Sec. IV.
- **Polynomial-scaling circuit knitting for tree circuits.** We consider applying the approximate rescaling-free wire cut to inter-cluster edges in two-layer ($L = 1$) tree-structured quantum circuits (Fig. 2(c3)). We show that by appropriately controlling the number of measurements in each tomography step, we can achieve a total number of measurements that scales polynomially with the number of cuts. We also account for the quantum and classical resources required to construct the corresponding decompositions. We then extend the discussion to decompositions of general multi-layer tree-structured quantum circuits as shown in Fig. 1(a) (Sec. V).

However, one may question whether this polynomial scaling is achieved simply due to the tree-like structure, and whether conventional quantum circuit cutting could

also achieve the same scaling for such circuits. To exclude this possibility, we further show:

- **Exponential separation from conventional wire-cutting.** Via an information-theoretic argument, we analytically demonstrate an exponential separation between our learning-based protocol and traditional wire-cutting approaches as shown in Fig. 2(b). For a two-layer tree ($L = 1$), we prove that any wire-cutting protocol requires at least $\Omega((d+1)^R/\epsilon^2)$ measurements under comparable assumptions (Sec. VI).

For the third contribution, we show that for a rooted tree-structured quantum circuit with maximum depth L , maximum branching factor R , and maximum bond dimension d , the expectation value of a product observable can be estimated to accuracy ϵ using

$$\mathcal{O}\left(\frac{4^L d^3 L^2 R^{3L}}{\epsilon^2} \ln\left(\frac{R^L d}{\delta}\right)\right) \quad (1)$$

measurements with probability at least $1 - \delta$. Since the number of cuts scales as $K = \tilde{\mathcal{O}}(R^L)$ for a complete R -ary tree, this yields an overall sampling cost of

$$\tilde{\mathcal{O}}\left(\frac{d^3 K^5}{\epsilon^2}\right), \quad (2)$$

indicating that our algorithm achieves polynomial scaling in the number of cuts K . Taken together with the fourth contribution, these results establish that our method provides a fundamentally more efficient framework for simulating large-scale tree-structured quantum systems on near-term quantum hardware.

For the fourth contribution, this separation suggests that the improvement is not merely a consequence of restricting to tree-structured circuits. Rather, it highlights the importance of adaptively constructing the decomposition using information obtained from quantum tomography. In conventional wire-cutting methods, one replaces a target identity channel with a measure-and-prepare (MP) channel sampled from a fixed, pre-specified classical probability distribution. Consequently, the choice of which basis information is transmitted across the cut is determined by this classical randomness. In contrast, our approach first performs a tomographic characterization on the receiving side (i.e., the state-preparation side in the MP channel) to identify the measurement bases that are most relevant to the receiving side. Using this information, we then adaptively choose the measurement bases on the sending (measurement) side. In this way, the learning-based protocol reduces redundant measurements on the sending side, and we expect that this is a key mechanism behind the improvement.

II. PRELIMINARIES

A. Notation

We use the following notation in this work. For a quantum system A , \mathcal{H}_A denotes the finite-dimensional Hilbert space of A . Throughout this paper, we consider qubit systems, and when writing the dimension as d , we assume $d = 2^n$ for some number of qubits n . For a d -dimensional complex vector space \mathbb{C}^d , we write $\mathcal{L}(\mathbb{C}^d)$ for the set of linear operators acting on \mathbb{C}^d , $\mathcal{H}(\mathbb{C}^d)$ for the set of Hermitian operators in $\mathcal{L}(\mathbb{C}^d)$, $\mathcal{D}(\mathbb{C}^d)$ for the set of density operators in $\mathcal{H}(\mathbb{C}^d)$, and $\mathcal{U}(\mathbb{C}^d)$ for the unitary group in $\mathcal{L}(\mathbb{C}^d)$. We denote by I_d the identity operator on \mathbb{C}^d , and by id^n the identity channel on $\mathcal{L}(\mathbb{C}^d)$; when the dimension is clear from context, we simply write I or id . For $d \in \mathbb{N}$, we use the shorthand $[d] := \{1, 2, \dots, d\}$. All matrix norms $\|\cdot\|_p$ are taken to be Schatten p -norms.

B. Quantum circuit cut

A quantum circuit cut is a technique that partitions a large quantum circuit into a collection of smaller subcircuits that can be executed on available quantum hardware [14, 24]. Such a partition can be implemented through the technique called quasiprobability simulation, which has been extensively employed across a wide range of quantum information and computation tasks, including quantum error mitigation [29, 31, 47], classical simulation of quantum systems [30, 48–50], and quantum circuit cutting. The key technical idea of the quasiprobability simulation is to express the target operation as a linear combination of implementable ones, referred to as a quasiprobability decomposition (QPD). Suppose that,

due to physical limitations or experimental costs, the available set of quantum operations is restricted to a family F , while the desired operation \mathcal{T} lies outside this set. Then, we represent \mathcal{T} as a linear combination of operations $\{\mathcal{E}_i\}_i \subseteq F$:

$$\mathcal{T} = \sum_i a_i \mathcal{E}_i, \quad (3)$$

where the coefficients a_i are real numbers that may take negative values. Building on this decomposition, quasiprobability simulation provides an unbiased estimator of the circuit output under \mathcal{T} using only the circuit outputs under $\{\mathcal{E}_i\}_i$ (see Appendix S1 for more detailed background). In the case of a quantum circuit cut, two types of QPDs are applied to entangling operations. The first technique replaces the multi-qubit identity channel (i.e., wire) with a linear combination of channels consisting of a measurement followed by a state preparation. This procedure is referred to as a wire cut, or equivalently, a timelike cut, as it effectively separates quantum operations along the temporal direction of the circuit [14, 19–23]. The second technique, known as a gate cut or spacelike cut, decomposes an entangling unitary operation into a linear combination of local unitaries acting on spatially separated subsystems [23–28]. In the following, we provide the key background of the wire cut, as it is more directly relevant to our main result.

In the wire cut, the target operation to be replaced is the n -qubit identity channel, denoted by id^n . The identity channel is defined as the completely positive and trace-preserving (CPTP) map that transmits any input exactly to itself without alteration. Formally, $\text{id}^n : \mathcal{L}(\mathbb{C}^d) \rightarrow \mathcal{L}(\mathbb{C}^d)$ is defined by

$$\text{id}^n(X) = X \quad \forall X \in \mathcal{L}(\mathbb{C}^d). \quad (4)$$

In contrast, the implementable operations are restricted to quantum channels that can be simulated using only local operations and classical communication (LOCC) between devices. Specifically, we consider a special class of quantum channels that can be realized through the following sequence of steps: (i) the sender performs a measurement on the input state ρ , (ii) communicates the measurement outcome to the receiver via a classical channel, and (iii) the receiver prepares a quantum state conditioned on the received outcome. Such channels are known as *measure-and-prepare* (MP) channels (or equivalently, *entanglement-breaking* channels) [51], and they take the general form $\sum_{\mu} \text{tr}(E_{\mu}\rho)\sigma_{\mu}$ where σ_{μ} are quantum states, and $\{E_{\mu}\}_{\mu}$ denotes a positive operator-valued measure (POVM) satisfying $\sum_{\mu} E_{\mu} = I$ and $E_{\mu} \geq 0$ for all μ . Moreover, building on the above quantum operations, when classical post-processing is allowed, where the post-processing consists of multiplying the circuit outputs by $c_{\mu} \in \{\pm 1\}$ depending on intermediate measurement outcomes μ , we can define the following channel:

$$\mathcal{M}(\rho) = \sum_{\mu} c_{\mu} \text{tr}(E_{\mu}\rho)\sigma_{\mu}. \quad (5)$$

In wire cutting, this channel is used as the decomposition basis; we refer to it as the MP channel in what follows. In summary, a wire cut represents the identity channel as a linear combination of MP channels:

$$\text{id}^n = \sum_i a_i \mathcal{M}_i. \quad (6)$$

In this way, the QPD-based circuit cut provides an unbiased estimator of the desired expectation value, but the statistical error is amplified by a rescaling (multiplicative) factor of $\gamma := \sum_i |a_i|$. According to Hoeffding's inequality [52], to estimate the expectation value with an additive error ϵ with high probability, it suffices to perform

$$N = \mathcal{O}\left(\frac{\gamma^2}{\epsilon^2}\right) \quad (7)$$

iterations. Hence, the sampling overhead scales quadratically with the ℓ_1 norm of the coefficients. In practice, partitioning a quantum circuit to fit within available hardware typically requires multiple applications. Let γ_k denote the rescaling factor associated with the k -th replacement. Since the estimator weights multiply across independent decompositions, the overall sampling overhead scales as $\prod_{k=1}^K \gamma_k^2$. Thus, it is of practical importance to minimize the rescaling factor γ , and a number of approaches have been proposed to reduce the γ in wire-cutting protocols [19–23]. However, it is known that γ is fundamentally lower bounded by $2d-1$, as established in the context of quantum circuit cutting [20] and independently in the resource theory of quantum memory [38]. Consequently, cutting a quantum circuit at multiple locations based on QPDs inevitably induces an exponential measurement overhead. For example, when cutting K instances of d -dimensional wires and estimating an expectation value within additive error ϵ , the sufficient number of measurements by Hoeffding's inequality scales as $\mathcal{O}(d^{2K}/\epsilon^2)$. This exponential overhead poses a major bottleneck for the practical application of quantum circuit cutting in near-term quantum computation.

III. EXISTENCE OF A RESCALING-FREE WIRE CUT

As introduced in Sec. II B, QPD represents a target operation as a linear combination of experimentally implementable operations, $\mathcal{T} = \sum_i a_i \mathcal{E}_i$, with the rescaling factor quantified by $\sum_i |a_i|$. However, considering that the goal is merely to recover the expectation value of an observable, i.e., $\text{tr}[O\mathcal{T}(\rho)] = \sum_i a_i \text{tr}[O\mathcal{E}_i(\rho)]$, such a full channel-level decomposition is unnecessarily expressive in general. In what follows, we demonstrate that in wire cutting the rescaling factor can be reduced dramatically by relaxing the requirement from a channel-level decomposition to an expectation-value-level decomposition; indeed, we prove the existence of a decomposition

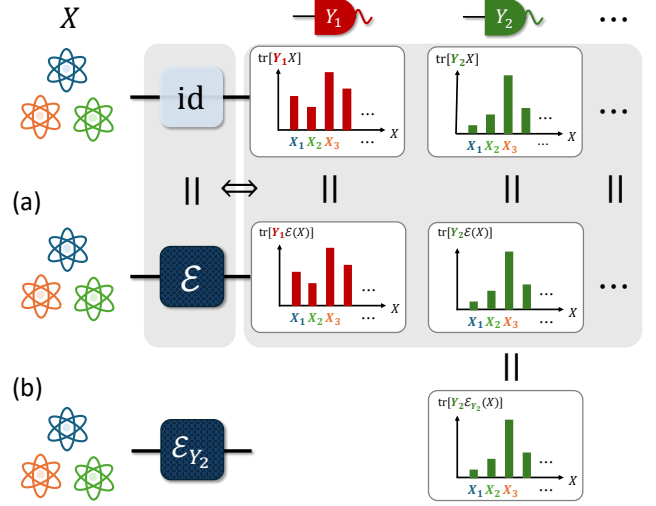


FIG. 3. (a) Characterization of the identity channel id in terms of the invariance under the Hilbert-Schmidt inner product (Eq. (8)). A linear map \mathcal{E} coincides with id if and only if it preserves the expectation value of any observable Y for any input X . (b) Schematic figure of the map \mathcal{E}_{Y_2} defined in Eq. (10). We focus on the decomposition of the map \mathcal{E}_{Y_2} that preserves the expectation value of a fixed observable Y_2 for any input X .

whose rescaling factor is unity in Sec. III A. To connect this existence result to practical protocols, in Sec. III B we further investigate approximate decompositions that inherit similar structural properties.

A. Existence of a rescaling-free wire cut

In Sec. II B, we introduced the identity channel as the map that transmits any quantum state to itself without alteration, i.e., $\text{id}^n(X) = X$. While this operational definition is straightforward, it is often more insightful to characterize the identity channel in terms of its invariance under the Hilbert-Schmidt inner product. Specifically, a linear map \mathcal{E} coincides with the identity channel id^n defined in Eq. (4) if and only if

$$\text{tr}[YX] = \text{tr}[Y\mathcal{E}(X)] \quad \forall X, Y \in \mathcal{L}(\mathbb{C}^d) \quad (8)$$

Proof. For any fixed $X \in \mathcal{L}(\mathbb{C}^d)$, define the linear functional

$$f_X(Y) := \text{tr}[Y(\mathcal{E}(X) - X)]. \quad (9)$$

By the assumption, $f_X(Y) = 0$ for all $Y \in \mathcal{L}(\mathbb{C}^d)$. Since the Hilbert-Schmidt inner product is nondegenerate, this implies $\mathcal{E}(X) - X = 0$. As this holds for every $X \in \mathcal{L}(\mathbb{C}^d)$, we conclude $\mathcal{E} = \text{id}^n$. \square

Eq. (8) thus indicates that id^n is the unique channel that preserves the expectation value of every observable Y for any (possibly unknown) input operator

X (Fig. 3(a)). From the perspective of wire cuts, this interpretation clarifies the origin of the sampling overhead $\gamma^2 = (2d-1)^2$, which scales quadratically with the input dimension d of the system on which id^n acts: reproducing the outcome statistics of all observables requires an MP decomposition that recovers the full information of the input quantum state, and such completeness inevitably entails a large sampling overhead γ^2 .

This observation naturally raises the following question: *If one is only interested in reproducing the expectation values of a fixed observable for arbitrary unknown inputs, can the rescaling factor γ be reduced below $2d-1$?* Formally, consider an MP decomposition of the form $\mathcal{E}_Y = \sum_i a_i \mathcal{M}_i$ with $\mathcal{M}_i \in \text{MP}$ and $a_i \in \mathbb{R}$. We ask whether, for a fixed $Y \in \mathcal{L}(\mathbb{C}^d)$,

$$\text{tr}[YX] = \text{tr}[Y\mathcal{E}_Y(X)] \quad \forall X \in \mathcal{L}(\mathbb{C}^d), \quad (10)$$

the minimal $\gamma := \sum_i |a_i|$ can be made smaller than $2d-1$; see Fig. 3(b) for the graphical representation of the map \mathcal{E}_Y . The following theorem provides an affirmative answer to this question.

Theorem 1 (Existence of a rescaling-free wire cut). *Let $\Phi : \mathcal{L}(\mathbb{C}^{d_{\text{in}}}) \rightarrow \mathcal{L}(\mathbb{C}^{d_{\text{out}}})$ be a CPTP map, and let $O \in \mathcal{H}(\mathbb{C}^{d_{\text{out}}})$ be a Hermitian operator. Then there exists a MP channel $\mathcal{M}_{\text{id}} : \mathcal{L}(\mathbb{C}^{d_{\text{in}}}) \rightarrow \mathcal{L}(\mathbb{C}^{d_{\text{in}}})$ such that, for any $X \in \mathcal{L}(\mathbb{C}^{d_{\text{in}}})$,*

$$\text{tr}[O\Phi(X)] = \text{tr}[O\Phi \circ \mathcal{M}_{\text{id}}(X)]. \quad (11)$$

An explicit construction of \mathcal{M}_{id} is given by

$$\mathcal{M}_{\text{id}}(X) = \sum_j \text{tr}[V|j\rangle\langle j|V^\dagger X] V|j\rangle\langle j|V^\dagger, \quad (12)$$

where $\{|j\rangle\}$ denotes the computational basis, and V is a unitary that diagonalizes $O_\Phi := \Phi^\dagger(O)$, i.e.,

$$O_\Phi := \Phi^\dagger(O) = VDV^\dagger. \quad (13)$$

The proof of Theorem 1 is provided in Appendix S2.1. We note that, although Φ is defined as a CPTP map in the theorem statement for generality, a concrete instance of Φ can take the form

$$\Phi(X) = U(X_{\text{in}} \otimes |0^m\rangle\langle 0^m|)U^\dagger \quad (14)$$

where U is a unitary and $m \in \mathbb{Z}$ denotes the number of ancilla qubits; see Fig. 4 (a).

Theorem 1 establishes the existence of a rescaling-free wire cut: for any observable O , there exists a MP channel \mathcal{M}_{id} that leaves the expectation value $\text{tr}[O\Phi(X)]$ invariant for all input operators X . In other words, there exists a wire cut whose rescaling factor is unity, i.e., $\gamma = 1$, in contrast to the conventional wire cut whose overhead scales as $\gamma = 2d-1$ (Fig. 4 (b)(c)). The key ingredient underlying the construction of the MP channel \mathcal{M}_{id} is the unitary V that diagonalizes the effective observable $O_\Phi := \Phi^\dagger(O)$. Operationally, \mathcal{M}_{id} projects the input onto the eigenbasis of O_Φ , measures in that basis, and then re-prepares the corresponding eigenstate; thereby transmitting precisely the information relevant to O_Φ .

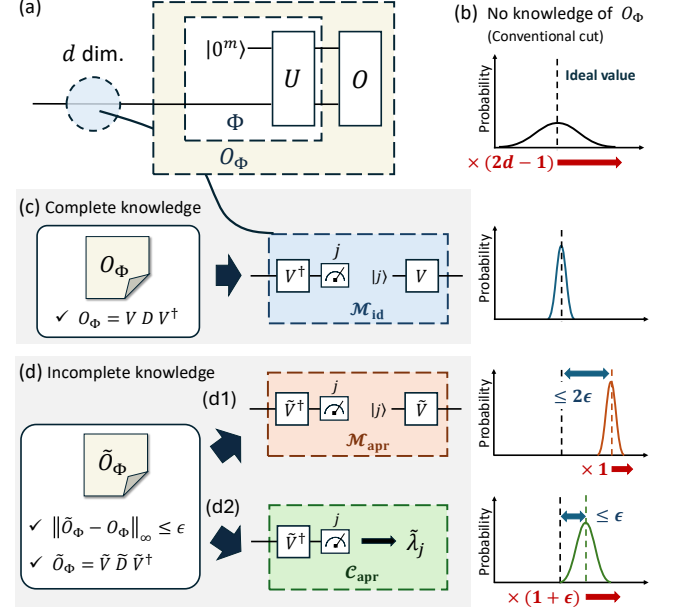


FIG. 4. (a) Original quantum circuit before decomposition. Here, Φ denotes a CPTP map, and O is a Hermitian operator satisfying $\|O\|_\infty \leq 1$. We consider a decomposition of the identity channel enclosed by the blue dashed circle. (b) When the conventional wire cut in Eq. (6) is applied to the dashed circuit in (a), a rescaling factor $2d-1$ is required, which consequently increases the variance. (c) There exists an MP channel \mathcal{M}_{id} that preserves the unbiasedness of the ideal expectation value without introducing any additional rescaling factor, i.e., without increasing the variance (Theorem 1). (d1) When the dashed circle is replaced by an MP channel \mathcal{M}_{apr} constructed from an approximate effective observable \tilde{O}_Φ satisfying $\|\tilde{O}_\Phi - O_\Phi\|_\infty \leq \epsilon$, the bias in the expectation value is bounded by 2ϵ , and no additional rescaling factor is required (Theorem 2). (d2) When a classical post-processing function \mathcal{C}_{apr} constructed from \tilde{O}_Φ is used, the bias is bounded by ϵ , and the additional rescaling factor is at most $1+\epsilon$ (Theorem 3).

B. Approximate version of the rescaling-free wire cut

It should be emphasized that Theorem 1 is primarily an existence result. The explicit construction of \mathcal{M}_{id} requires knowledge of the unitary V that diagonalizes O_Φ . However, complete knowledge of O_Φ (that is, a full classical description without any error) is typically unavailable unless Φ admits a classical description or possesses a known structure (e.g., Clifford circuits). Nevertheless, even without complete knowledge of O_Φ , having only an imperfect approximation \tilde{O}_Φ with bounded error is sufficient to construct a rescaling-free wire cut that faithfully reproduces the desired expectation values up to a bounded bias. Theorem 2 formalizes this statement.

Theorem 2 (Approximate rescaling-free wire cut). *Let $\Phi : \mathcal{L}(\mathbb{C}^{d_{\text{in}}}) \rightarrow \mathcal{L}(\mathbb{C}^{d_{\text{out}}})$ be a CPTP map, and let $O \in \mathcal{H}(\mathbb{C}^{d_{\text{out}}})$ be a Hermitian operator. Denote by $O_\Phi :=$*

$\Phi^\dagger(O)$ the corresponding effective observable, and let \tilde{O}_Φ be its Hermitian approximation satisfying $\|\tilde{O}_\Phi - O_\Phi\|_\infty \leq \epsilon$. Define the MP channel $\mathcal{M}_{\text{apr}} : \mathcal{L}(\mathbb{C}^{d_{\text{in}}}) \rightarrow \mathcal{L}(\mathbb{C}^{d_{\text{in}}})$ given by

$$\mathcal{M}_{\text{apr}}(X) := \sum_j \text{tr} \left[\tilde{V} |j\rangle \langle j| \tilde{V}^\dagger X \right] \tilde{V} |j\rangle \langle j| \tilde{V}^\dagger, \quad (15)$$

where $\{|j\rangle\}$ denotes the computational basis, and \tilde{V} is a unitary that diagonalizes \tilde{O}_Φ (i.e., $\tilde{O}_\Phi = \tilde{V} \tilde{D} \tilde{V}^\dagger$). Then for any $X \in \mathcal{L}(\mathbb{C}^{d_{\text{in}}})$,

$$|\text{tr}[O\Phi \circ \mathcal{M}_{\text{apr}}(X)] - \text{tr}[O\Phi(X)]| \leq 2\epsilon \|X\|_1. \quad (16)$$

The proof of Theorem 2 can be found in Appendix S2.2. In particular, for any input state $\rho \in \mathcal{D}(\mathbb{C}^{d_{\text{in}}})$, this theorem guarantees the bounded bias as

$$|\text{tr}[O\Phi \circ \mathcal{M}_{\text{apr}}(\rho)] - \text{tr}[O\Phi(\rho)]| \leq 2\epsilon. \quad (17)$$

This argument is schematically depicted in Fig. 4(d1).

We remark that the above strategy assumes that one has access to a reasonably accurate classical description of the effective observable O_Φ . Hence, in order for Theorem 2 to work meaningfully, it is required to construct a learning protocol for O_Φ , with controlled accuracy in the operator norm. In the next section, we establish a practical tomography procedure that enables such estimation.

Theorem 2 naturally motivates a constructive strategy for realizing rescaling-free wire cuts in practice. For each cut location satisfying the conditions of Theorem 2, one may proceed as follows: (i) estimate the effective observable $O_\Phi^{(k)}$ of the target subcircuit and obtain an estimator $\tilde{O}_\Phi^{(k)}$, (ii) diagonalize $\tilde{O}_\Phi^{(k)}$ to obtain the corresponding unitary $\tilde{V}^{(k)}$ such that $\tilde{O}_\Phi^{(k)} = \tilde{V}^{(k)} \tilde{D}^{(k)} \tilde{V}^{(k)\dagger}$, and (iii) construct the local MP channel $\mathcal{M}_{\text{apr}}^{(k)}$ from this basis. By controlling the estimation error of each $\tilde{O}_\Phi^{(k)}$ so that the accumulated bias remains negligible, one can achieve a faithful global reconstruction of the circuit's output expectation value while maintaining a rescaling factor of unity.

From an implementation point of view, however, it is important to note that constructing a single rescaling-free wire cut requires classical and quantum resources. The procedure incurs an additional classical computational cost of order $\mathcal{O}(d_{\text{in}}^3)$, coming from the tomography of O_Φ (Sec. IV C) and its diagonalization, and it also requires implementing the MP channel \mathcal{M}_{apr} . In the worst case, realizing \mathcal{M}_{apr} needs quantum circuits of $\mathcal{O}(d_{\text{in}}^2)$ elementary gates [53, 54]. Therefore, for a single cut, applying Theorem 2 can look less attractive than existing optimal wire-cutting methods [21–23] that avoid tomography and can be executed with $\mathcal{O}(\text{polylog}(d_{\text{in}}))$ elementary gates.

However, the distinctive advantage of this approach is that, because it removes the rescaling factor, the main

trade-off shifts from variance amplification to bias control. This change becomes particularly significant when multiple cuts are applied. Conventional QPD-based wire cuts accumulate rescaling factors $\gamma = \mathcal{O}(d_{\text{in}})$, so the variance typically scales as $\gamma^{2K} = \mathcal{O}(d_{\text{in}}^{2K})$, leading to an exponential increase in the required number of measurements. In contrast, when the approximate rescaling-free construction is combined with the tomography procedures in Sec. IV, which provide rigorous operator-norm guarantees, the total error can be controlled by appropriately allocating per-cut bias budgets, and the dominant classical cost grows only polynomially with the number of cuts as $\mathcal{O}(\text{poly}(d_{\text{in}}, K))$. As a concrete practical application, Sec. V demonstrates the effectiveness of this approach for decomposing tree-structured quantum circuits.

Up to this point, we have considered constructing an approximate rescaling-free wire cut based on Theorem 2. In this framework, we utilize only the diagonalizing unitary \tilde{V} obtained from the approximate observable, while we have not exploited the corresponding approximate eigenvalues $\tilde{\lambda}_j$ in \tilde{D} . Nevertheless, these eigenvalues may contain additional information about the effective observable O_Φ that can be leveraged to improve estimation accuracy. Indeed, as shown in the following theorem, the approximate eigenvalues $\tilde{\lambda}_j$ allow us to construct an estimator with a smaller bias than that obtained in Theorem 2.

Theorem 3. *Let $\Phi : \mathcal{L}(\mathbb{C}^{d_{\text{in}}}) \rightarrow \mathcal{L}(\mathbb{C}^{d_{\text{out}}})$ be a CPTP map, and let $O \in \mathcal{H}(\mathbb{C}^{d_{\text{out}}})$ be a Hermitian operator. Denote by $O_\Phi := \Phi^\dagger(O)$ the corresponding effective observable, and let \tilde{O}_Φ be its Hermitian approximation satisfying $\|\tilde{O}_\Phi - O_\Phi\|_\infty \leq \epsilon$. Define the classical post-processing function*

$$\mathcal{C}_{\text{apr}}(X) := \sum_j \text{tr} \left[\tilde{V} |j\rangle \langle j| \tilde{V}^\dagger X \right] \tilde{\lambda}_j, \quad (18)$$

where $\{|j\rangle\}$ denotes the computational basis, \tilde{V} is a unitary that diagonalizes \tilde{O}_Φ (i.e., $\tilde{O}_\Phi = \tilde{V} \tilde{D} \tilde{V}^\dagger$), and $\tilde{D} := \sum_j \tilde{\lambda}_j |j\rangle \langle j|$. Then, for any $X \in \mathcal{L}(\mathbb{C}^{d_{\text{in}}})$,

$$|\mathcal{C}_{\text{apr}}(X) - \text{tr}[O\Phi(X)]| \leq \epsilon \|X\|_1, \quad (19)$$

$$\max_j |\tilde{\lambda}_j| \leq \|O\|_\infty + \epsilon. \quad (20)$$

The proof of Theorem 3 is provided in Appendix S2.3. Similar to Theorem 2, for any input state $\rho \in \mathcal{D}(\mathbb{C}^{d_{\text{in}}})$ and a bounded observable O satisfying $\|O\|_\infty \leq 1$, the theorem ensures that

$$|\mathcal{C}_{\text{apr}}(\rho) - \text{tr}[O\Phi(\rho)]| \leq \epsilon \quad (21)$$

and

$$\max_j |\tilde{\lambda}_j| \leq 1 + \epsilon. \quad (22)$$

Fig. 4 (d2) shows the graphical expression of this statement.

Now, comparing Theorem 2 and Theorem 3, we can see the trade-off between the two approaches. Using the approximate MP channel \mathcal{M}_{apr} of Theorem 2, one can estimate the expectation value with a unity rescaling factor (i.e., without additional multiplicative factor) but with an increased bias 2ϵ . In contrast, the post-processing function \mathcal{C}_{apr} of Theorem 3 achieves a smaller bias ϵ , albeit with a non-unity rescaling factor bounded by $1 + \epsilon$, i.e., a non-unity multiplicative factor. When we implement $\mathcal{C}_{\text{apr}}^{(k)}$ at multiple places, such a non-unity rescaling in Theorem 3 seems to become a large overhead in total, similar to the conventional wire cut; however, as discussed in Sec. V, both approaches exhibit comparable sample efficiency when \tilde{O}_Φ is estimated with the same level of accuracy.

In terms of ease of implementation, the protocol based on Theorem 3 offers a practical advantage. Once a sufficiently accurate approximation \tilde{O}_Φ is available, the estimation can be performed purely classically using only the approximate eigenvalue $\tilde{\lambda}_j$, without implementing Φ and directly measuring O . In addition, whereas the protocol based on Theorem 2 requires a feedforward operation in realizing the MP channel \mathcal{M}_{apr} , the protocol derived from Theorem 3 does not.

Lastly, we note that Appendix S6 provides a detailed discussion of how Theorem 1 relates to existing QPD-based wire-cutting methods.

IV. LEARNING HEISENBERG-EVOLVED OBSERVABLES UNDER UNKNOWN QUANTUM CHANNELS

In the previous section, Theorems 2 and 3 established that, given an accurate estimate of O_Φ , one can construct either a well-approximated rescaling-free wire cut \mathcal{M}_{apr} or a post-processing function \mathcal{C}_{apr} , which maintains a unity or near-unity rescaling factor. These constructions fundamentally rely on the knowledge of the effective observable O_Φ , which corresponds to the Heisenberg-evolved version of the measurement operator O under the unknown quantum channel Φ . However, in many practical scenarios, a classical description of Φ is not available.

To bridge the gap, we develop a practical learning framework for estimating such unknown effective observables O_Φ directly from experimental data, with controllable accuracy guarantees. In what follows, we formalize the problem setup in Sec. IV A, introduce concrete learning protocols in Sec. IV B, and provide performance guarantees and operator-norm accuracy in Sec. IV C.

A. Problem setup

Suppose we are given a known Hermitian operator $O \in \mathcal{H}(\mathbb{C}^{d_{\text{out}}})$ and an unknown CPTP map $\Phi : \mathcal{L}(\mathbb{C}^{d_{\text{in}}}) \rightarrow$

$\mathcal{L}(\mathbb{C}^{d_{\text{out}}})$. We denote d_{in} by 2^n , depending on the context. We assume that Φ is specified only as a quantum circuit, and thus its full classical description is inaccessible. The observable O admits the spectral decomposition

$$O = W \Lambda W^\dagger \quad (23)$$

where $\Lambda := \sum_j \nu_j |j\rangle\langle j|$ is diagonal in the computational basis $\{|j\rangle\}$, and W is a unitary operator. Our goal is to obtain a classical description of $O_\Phi = \Phi^\dagger(O) \in \mathcal{H}(\mathbb{C}^{d_{\text{in}}})$, where Φ^\dagger denotes the adjoint map of Φ . Formally, given a target accuracy $\epsilon > 0$, we aim to construct an estimator \hat{O}_Φ satisfying

$$\|\hat{O}_\Phi - O_\Phi\|_\infty \leq \epsilon \quad (24)$$

with probability at least $1 - \delta$.

B. Learning protocols

We here introduce three protocols for learning the unknown observable O_Φ . Before presenting the specific procedures, we outline the common structure shared by all of them. To obtain an estimator \hat{O}_Φ satisfying Eq. (24), we need to collect measurement data from the circuit composed of the unknown quantum channel Φ followed by the measurement of O . Such data are obtained by probing the circuit with an appropriately chosen ensemble of input states (i.e., a probability distribution over pure states):

$$\mathcal{S} := \{(p_i, |\psi_i\rangle)\}, \quad (25)$$

where p_i denotes the sampling probability associated with the pure states $|\psi_i\rangle$. As will be discussed below and in Appendix S3 1b, the probe states $|\psi_i\rangle$ in all of our schemes can be prepared efficiently on a quantum device, and their classical descriptions can be stored efficiently in classical memory. Given \mathcal{S} , we perform the following randomized procedure consisting of random sampling of input states, circuit measurement, and data storage:

1. **Random sampling:** Draw an input state $|\psi_i\rangle$ from \mathcal{S} according to the probability distribution p_i .
2. **Measurement:** Prepare $|\psi_i\rangle$ on the input register, evolve it under Φ , and measure the output using the observable O . Operationally, this corresponds to applying the unitary rotation W^\dagger immediately before measurement in the computational basis $\{|j\rangle\}$. Denote the observed outcome by j , associated with the eigenvalue ν_j of O .
3. **Data storage:** Store the pair $(|\psi_i\rangle, \nu_j)$ in classical memory.

Repeating the above procedure N times, we obtain an empirical dataset

$$\mathcal{D}_N := \{(|\psi_{i_k}\rangle, \nu_{j_k})\}_{k=1}^N \quad (26)$$

where i_k and j_k respectively denote the indices of the sampled input state and the corresponding measurement outcome in the k -th trial. By appropriately choosing the ensemble \mathcal{S} and sufficient sample size N , the empirical dataset \mathcal{D}_N encodes enough information to reconstruct O_Φ . Thus, by performing classical post-processing on \mathcal{D}_N , which depends on the choice of ensemble, we obtain an estimate of the classical description of O_Φ .

In the following, we present three concrete realizations of this framework. The first two protocols employ ensembles that form (i) a state 2-design (Sec. IV B 1), and (ii) the uniform tensor product of single-qubit stabilizer states (Sec. IV B 2). Both protocols can be described within the framework presented above. We present these two realizations because each has its own strengths and weaknesses in terms of sample efficiency and ease of implementation. Protocol (ii) is more hardware-friendly, as its input-state-preparation can be executed with a circuit depth of at most two, using only single-qubit Clifford gates. In contrast, implementing the protocol (i) using a Clifford ensemble requires $\mathcal{O}(n^2/\log n)$ Clifford gates. However, protocol (i) offers better sample efficiency, as established in Theorem 4. We also introduce a third protocol in Sec. IV B 3, which instead employs the uniform distribution over n -qubit Pauli operators and their eigenstates. This protocol uses input states similar to those in protocol (ii), but relies on a different classical post-processing method.

We mention the derivation of an unbiased estimator for O_Φ and the error analysis. To derive the unbiased estimator, we adopt the following strategy. We view the sequence of random procedures (Steps 1-3) as a random map. By computing the average output of this channel, we construct an unbiased estimator via classical post-processing, which is also related to the linear-inversion methods [55, 56]. For the error analysis, we employ the matrix Bernstein inequality [57]. The necessary background, tools for the derivation, and detailed proofs are provided in Appendix S3.

1. 2-design ensemble

Let $\mathcal{S}_{2\text{-dgn}} := \{(p_i, |\psi_i\rangle)\}$ be a state ensemble forming a state 2-design, i.e., it satisfies

$$\sum_i p_i (|\psi_i\rangle \langle \psi_i|)^{\otimes t} = \int_{\phi} d\phi (|\phi\rangle \langle \phi|)^{\otimes t}, \quad t = 1, 2 \quad (27)$$

where the integral is taken with respect to the normalized Haar measure on the unit sphere of $\mathbb{C}^{d_{\text{in}}}$. As concrete examples of state 2-designs, one may consider ensembles constructed from mutually unbiased bases (MUBs) and from symmetric informationally complete POVMs (SIC-POVMs). Moreover, the set $\{U|0^n\rangle : U \in \text{Cl}(2^n)\}$, where $\text{Cl}(2^n)$ denotes the n -qubit Clifford group, also forms a state 2-design, since $\text{Cl}(2^n)$ is known to form a unitary 3-design [58] (see Appendix S3 1b for additional

background). In addition, Clifford circuits can be stored efficiently in a classical computer.

Using $\mathcal{S}_{2\text{-dgn}}$, we perform the following procedure for $k = 1, \dots, N$:

1. **Random sampling:** Sample a pure state $|\psi_{i_k}\rangle$ from $\mathcal{S}_{2\text{-dgn}}$.
2. **Measurement:** Prepare $|\psi_{i_k}\rangle$, apply Φ , and measure the observable O . Let j_k be the observed outcome associated with eigenvalue ν_{j_k} .
3. **Data storage:** Store the pair $(|\psi_{i_k}\rangle, \nu_{j_k})$ in classical memory.

After repeating this procedure N times, we classically post-process each pair $(|\psi_{i_k}\rangle, \nu_{j_k})$ as

$$\hat{\omega}_{2\text{-dgn}}^{(k)} := \nu_{j_k} (d_{\text{in}}(d_{\text{in}} + 1) |\psi_{i_k}\rangle \langle \psi_{i_k}| - d_{\text{in}} I_{d_{\text{in}}}). \quad (28)$$

By averaging these matrices, we obtain

$$\hat{O}_{\Phi, 2\text{-dgn}} := \frac{1}{N} \sum_{k=1}^N \hat{\omega}_{2\text{-dgn}}^{(k)} \quad (29)$$

$$= \frac{1}{N} \sum_{k=1}^N \nu_{j_k} (d_{\text{in}}(d_{\text{in}} + 1) |\psi_{i_k}\rangle \langle \psi_{i_k}| - d_{\text{in}} I_{d_{\text{in}}}), \quad (30)$$

which is an unbiased estimator of O_Φ , i.e., $\mathbb{E}[\hat{O}_{\Phi, 2\text{-dgn}}] = O_\Phi$. A proof of its unbiasedness is given in Appendix S3 2a.

2. Tensor product single-qubit stabilizer states

We consider the input ensemble $\mathcal{S}_{\text{stab}}$, defined as the uniform distribution over all n -fold tensor products of single-qubit stabilizer states. Let $|\pm\rangle$ and $|\pm i\rangle$ denote the eigenstates of the Pauli operators X and Y , respectively, and define the set of single-qubit stabilizer states as

$$\mathcal{Q}_{\text{stab}} := \{|0\rangle, |1\rangle, |+\rangle, |-\rangle, |+i\rangle, |-i\rangle\}. \quad (31)$$

The ensemble $\mathcal{S}_{\text{stab}}$ is then formally given by

$$\mathcal{S}_{\text{stab}} := \left\{ \left(\frac{1}{6^n}, \bigotimes_{s=1}^n |u^s\rangle \right) : |u^s\rangle \in \mathcal{Q}_{\text{stab}} \right\} \quad (32)$$

Using $\mathcal{S}_{\text{stab}}$, we perform the following protocol for $k = 1, \dots, N$:

1. **Random sampling:** Sample a product state $\bigotimes_{s=1}^n |u_k^s\rangle$ from $\mathcal{S}_{\text{stab}}$.
2. **Measurement:** Prepare the state $\bigotimes_{s=1}^n |u_k^s\rangle$, apply Φ , and measure the observable O . Let j_k be the observed outcome corresponding to eigenvalue ν_{j_k} .

3. **Data storage:** Store the pair $(\bigotimes_{s=1}^n |u_k^s\rangle, \nu_{j_k})$ in classical memory.

After N iterations, we perform classical post-processing on each pair $(\bigotimes_{s=1}^n |u_k^s\rangle, \nu_{j_k})$ and define

$$\hat{\omega}_{\text{stab}}^{(k)} := \nu_{j_k} \bigotimes_{s=1}^n (6|u_k^s\rangle\langle u_k^s| - 2I). \quad (33)$$

The empirical estimator is obtained as the sample average

$$\hat{O}_{\Phi, \text{stab}} := \frac{1}{N} \sum_{k=1}^N \hat{\omega}_{\text{stab}}^{(k)} \quad (34)$$

$$= \frac{1}{N} \sum_{k=1}^N \nu_{j_k} \bigotimes_{s=1}^n (6|u_k^s\rangle\langle u_k^s| - 2I), \quad (35)$$

which is an unbiased estimator of O_Φ . A proof of its unbiasedness can be found in Appendix S3 2b.

3. *n*-qubit Pauli operator

In the protocol based on a 2-design (Sec. IV B 1) or a uniform tensor product of single-qubit stabilizer states (Sec. IV B 2), the unknown observable O_Φ is estimated by random sampling of quantum states from the corresponding ensemble. Here, we instead consider an alternative model where we randomly sample an n -qubit Pauli operator and one of its eigenstates as the input state.

We begin by recalling the single-qubit Pauli operators and their eigenvalue decompositions:

$$P_i = \sum_{e \in [2]} c_{i,e} |v_{i,e}\rangle\langle v_{i,e}| \quad i \in [4], \quad (36)$$

where we set P_1, P_2, P_3, P_4 to be the identity and the Pauli operators X, Y, and Z, respectively. Their eigenstates and corresponding eigenvalues are given by

$$\begin{aligned} |v_{1,1}\rangle &= |0\rangle, & c_{1,1} &= +1, & |v_{1,2}\rangle &= |1\rangle, & c_{1,2} &= +1, \\ |v_{2,1}\rangle &= |+\rangle, & c_{2,1} &= +1, & |v_{2,2}\rangle &= |-\rangle, & c_{2,2} &= -1, \\ |v_{3,1}\rangle &= |+\rangle, & c_{3,1} &= +1, & |v_{3,2}\rangle &= |-\rangle, & c_{3,2} &= -1, \\ |v_{4,1}\rangle &= |0\rangle, & c_{4,1} &= +1, & |v_{4,2}\rangle &= |1\rangle, & c_{4,2} &= -1. \end{aligned} \quad (37)$$

From these local definitions, we define the n -qubit Pauli ensemble as

$$\mathcal{S}_{\text{Paulis}} := \left\{ \left(\frac{1}{4^n}, P_i := \bigotimes_{s=1}^n P_{i_s} \right) : \mathbf{i} \in [4]^n \right\}, \quad (38)$$

where $\mathbf{i} := (i_1, \dots, i_n)$. Each n -qubit Pauli operator admits the eigenvalue decomposition

$$\begin{aligned} P_i &:= \sum_{\mathbf{e} := (e_1, \dots, e_n) \in [2]^n} c_{\mathbf{i}, \mathbf{e}} |v_{\mathbf{i}, \mathbf{e}}\rangle\langle v_{\mathbf{i}, \mathbf{e}}|, \\ c_{\mathbf{i}, \mathbf{e}} &:= \prod_{s=1}^n c_{i_s, e_s}, \quad |v_{\mathbf{i}, \mathbf{e}}\rangle := \bigotimes_{s=1}^n |v_{i_s, e_s}\rangle. \end{aligned} \quad (39)$$

We now consider the following sampling procedure, repeated for $k = 1, \dots, N$, where a Pauli operator and one of its eigenstates are chosen at random:

1. **Random sampling:** Sample a Pauli operator $P_{\mathbf{i}_k}$ and its eigenstates $|v_{\mathbf{i}_k, \mathbf{e}_k}\rangle$ uniformly at random.
2. **Measurement:** Prepare $|v_{\mathbf{i}_k, \mathbf{e}_k}\rangle$, evolve it under Φ , and measure the observable O . Denote the measurement outcome by j_k
3. **Data storage:** Store the triple $(P_{\mathbf{i}_k}, |v_{\mathbf{i}_k, \mathbf{e}_k}\rangle, j_k)$ in classical memory.

After repeating the above procedure N times, we classically post-process each stored triple $(P_{\mathbf{i}_k}, |v_{\mathbf{i}_k, \mathbf{e}_k}\rangle, j_k)$ as

$$\hat{\omega}_{\text{pauli}}^{(k)} := 4^n \nu_{j_k} c_{\mathbf{i}_k, \mathbf{e}_k} P_{\mathbf{i}_k}. \quad (40)$$

By averaging over these matrices, we obtain the empirical estimator

$$\hat{O}_{\Phi, \text{pauli}} := \frac{1}{N} \sum_{k=1}^N \hat{\omega}_{\text{pauli}}^{(k)} \quad (41)$$

$$= \frac{1}{N} \sum_{k=1}^N 4^n \nu_{j_k} c_{\mathbf{i}_k, \mathbf{e}_k} P_{\mathbf{i}_k}. \quad (42)$$

The resulting estimator is unbiased with respect to O_Φ ; see Appendix S3 2c for a detailed proof.

C. Performance guarantees

We establish a performance guarantee for the empirical estimator $\hat{O}_{\Phi, x}$ for each $x \in \{2\text{-dgn, stab, pauli}\}$, introduced in Sec. IV B.

Theorem 4 (Performance guarantee for $\hat{O}_{\Phi, x}$). *Let $\Phi : \mathcal{L}(\mathbb{C}^{d_{\text{in}}}) \rightarrow \mathcal{L}(\mathbb{C}^{d_{\text{out}}})$ be an unknown CPTP map, and let $O \in \mathcal{H}(\mathbb{C}^{d_{\text{out}}})$ be a known Hermitian operator. Denote by $O_\Phi := \Phi^\dagger(O)$ the corresponding effective observable. Fix a probability distribution over sets of quantum states or Pauli operators associated with $x \in \{2\text{-dgn, stab, pauli}\}$. Then the following number of iterations suffices to ensure that the learning protocol defined in Sec. IV B produces an estimate $\hat{O}_{\Phi, x}$ satisfying $\|\hat{O}_{\Phi, x} - O_\Phi\|_\infty \leq \epsilon$ with probability at least $1 - \delta$, for any $\epsilon > 0$:*

$x = 2\text{-dgn}:$

$$\frac{2 \max\{1, \|O\|_\infty^2\} (d_{\text{in}}^2 + 1) (d_{\text{in}} + 1 + \epsilon/3)}{\epsilon^2} \ln \left(\frac{d_{\text{in}}}{\delta} \right),$$

$x = \text{stab}:$

$$\frac{2 \max\{1, \|O\|_\infty^2\} (d_{\text{in}}^{3.33} + (\epsilon/3)(d_{\text{in}}^2 + 1))}{\epsilon^2} \ln \left(\frac{d_{\text{in}}}{\delta} \right),$$

$x = \text{pauli}:$

$$\frac{2 \max\{1, \|O\|_\infty^2\} (d_{\text{in}}^4 + 1 + (\epsilon/3)(d_{\text{in}}^2 + 1))}{\epsilon^2} \ln \left(\frac{d_{\text{in}}}{\delta} \right).$$

For a detailed proof, see Appendix S3 3.

V. POLYNOMIAL-SCALING CIRCUIT KNITTING FOR TREE QUANTUM CIRCUITS

In this section, we show that, by combining either Theorems 2 or 3 with the learning protocol introduced in Sec. IVB, one can estimate expectation values of quantum circuits with a clustered tree structure using fewer measurements than conventional circuit-cutting-based methods, whose measurement cost scales exponentially with the number of cuts. In Sec. VA, we describe the problem setup. In Sec. VB, we study the cluster simulation of a two-layer tree quantum circuit using protocols based on Theorem 2 and Theorem 3. In Sec. VC, we present a theorem that extends the result of Sec. VB from the two-layer case ($L = 1$) to the general multi-layer case ($L \geq 2$).

A. Problem setup

We consider a rooted tree with maximum depth L , maximum branching factor R , and bond dimension bounded by d ; see Fig. 5. Each edge carries a Hilbert space of dimension at most d , and each node has at most R outgoing edges. We refer to such a structure as an (L, R, d) -tree quantum circuit. The root is defined to be at depth 0. Each node at depth $l (\geq 1)$ is uniquely labeled by a tuple (i_1, \dots, i_l) with $i_k \in [R]$, specifying the path from the root through the i_1 -th, i_2 -th, ..., i_l -th child.

Quantum state and channels. Each circle node in

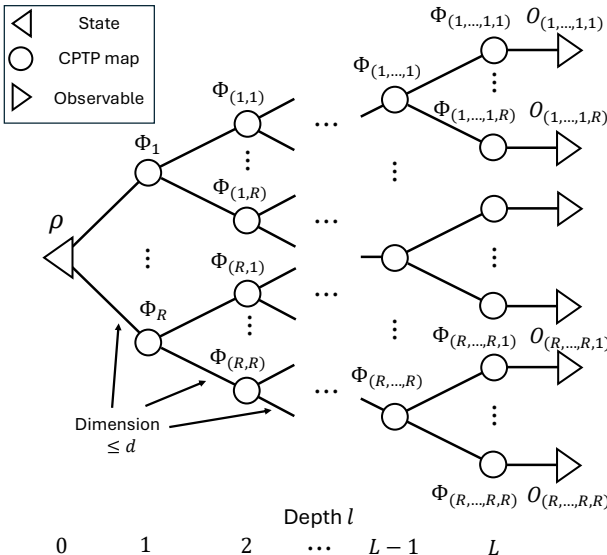


FIG. 5. Tensor-network representation of an (L, R, d) -tree quantum circuit. Nodes correspond to a quantum state ρ , CPTP maps $\Phi_{(i_1, \dots, i_l)}$ ($l = 1, \dots, L$), and local observables $O_{(i_1, \dots, i_L)}$ with $\|O_{(i_1, \dots, i_L)}\|_\infty \leq 1$. Each edge represents the identity channel of dimension at most d , except for those connecting a CPTP map (circle node) to an observable (triangle node).

Fig. 5 is associated with a CPTP map

$$\Phi_{(i_1, \dots, i_l)} : \mathcal{L}(\mathbb{C}^{d_{\text{in}}}) \rightarrow \mathcal{L}(\mathbb{C}^{d_{\text{out}}}), \quad (43)$$

where $d_{\text{in}} \leq d$ denotes the dimension of the input Hilbert space, and d_{out} is the dimension of the output space associated with its $r \leq R$ children. Since each outgoing edge carries a subsystem of dimension at most d , the total output dimension satisfies $d_{\text{out}} \leq d^r$. Let $\mathcal{I}_l \subseteq [R]^l$ denote the set of all nodes at depth l . The joint action of the nodes is given by

$$\Phi^{[l]} := \bigotimes_{(i_1, \dots, i_l) \in \mathcal{I}_l} \Phi_{(i_1, \dots, i_l)}. \quad (44)$$

The root nodes correspond to an initial state ρ . Starting from ρ , the state after depth l is defined as

$$\rho^{[l]} := \Phi^{[l]} \circ \dots \circ \Phi^{[1]}(\rho), \quad \text{and} \quad \rho^{[0]} := \rho. \quad (45)$$

We denote the final state at depth L by $\rho_{\text{tree}} := \rho^{[L]}$.

Local and global observables. At each leaf, we place an observable $O_{(i_1, \dots, i_L)}$ acting on the Hilbert space associated with node $\Phi_{(i_1, \dots, i_L)}$, where the operator norm is bounded by 1. A typical example of $O_{(i_1, \dots, i_L)}$ is a Pauli string, e.g., $X \otimes Y \otimes \dots \otimes Z$. By taking the tensor product of all leaf observables, we obtain the global observable

$$O := \bigotimes_{(i_1, \dots, i_L) \in \mathcal{I}_L} O_{(i_1, \dots, i_L)}. \quad (46)$$

The expectation value of O with respect to ρ_{tree} is

$$\langle O \rangle_{\rho_{\text{tree}}} := \text{tr}(O \rho_{\text{tree}}). \quad (47)$$

Effective observables. To evaluate the expectation value, it is convenient to introduce the effective observables $M_{(i_1, \dots, i_l)}$, obtained by contracting the subtree rooted at (i_1, \dots, i_l) in the Heisenberg picture. At depth L , we set $M_{(i_1, \dots, i_L)} := \Phi_{(i_1, \dots, i_L)}^\dagger(O_{(i_1, \dots, i_L)})$. For $1 \leq l < L$, let $\text{Ch}(i_1, \dots, i_l)$ denote the set of child indices of the node (i_1, \dots, i_l) . Then, we recursively define

$$M_{(i_1, \dots, i_l)} := \Phi_{(i_1, \dots, i_l)}^\dagger \left(\bigotimes_{j \in \text{Ch}(i_1, \dots, i_l)} M_{(i_1, \dots, i_l, j)} \right). \quad (48)$$

With the effective observable $M_{(i_1, \dots, i_l)}$, the expectation value can be expressed as

$$\langle O \rangle_{\rho_{\text{tree}}} = \text{tr} \left(\rho^{[l-1]} \bigotimes_{(i_1, \dots, i_l) \in \mathcal{I}_l} M_{(i_1, \dots, i_l)} \right) \quad (49)$$

for $1 \leq l \leq L$.

B. 2-layer tree-structured quantum circuit

As a simple example to illustrate our idea, we here focus on the case $L = 1$. In the following, we consider

the task of estimating the expectation value $\langle O \rangle_{\rho_{\text{tree}}} = \text{tr}(O\rho_{\text{tree}})$ up to additive error $\epsilon \in (0, 1]$ with success probability at least $1 - \delta$, where the observable is given by the product form $O := O_1 \otimes \cdots \otimes O_R$ with $\|O_k\|_\infty \leq 1$ for all k . The state ρ_{tree} is a two-layer tree-structured quantum state generated by a $(1, R, d)$ -tree quantum circuit, namely

$$\rho_{\text{tree}} := (\Phi_1 \otimes \cdots \otimes \Phi_R)(\rho). \quad (50)$$

In addition, we assume that the available quantum hardware is strictly local. That is, we address the above estimation task under the constraint that we can access only devices whose size is bounded by the maximal number of qubits required to represent the state ρ and the local maps Φ_k .

Having set up the estimation problem, we now analyze how it can be solved using protocols based on Theorems 2 and 3. We first examine the approach derived from Theorem 2. Recall that this theorem guarantees the existence of an MP channel \mathcal{M}_{apr} whose output is biased by at most 2ϵ , provided that we have access to an operator \tilde{O}_Φ satisfying

$$\|\tilde{O}_\Phi - O_\Phi\|_\infty \leq \epsilon. \quad (51)$$

By combining this with the estimation protocol for O_Φ introduced in Sec. IV B, one may naturally consider the following procedure.

Protocol based on Theorem 2

(a-1): Estimate the effective observable $M_k := \Phi_k^\dagger(O_k)$ for each local subsystem $k = 1, \dots, R$ using a finite number of shots $N_{a,k}$, and obtain an estimator \tilde{M}_k .

(a-2): Diagonalize each operator $\tilde{M}_k := \tilde{V}_k \tilde{D}_k \tilde{V}_k^\dagger$, and construct the MP channel

$$\mathcal{M}_{\text{apr}}^{(k)}(\bullet) := \sum_j \text{tr} \left[\tilde{V}_k |j\rangle \langle j| \tilde{V}_k^\dagger \bullet \right] \tilde{V}_k |j\rangle \langle j| \tilde{V}_k^\dagger \quad (52)$$

where $\{|j\rangle\}$ is the computational basis.

(a-3): Replace the identity channels connecting ρ and Φ_k by $\mathcal{M}_{\text{apr}}^{(k)}$, execute the resulting quantum circuit for $N_{a,0}$ shots, and take the empirical mean $\hat{\mu}_a$ as the estimator of $\langle O \rangle_{\rho_{\text{tree}}}$.

Note that Step **(a-3)** does not violate the locality constraint, as the systems ρ and Φ_k interact only through local operations and classical communication. A key caveat of this approach is that the estimator $\hat{\mu}_a$ incurs a bias due to the approximate nature of the MP channels $\mathcal{M}_{\text{apr}}^{(k)}$ for $k = 1, \dots, R$. Consequently, the number of measurements $N_{a,k}$ in Step **(a-1)** must be chosen sufficiently large, while still being kept as small as possible, to ensure that the total bias remains within ϵ . In the subsequent analysis, we carefully account for the accumulation of this bias when choosing the number of measurements $N_{a,k}$.

Next, we consider the protocol based on Theorem 3. Under the same assumption on \tilde{O}_Φ , this theorem uses a measurement with the classical post-processing \mathcal{C}_{apr} . This yields the estimator whose bias is at most ϵ and whose rescaling factor is at most $1 + \epsilon$. Combining this with the protocol of Sec. IV B, we obtain the following estimation protocol.

Protocol based on Theorem 3

(b-1): Estimate the effective observable $M_k := \Phi_k^\dagger(O_k)$ for each local subsystem $k = 1, \dots, R$ using a finite number of shots $N_{b,k}$, and obtain an estimator \tilde{M}_k .

(b-2): Diagonalize each operator $\tilde{M}_k := \tilde{V}_k \tilde{D}_k \tilde{V}_k^\dagger$ with $\tilde{D}_k := \sum_j \tilde{\lambda}_{k,j} |j\rangle \langle j|$, and construct the measurement with classical post-processing

$$\mathcal{C}_{\text{apr}}^{(k)}(\bullet) := \sum_j \text{tr} \left[\tilde{V}_k |j\rangle \langle j| \tilde{V}_k^\dagger \bullet \right] \tilde{\lambda}_{k,j} \quad (53)$$

where $\{|j\rangle\}$ is the computational basis.

(b-3): Measure ρ using $\bigotimes_{k=1}^R \mathcal{C}_{\text{apr}}^{(k)}$ for $N_{b,0}$ times, and take the empirical mean of the classical outputs $\hat{\mu}_b$ as the estimator.

As in the Theorem 2-based protocol, the estimator in Step **(b-3)** is biased. Moreover, this method incurs a rescaling factor that grows exponentially with the number of subsystems R .

In what follows, we provide an upper bound on the sample complexity of these two protocols in solving the estimation task of $\langle O \rangle_{\rho_{\text{tree}}}$. Let

$$N_{a,\text{tot}} = \sum_{k=0}^R N_{a,k}, \quad N_{b,\text{tot}} = \sum_{k=0}^R N_{b,k}, \quad (54)$$

denote the total number of measurements used by protocols based on Theorems 2 and 3.

Theorem 5 (Two-layer tree circuits). *Both the protocol based on Theorem 2 and the protocol based on Theorem 3 estimate $\langle O \rangle_{\rho_{\text{tree}}}$ up to additive error $\epsilon \in (0, 1]$ with probability at least $1 - \delta$, provided that the numbers of measurements satisfy, for $k = 1, \dots, R$,*

$$\begin{aligned} N_{a,k} = N_{b,k} &= \mathcal{O} \left(\frac{d^3 R^2}{\epsilon^2} \ln \left(\frac{(R+1)d}{\delta} \right) \right), \\ N_{a,0} = N_{b,0} &= \mathcal{O} \left(\frac{1}{\epsilon^2} \ln \left(\frac{R+1}{\delta} \right) \right). \end{aligned} \quad (55)$$

Consequently, the total numbers of measurements scale as

$$N_{a,\text{tot}} = N_{b,\text{tot}} = \mathcal{O} \left(\frac{d^3 R^3}{\epsilon^2} \ln \left(\frac{(R+1)d}{\delta} \right) \right). \quad (56)$$

We remark that the above complexity assumes the use of the learning procedure based on 2-design ensemble (Sec. IV B 1). If we replace it with tensor product single-qubit stabilizer states (Sec. IV B 2) or n -qubit Pauli operators (Sec. IV B 3), the total number of measurements becomes

$$N_{a,\text{tot}} = N_{b,\text{tot}} = \mathcal{O} \left(\frac{d^{3.33} R^3}{\epsilon^2} \ln \left(\frac{(R+1)d}{\delta} \right) \right) \quad (57)$$

and

$$N_{a,\text{tot}} = N_{b,\text{tot}} = \mathcal{O} \left(\frac{d^4 R^3}{\epsilon^2} \ln \left(\frac{(R+1)d}{\delta} \right) \right), \quad (58)$$

respectively.

In addition, we emphasize that both protocols based on Theorem 2 and 3 are compatible with the circuit-knitting/cutting setting: they require access only to local devices whose size is bounded by the maximal number of qubits needed to represent ρ and each intermediate object $\Phi_{(i_1, \dots, i_l)}$ ($l = 1, \dots, L$). No coherent quantum operation on the full system is ever required; different devices are combined only through classical communication and classical post-processing of measurement outcomes.

In the following, we sketch the proof of Theorem 5; a detailed version is provided in Appendix S4.2.

Proof sketch of Theorem 5. We first sketch the proof in solving the estimation task using the protocol based on Theorem 2.

1. Proof of the protocol based on Theorem 2

We begin by assuming that the operator-norm error of each estimated observable \tilde{M}_k in Step (a-1) is upper bounded by η , i.e.,

$$\left\| \tilde{M}_k - M_k \right\|_{\infty} \leq \eta, \quad k = 1, \dots, R. \quad (59)$$

Under this assumption, we will relate the individual errors η to the total bias in Step (a-3):

$$\text{Bias}_a := \left| \text{tr} \left[O \left(\bigotimes_{k=1}^R \Phi_k \circ \mathcal{M}_{\text{apr}}^{(k)} \right) (\rho) \right] - \langle O \rangle_{\rho_{\text{tree}}} \right|. \quad (60)$$

Using the telescoping identity (see Lemma 6 in Appendix S4.1) and Theorem 2, we can express the bias solely in terms of the quantity η as

$$\text{Bias}_a \leq 2R\eta. \quad (61)$$

Here, by choosing $\eta = \epsilon/(4R)$, the total bias Bias_a is upper bounded by $\epsilon/2$:

$$\text{Bias}_a \leq \frac{\epsilon}{2}. \quad (62)$$

As a consequence, after implementing the MP channels $\mathcal{M}_{\text{apr}}^{(k)}$ at R locations, an additional estimation with accuracy $\epsilon/2$ suffices to ensure that the overall estimation error is at most ϵ :

$$\left| \hat{\mu}_a - \langle O \rangle_{\rho_{\text{tree}}} \right| \leq \text{Bias}_a + \frac{\epsilon}{2} \leq \epsilon. \quad (63)$$

From the above discussion, we have identified a set of conditions on the estimate at each step that guarantee that the final estimator $\hat{\mu}_a$ achieves additive error at most ϵ . Based on these conditions, we determine the sufficient numbers of measurements so that they hold simultaneously with probability at least $1 - \delta$. According to the analysis so far, the condition for Step (a-1) is

$$\left\| \tilde{M}_k - M_k \right\|_{\infty} \leq \frac{\epsilon}{4R} \quad (k = 1, \dots, R) \quad (64)$$

and the condition for Step (a-3) is

$$\left| \hat{\mu}_a - \text{tr} \left[O \left(\bigotimes_{k=1}^R \Phi_k \circ \mathcal{M}_{\text{apr}}^{(k)} \right) (\rho) \right] \right| \leq \frac{\epsilon}{2}. \quad (65)$$

Note that since Step (a-3) is performed after the learning stage (Step (a-1)), $\hat{\mu}_a$ is conditionally distributed given the learned observables $\{\tilde{M}_k\}$. However, each single-shot outcome in Step (a-3) is always bounded in $[-1, 1]$, because we measure $O = \bigotimes_{k=1}^R O_k$ with $\|O_k\|_{\infty} \leq 1$. Thus, Hoeffding's inequality is uniform in the learning outcomes and can be made unconditional by the tower property (see Appendix S4.2 for detailed discussion).

Thus, there are $R+1$ events; one for each k in Step (a-1) and one for (a-3). By the union bound (Lemma 7), it is sufficient to ensure that each event holds with probability at least $1 - \delta/(R+1)$. Under this requirement, a sufficient number of measurements $N_{a,k}$ in Step (a-1) is

$$N_{a,k} = \mathcal{O} \left(\frac{d^3 R^2}{\epsilon^2} \ln \left(\frac{(R+1)d}{\delta} \right) \right). \quad (66)$$

Similarly, by Hoeffding's inequality, a sufficient number of measurements in Step (a-3) is

$$N_{a,0} = \mathcal{O} \left(\frac{1}{\epsilon^2} \ln \left(\frac{R+1}{\delta} \right) \right). \quad (67)$$

2. Proof of the protocol based on Theorem 3

We assume that the operator-norm error of each estimated observable \tilde{M}_k in Step (b-1) is upper bounded by ξ , namely,

$$\left\| \tilde{M}_k - M_k \right\|_{\infty} \leq \xi, \quad k = 1, \dots, R. \quad (68)$$

Under this assumption, we first investigate the relationship between the individual errors ξ and the total bias in Step (b-3):

$$\text{Bias}_b := \left| \text{tr} \left[\left(\bigotimes_{k=1}^R \tilde{M}_k \right) \rho \right] - \langle O \rangle_{\rho_{\text{tree}}} \right|. \quad (69)$$

Here, we used $\bigotimes_{k=1}^R \mathcal{C}_{\text{apr}}^{(k)}(\rho) = \text{tr}[(\bigotimes_{k=1}^R \tilde{M}_k)\rho]$. Moreover, using $\langle O \rangle_{\rho_{\text{tree}}} = \text{tr}[(\bigotimes_{k=1}^R M_k)\rho]$, the telescoping identity (Lemma 6), and Theorem 3, we obtain

$$\text{Bias}_b \leq R\xi(1 + \xi)^{R-1}. \quad (70)$$

Using Eq. (70) and $(1+x)^r \leq 1 + (e-1)rx$ for $0 \leq x \leq 1/r$ (Lemma 5), we find that setting $\xi = \epsilon/[2R(e-1)]$ yields

$$\text{Bias}_b \leq \frac{\epsilon}{2}. \quad (71)$$

Therefore, with the choice

$$\xi = \frac{\epsilon}{2R(e-1)}, \quad (72)$$

the total bias Bias_b is upper bounded by $\epsilon/2$. Thus, it is sufficient to perform the estimation with accuracy $\epsilon/2$ in Step (b-3) to ensure that the overall estimation error is at most ϵ :

$$|\hat{\mu}_b - \langle O \rangle_{\rho_{\text{tree}}}| \leq \text{Bias}_b + \frac{\epsilon}{2} \leq \epsilon. \quad (73)$$

We now discuss the statistical error in Step (b-3). Define the good-tomography event

$$T := \bigcap_{k=1}^R \left\{ \left\| \tilde{M}_k - M_k \right\|_{\infty} \leq \xi \right\} \quad (74)$$

and define the statistical event

$$E_0^b := \left\{ \left| \hat{\mu}_b - \text{tr} \left[\left(\bigotimes_{k=1}^R \tilde{M}_k \right) \rho \right] \right| \leq \frac{\epsilon}{2} \right\}. \quad (75)$$

On the event T , we have $\|\tilde{M}_k\|_{\infty} \leq \|M_k\|_{\infty} + \|\tilde{M}_k - M_k\|_{\infty} \leq 1 + \xi$ and hence

$$\left\| \bigotimes_{k=1}^R \tilde{M}_k \right\|_{\infty} \leq \prod_{k=1}^R \|\tilde{M}_k\|_{\infty} \leq (1 + \xi)^R \leq 1 + \frac{\epsilon}{2} \leq \frac{3}{2}, \quad (76)$$

where we used $\xi = \epsilon/[2R(e-1)]$ and Lemma 5 in the fourth inequality.

Consequently, we apply Hoeffding's inequality conditioned on the learning outcomes $\{\tilde{M}_k\}$. On the event T , the single-shot output in Step (b-3) is bounded by a constant, and Hoeffding's inequality holds uniformly for every realization on T . Averaging over the learning step gives an unconditional bound

$$\Pr [(E_0^b)^c \cap T] \leq 2 \exp \left(-\frac{N_{b,0}\epsilon^2}{18} \right), \quad (77)$$

where we used the norm upper bound in Eq. (76). See Appendix S4.2 for details.

From the above discussion, Step (b-1) requires that

$$\left\| \tilde{M}_k - M_k \right\|_{\infty} \leq \frac{\epsilon}{2R(e-1)} \quad (k = 1, \dots, R) \quad (78)$$

and Step (b-3) requires that

$$\left| \hat{\mu}_b - \text{tr} \left[\left(\bigotimes_{k=1}^R \tilde{M}_k \right) \rho \right] \right| \leq \frac{\epsilon}{2}. \quad (79)$$

Thus, there are $R+1$ events; the R tomography events in Step (b-1) and the statistical event E_0^b for Step (b-3) on the event T . By the union bound (Lemma 7), it is sufficient to ensure that each of the R tomography events holds with probability at least $1 - \delta/(R+1)$ and that $\Pr [(E_0^b)^c \cap T] \leq \delta/(R+1)$.

Under this requirement, a sufficient number of measurements $N_{b,k}$ in Step (b-1) is

$$N_{b,k} = \mathcal{O} \left(\frac{d^3 R^2}{\epsilon^2} \ln \left(\frac{(R+1)d}{\delta} \right) \right), \quad (80)$$

and Hoeffding's inequality gives that a sufficient number of measurements in Step (b-3) is

$$N_{b,0} = \mathcal{O} \left(\frac{1}{\epsilon^2} \ln \left(\frac{R+1}{\delta} \right) \right). \quad (81)$$

□

Finally, we comment on the implementation cost of $\mathcal{C}_{\text{apr}}^{(k)}$ and $\mathcal{M}_{\text{apr}}^{(k)}$. Both $\mathcal{C}_{\text{apr}}^{(k)}$ and $\mathcal{M}_{\text{apr}}^{(k)}$ involve a unitary that diagonalizes an effective observable \tilde{M}_k of size at most $d \times d$. Hence, one has to perform this diagonalization classically on \tilde{M}_k ($k = 1, \dots, R$). The associated classical computational cost scales as $\mathcal{O}(d^3)$. In the example of a two-layer tree quantum circuit, this procedure is repeated R times, leading to an overall scaling of $\mathcal{O}(d^3R)$. The number of elementary gates of the corresponding unitary U scales at worst as $\mathcal{O}(d^2)$ [53, 54].

C. Multi-layer tree-structured quantum circuit

Here, we extend the result of Sec. V B from the case $L = 1$ to the general case $L \geq 2$. Formally, the following theorem states the general result.

Theorem 6 (Multi-layer tree circuits). *Suppose ρ_{tree} is the quantum state generated by an (L, R, d) -tree quantum circuit with $R \geq 2$, $L \geq 1$, and $d = 2^n$, and let O be the observable defined in Eq. (46). Assume that we have access only to devices whose size is bounded by the maximal number of qubits required to represent ρ and $\Phi_{(i_1, \dots, i_l)}$ for each $l = 1, \dots, L$. Then the total number of measurements*

$$\mathcal{O} \left(\frac{4^L d^3 L^2 R^{3L}}{\epsilon^2} \ln \left(\frac{R^L d}{\delta} \right) \right) \quad (82)$$

is sufficient to estimate $\langle O \rangle_{\rho_{\text{tree}}}$ within additive error $\epsilon \in (0, 1]$ with probability at least $1 - \delta$.

The detailed proof can be found in Appendix S4.3. Theorem 6 indicates that the shot allocation for estimating $M_{(i_1, \dots, i_l)}$ at each step is not uniform; see Fig. 6. This reflects the fact that the estimation errors from deeper layers propagate to shallower layers. Therefore, to keep the total accumulated error under control, we need to allocate more shots to the deeper-layer estimations. Moreover, Theorem 6 yields the following scaling

for a complete R -ary tree, i.e., a tree in which every node has exactly R children. Suppose that we decompose ρ_{tree} into local channels $\Phi_{(i_1, \dots, i_L)}$ and a quantum state ρ . For a complete R -ary tree, the number of cuts (or clusters) scales as $K = \mathcal{O}(R^L)$. The theorem then implies that $\langle O \rangle_{\rho_{\text{tree}}}$ can be estimated within additive error ϵ using a total number of measurements

$$\tilde{\mathcal{O}}\left(\frac{d^3 K^5}{\epsilon^2}\right), \quad (83)$$

where $\tilde{\mathcal{O}}$ suppresses polylogarithmic factors. This scaling is exponentially smaller in K than the existing estimate based on wire cutting, $\mathcal{O}(d^{2K}/\epsilon^2)$. We note that, consistent with previous studies of wire cutting [14, 19–23], the measurement bound for wire cutting is a sufficient bound derived from Hoeffding’s inequality. In the two-layer case, however, we prove that an exponential number of measurements in the number of cuts is also necessary in the next section.

We also note that, in the special case of $R = 1$, Theorem 6 implies that while the number of cuts K scales linearly with L , the total number of measurements scales as $\tilde{\mathcal{O}}(d^3 L^2 4^L \epsilon^{-2})$. Although this scaling is exponential in the number of cuts K and is the same as that of the conventional wire-cutting method, it is merely an artifact of the looseness of the evaluation. The following remark supplements this discussion.

Remark 1 ($R = 1$). Consider partitioning the quantum circuit in Fig. 7 at the wires between Φ_i and Φ_{i+1} for

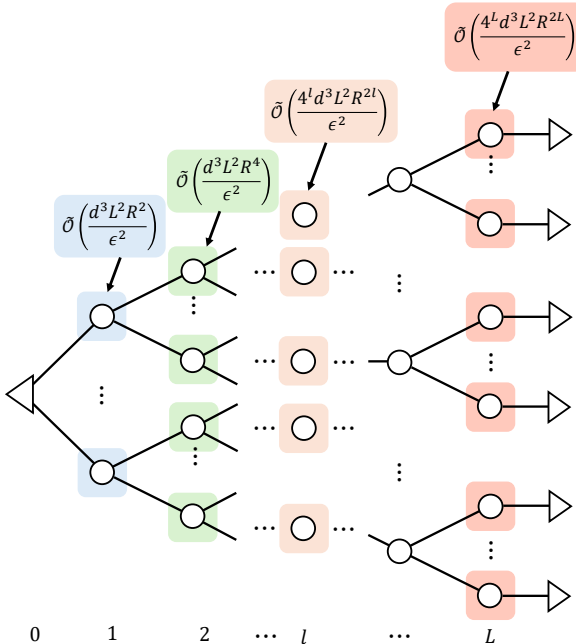


FIG. 6. Schematic of the shot allocation required for estimating $M_{(i_1, \dots, i_l)}$ in a multi-layer tree quantum circuit.

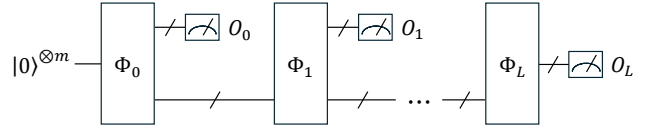


FIG. 7. Quantum circuit considered in Remark 1. Each Φ_i is an unknown CPTP map, and Φ_i and Φ_{i+1} ($i = 0, \dots, L - 1$) are connected by a wire of dimension at most d . Here, $m \in \mathbb{N}$, and O_0, \dots, O_L are Hermitian operators satisfying $\|O_i\|_\infty \leq 1$.

$i = 0, \dots, L - 1$. Then the total number of measurements

$$\mathcal{O}\left(\frac{L^3 d^3}{\epsilon^2} \ln\left(\frac{(L+1)d}{\delta}\right)\right) \quad (84)$$

is sufficient to estimate the expectation value within additive error $\epsilon \in (0, 1]$ with probability at least $1 - \delta$.

For the detailed proof of this remark, see Appendix S4.4. In the following, we show the proof sketch of Theorem 6.

Proof sketch of Theorem 6. For simplicity, we consider an (L, R, d) -tree quantum circuit that forms a complete R -ary tree of depth L with bond dimension $d = 2^n$. We note that when the branching factor and the bond dimension are non-uniform, our algorithm below allows one to estimate the expectation value with fewer measurements than the bound, by appropriately optimizing the shot allocation.

Our basic computational strategy is to apply the learning protocol sequentially, constructing the corresponding classical functions \mathcal{C}_{apr} from the part of the circuit closest to the observable O . More concretely, we repeatedly construct estimators of the effective observables $M_{(i_1, \dots, i_l)}$, denoted by $\tilde{M}_{(i_1, \dots, i_l)}$, in the order of

$$\{\tilde{M}_{(i_1, \dots, i_L)} : (i_1, \dots, i_L) \in [R]^L\} \rightarrow \dots \rightarrow \{\tilde{M}_{i_1} : i_1 \in [R]\}.$$

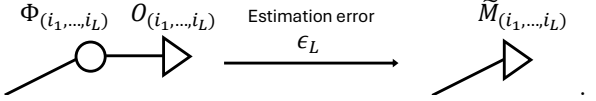
On the other hand, since the learning protocol relies on finite-shot estimation, the estimation error accumulates as we move towards the lower-depth part of the circuit. In what follows, we track how these estimation errors propagate, and then choose the target accuracy at each estimation step so that the final estimate of $\langle O \rangle_{\rho_{\text{tree}}}$ achieves an overall precision ϵ with probability at least $1 - \delta$. For the subsequent analysis, we define an upper bound on the deviations between the estimated effective observable $\tilde{M}_{(i_1, \dots, i_l)}$ and the ideal effective observable $M_{(i_1, \dots, i_l)}$ for each depth $l = 1, \dots, L$ by

$$\|\tilde{M}_{(i_1, \dots, i_l)} - M_{(i_1, \dots, i_l)}\|_\infty \leq x_l \quad \text{for all } (i_1, \dots, i_l). \quad (85)$$

(i) Learning process at depth L

Given the known observable $O_{(i_1, \dots, i_L)}$ and the unknown quantum channel $\Phi_{(i_1, \dots, i_L)}$, we estimate

$M_{(i_1, \dots, i_L)} := \Phi_{(i_1, \dots, i_L)}^\dagger(O_{(i_1, \dots, i_L)})$ using the learning protocol introduced in Sec. IV:

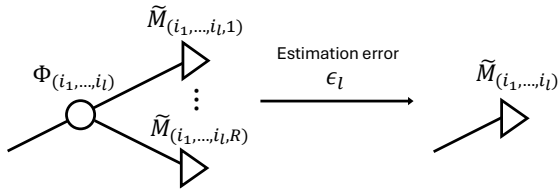


Denoting by ϵ_L an upper bound on the estimation error at depth L , the definition of x_l gives:

$$x_L = \epsilon_L. \quad (86)$$

(ii) Learning process at depth $l = 1, \dots, L-1$

Given the estimated effective observables $\tilde{M}_{(i_1, \dots, i_{l+1})}$ at depth $l+1$ and the unknown quantum channel $\Phi_{(i_1, \dots, i_l)}$, we apply the learning procedure to estimate $M_{(i_1, \dots, i_l)}$:



Denoting by ϵ_l an upper bound on the estimation error introduced at depth l , we can bound the error x_l as

$$x_l \leq \epsilon_l + Rx_{l+1} (1 + x_{l+1})^{R-1}. \quad (87)$$

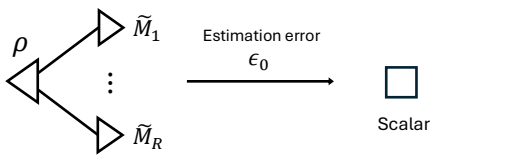
In addition, assuming that x_{l+1} is upper bounded by $1/[(e-1)R]$, Eq. (87) can be further simplified to

$$x_l \leq 2Rx_{l+1} + \epsilon_l. \quad (88)$$

For the detailed calculations of Eqs. (87) and (88), see Appendix S4.3. This yields a simple interpretation of how the errors propagate across the tree: at depth l , the total error is at most the sum of the estimation error ϵ_l at this step and (at most) twice the sum of the R errors coming from depth $l+1$.

(iii) Learning process at depth 0

Given the estimated effective observables $\tilde{M}_1, \dots, \tilde{M}_R$ and the unknown quantum state ρ , we finally calculate the estimate of $\langle O \rangle_{\rho_{\text{tree}}}$ as



Denoting by ϵ_0 an upper bound on the estimation error at this step, the discussion in the case of $L=1$ (Sec. V B) indicates that it is sufficient to take

$$\epsilon_0 = \frac{\epsilon}{2}, \quad x_1 = \frac{\epsilon}{2R(e-1)}. \quad (89)$$

Here, by repeatedly substituting Eq. (88), we obtain the following expression:

$$x_1 \leq \sum_{l=1}^L (2R)^{l-1} \epsilon_l. \quad (90)$$

Thus, to satisfy the condition (89), it suffices to choose

$$\epsilon_k = \frac{\epsilon}{(2R)^k (e-1)L}, \quad k = 1, \dots, L. \quad (91)$$

We remark that if this condition is satisfied, x_l ($l = 1, \dots, L$) is upper bounded as $1/[R(e-1)]$. In addition, under this choice, the operator norm of the product of $\tilde{M}_{(i_1, \dots, i_{l+1})}$ ($l = 1, \dots, L-1$) can be upper bounded as

$$\left\| \bigotimes_{k=1}^R \tilde{M}_{(i_1, \dots, i_l, k)} \right\|_\infty \leq 2. \quad (92)$$

Building on the discussion so far, we now choose the numbers of measurements so that all accuracy requirements hold simultaneously with probability at least $1-\delta$. As in the depth-1 case (Sec. V B), we allocate the total failure probability δ via a union bound (Lemma 7). Here, the input observables $\{\tilde{M}_{(i_1, \dots, i_l, k)}\}_k$ at depth l depend on the random outcomes at deeper depths, and their operator norms affect the sample size as shown in Theorem 4. Hence, we apply the learning guarantee conditionally on the event where all deeper-depth learning steps succeed, and then remove the conditioning via the tower property; see Appendix S4.3 for details.

Putting these together, it is sufficient to take

$$N_{(i_1, \dots, i_l)} = \mathcal{O} \left(\frac{d^3 (2R)^{2l} L^2}{\epsilon^2} \ln \left(\frac{R^L d}{\delta} \right) \right), \quad (93)$$

$$N_0 = \mathcal{O} \left(\frac{1}{\epsilon^2} \ln \left(\frac{R^L}{\delta} \right) \right), \quad (94)$$

where $N_{(i_1, \dots, i_l)}$ and N_0 denote the numbers of measurements used to estimate $M_{(i_1, \dots, i_l)}$ and $\langle O \rangle_{\rho_{\text{tree}}}$, respectively. Thus, the total number of measurements N_{tot} is

$$N_{\text{tot}} = N_0 + \sum_{l=1}^L \sum_{(i_1, \dots, i_l) \in [R]^l} N_{(i_1, \dots, i_l)} \quad (95)$$

$$= \mathcal{O} \left(\frac{4^L d^3 L^2 R^{3L}}{\epsilon^2} \ln \left(\frac{R^L d}{\delta} \right) \right), \quad (96)$$

as claimed. \square

VI. EXPONENTIAL SEPARATION IN THE NUMBER OF CUTS COMPARED TO CONVENTIONAL WIRE-CUTTING METHODS

We demonstrate a polynomial-exponential separation in the scaling with respect to the number of cuts between our learning-based approach and conventional

Algorithm 1: Cluster simulation of a two-layer tree circuit with quantum circuit cut

Input: Unknown CPTP maps $\{\Phi_k\}_{k=1}^R$; an unknown quantum state ρ ; known observables $O = \bigotimes_{k=1}^R O_k$ with $\|O_k\|_\infty \leq 1$; and accuracy ϵ

Output: Estimate $\hat{\mu}$ of $\text{tr}(O\rho_{\text{tree}})$

for $i = 1, 2, \dots, N$ **do**

Sample η_i according to the probability distribution p ;

Measure ρ with the POVM $\{M_{\eta_i, y_i} = \bigotimes_{k=1}^R M_{\eta_i, y_i^k}^k\}_{y_i}$, deriving the outcome $y_i = (y_i^1, \dots, y_i^R)$;

Prepare $\bigotimes_{k=1}^R \sigma_{\eta_i, y_i^k}^k$ and evolve it under the CPTP map $\bigotimes_{k=1}^R \Phi_k$;

Rotate the state with $\bigotimes_{k=1}^R W_k^\dagger$ where each W_k is a unitary defined by the eigenvalue decomposition $O_k := W_k \Lambda_k W_k^\dagger$;

Measure the resulting state in the computational basis, deriving the bitstrings $z_i := (z_i^1, \dots, z_i^R)$;

$\hat{\mu} \leftarrow \text{ClassicalProcessing}((\eta_1, y_1, z_1), \dots, (\eta_N, y_N, z_N))$;

return $\hat{\mu}$;

quasiprobability-based circuit cutting approaches, especially wire cut [14, 19–23], for the distributed expectation estimation task in a two-layer tree-structured quantum circuit. Here, we consider the following task.

Task 1 (Distributed expectation estimation for a two-layer tree quantum circuit). *Let $\rho_{\text{targ}} := (\Phi_1 \otimes \dots \otimes \Phi_R)(\rho)$ be an unknown quantum state acting on the Hilbert space $\bigotimes_{k=1}^R \mathcal{H}_{\text{out}}^{(k)}$, where ρ is an unknown quantum state on $\bigotimes_{k=1}^R \mathcal{H}_{\text{in}}^{(k)}$, and each $\Phi_k : \mathcal{L}(\mathbb{C}^d) \rightarrow \mathcal{L}(\mathbb{C}^{d'})$ is an unknown CPTP map with $d = 2^n$ and $d \leq d'$. We are also given a known Hermitian observable $O := \bigotimes_{k=1}^R O_k$ where each $O_k \in \mathcal{H}(\mathbb{C}^{d'})$ satisfies $\|O_k\|_\infty \leq 1$. The goal is to estimate the expectation value $\text{Tr}(O\rho_{\text{targ}})$ up to additive error ϵ with high probability, under the constraint that we do not have access to any quantum device larger than the maximum number of qubits required to represent either ρ or any of the channels Φ_k for $k = 1, \dots, R$.*

We can solve this problem using the learning-based cutting method. In this approach, we first approximate the effective observable $M_k = \Phi_k^\dagger(O_k)$ for each $k = 1, \dots, R$ using the learning protocol described in Sec. IV, obtaining an estimated matrix \tilde{M}_k . Next, we perform the eigenvalue decomposition of each estimated observable as $\tilde{M}_k := \tilde{V}_k (\sum_{j_k} \tilde{\lambda}_{k,j} |j\rangle\langle j|) \tilde{V}_k^\dagger$ where $\{|j\rangle\}$ denotes the computational basis. We then construct MP channels $\mathcal{M}_{\text{apr}}^{(k)}$ ($k = 1, \dots, R$), replace the identity channels connecting ρ and Φ_k by $\mathcal{M}_{\text{apr}}^{(k)}$ for $k = 1, \dots, R$, and execute the resulting quantum circuit. Finally, we obtain the estimator $\hat{\mu}$ by computing the arithmetic mean of the

weighted outcomes. Following this procedure, Theorem 5 shows that the task can be solved using at most

$$N = \mathcal{O}\left(\frac{d^3 R^3}{\epsilon^2} \ln\left(\frac{(R+1)d}{\delta}\right)\right) \quad (97)$$

total measurements.

In contrast, a conventional approach to solving the distributed expectation value estimation task is based on quantum circuit cutting, particularly wire-cutting methods. As introduced in Sec. II B, a conventional QPD-based wire cut simulates an identity channel by probabilistically replacing it with an MP channel, followed by appropriate classical post-processing of the measurement outcomes. With this wire cut, we can accomplish the Task 1 by replacing the R identity channels

$$\text{id}^{(k)} : \mathcal{L}(\mathbb{C}^d) \rightarrow \mathcal{L}(\mathbb{C}^d) \quad \text{for } k = 1, \dots, R \quad (98)$$

that connect ρ and each Φ_k with such probabilistic measure-and-prepare channels, and subsequently applying classical post-processing to reconstruct the desired expectation value. However, as we prove in Appendix S5, any conventional wire-cutting approach requires at least an exponential number of measurements in R to achieve the same accuracy. Formally, we establish the following theorem.

Theorem 7. *Consider solving Task 1 using either the learning-based approach described in Sec. V B or a conventional quasiprobability-based wire-cutting approach described in Algorithm 1.*

- **Upper bound:** *The learning-based approach can solve Task 1 using at most $\mathcal{O}(R^3 d^3 \ln((R+1)d)/\epsilon^2)$ total measurements, for any quantum state ρ , CPTP maps Φ_k , and observable O .*
- **Lower bound:** *Any quasiprobability-based wire-cutting requires at least $\Omega((d+1)^R/\epsilon^2)$ measurements to solve Task 1.*

The proof is provided in Appendix S5. We here outline the main proof idea as follows. The upper bound can be directly derived from Theorem 5. To prove the lower bound, we use the fact that randomized measurements are effective at capturing the low-rank properties of input quantum states, but are not effective at capturing their high-rank properties in general. For example, the classical shadow tomography is a prominent example of the learning protocol using randomized measurements [59, 60]. It enables the prediction of multiple properties of arbitrary observables from data obtained via randomized measurements performed before the set of target observables is specified. However, it has been proven that, in the setting of independent measurements and mixed input quantum states, achieving a desired estimation accuracy requires a number of measurements that scales proportionally with the rank r of the observable [59]. Similarly, it is known that wire cutting

is more effective at estimating low-rank properties than high-rank ones [19, 23]. Building on this intuition, we establish an exponential separation by reducing the problem to a two-state discrimination task associated with properties of high-rank observables.

VII. CONCLUSION AND DISCUSSIONS

In this work, we introduced a new framework for circuit knitting with quantum tomography that achieves unit rescaling locally and ensures that the total number of measurements scales polynomially with the number of circuit cuts. This sharply contrasts with conventional QPD-based or virtual-protocol approaches in which decomposing target operations into linear combinations of implementable ones induces an exponential sampling overhead in the number of applications. The core idea underlying our protocol is that local tomography can regulate the rescaling factor at each cut, converting global multiplicative rescaling factors into locally controlled additive measurement costs. Through this mechanism, we avoid exponential blow-ups and establish a scalable pathway for virtual circuit reconstruction.

To realize this framework, we developed a randomized estimation procedure for quantum tomography. Our analytical results confirm that recursive applications of the tomography protocol guarantee polynomial measurement scaling in the number of cuts or clusters. Moreover, we prove an exponential separation in the number of cut locations compared to any conventional QPD-based wire-cutting method in the two-layer tree case. These results collectively demonstrate that incorporating tomography into circuit knitting enables a fundamentally more scalable approach to expectation-value estimation in structured quantum circuits.

A natural and compelling direction for future work is to extend our methodology beyond tree-structured circuits. While our analysis establishes polynomial measurement scaling for trees, it remains an open challenge to characterize the complexity for more general circuit architectures—such as planar graphs, low-treewidth circuits, or tensor-network amenable structures. An especially intriguing possibility is to employ gate cuts [23–28] to transform an arbitrary quantum circuit into a tree-like decomposition, followed by the application of our learning-based procedure. This hybrid approach, combining circuit cutting with our proposal, has the potential to enable efficient simulation even when the original

circuit does not have an inherent tree structure. When the resulting graph exhibits bounded treewidth, or when controlled tensor-contraction strategies are available, this combined method may yield further reductions in complexity, facilitated by optimized contraction orders and graph-specific decomposition rules. Understanding the precise regimes in which such hybrid constructions offer meaningful advantages constitutes a key avenue for future research.

Our framework may be naturally helpful for the realization of efficient distributed quantum computation [61–63], in which a global task is decomposed into smaller quantum subsystems coordinated via quantum information flow. Examining how tomographic protocols integrate with distributed architectures, such as modular quantum processors or multi-node hybrid systems [64], may reveal new pathways for scalable computation under realistic hardware constraints.

Potential complexity improvements may also arise when each subsystem has limited non-Clifford depth or restricted gate sets. It remains to understand how these structural restrictions would improve sample and runtime bounds within our tomographic contraction protocol.

Our findings suggest broader implications for virtual quantum simulation techniques [65–70]. The principle underlying our approach, which uses local tomography to suppress the global rescaling factor, shares conceptual similarities with the coherent-resource versus rescaling-factor trade-off observed in the recently introduced virtual simulation framework [71]. In both contexts, the introduction of an additional local resource mitigates exponential rescaling growth, offering a unifying conceptual insight for designing scalable near-term algorithms across quantum circuit cutting, quantum error mitigation [29, 31, 47], and hybrid quantum-classical simulations [72].

ACKNOWLEDGMENTS

H.H. and S.E. thank Kosuke Mitarai and Bo Yang for fruitful discussions at the early stage of this work. This work was supported by JST [Moonshot R&D] Grant No. JPMJMS2061; MEXT Q-LEAP, Grant No. JPMXS0120319794 and JPMXS0118067285; JST CREST Grant No. JPMJCR23I4, and No. JPMJCR25I4. K.W. was supported by JSPS KAKENHI Grant Number JP24KJ1963.

[1] L. K. Grover, A fast quantum mechanical algorithm for database search, in *Proceedings of the Twenty-Eighth Annual ACM Symposium on Theory of Computing*, STOC '96 (Association for Computing Machinery, New York, NY, USA, 1996) p. 212–219.

[2] P. W. Shor, Polynomial-time algorithms for prime factorization and discrete logarithms on a quantum computer, *SIAM Journal on Computing* **26**, 1484 (1997).

[3] A. Peruzzo, J. McClean, P. Shadbolt, M.-H. Yung, X.-Q. Zhou, P. J. Love, A. Aspuru-Guzik, and J. L. O'Brien,

A variational eigenvalue solver on a photonic quantum processor, *Nature communications* **5**, 4213 (2014).

[4] A. Kandala, A. Mezzacapo, K. Temme, M. Takita, M. Brink, J. M. Chow, and J. M. Gambetta, Hardware-efficient variational quantum eigensolver for small molecules and quantum magnets, *Nature* **549**, 242 (2017).

[5] B. Bauer, S. Bravyi, M. Motta, and G. K.-L. Chan, Quantum algorithms for quantum chemistry and quantum materials science, *Chemical Reviews* **120**, 12685 (2020).

[6] H. Ma, M. Govoni, and G. Galli, Quantum simulations of materials on near-term quantum computers, *npj Computational Materials* **6**, 85 (2020).

[7] N. Moll, P. Barkoutsos, L. S. Bishop, J. M. Chow, A. Cross, D. J. Egger, S. Filipp, A. Fuhrer, J. M. Gambetta, M. Ganzhorn, A. Kandala, A. Mezzacapo, P. Müller, W. Riess, G. Salis, J. Smolin, I. Tavernelli, and K. Temme, Quantum optimization using variational algorithms on near-term quantum devices, *Quantum Science and Technology* **3**, 030503 (2018).

[8] V. Havlíček, A. D. Córcoles, K. Temme, A. W. Harrow, A. Kandala, J. M. Chow, and J. M. Gambetta, Supervised learning with quantum-enhanced feature spaces, *Nature* **567**, 209 (2019).

[9] D. Amaro, M. Rosenkranz, N. Fitzpatrick, K. Hirano, and M. Fiorentini, A case study of variational quantum algorithms for a job shop scheduling problem, *EPJ Quantum Technology* **9**, 5 (2022).

[10] B. Fuller, C. Hadfield, J. R. Glick, T. Imamichi, T. Itoko, R. J. Thompson, Y. Jiao, M. M. Kagele, A. W. Blom-Schieber, R. Raymond, and A. Mezzacapo, Approximate solutions of combinatorial problems via quantum relaxations, *IEEE Transactions on Quantum Engineering* **5**, 1 (2024).

[11] R. Orús, S. Mugel, and E. Lizaso, Quantum computing for finance: Overview and prospects, *Reviews in Physics* **4**, 100028 (2019).

[12] D. Herman, C. Googin, X. Liu, A. Galda, I. Safro, Y. Sun, M. Pistoia, and Y. Alexeev, A survey of quantum computing for finance (2022), [arXiv:2201.02773 \[quant-ph\]](https://arxiv.org/abs/2201.02773).

[13] S. Bravyi, G. Smith, and J. A. Smolin, Trading classical and quantum computational resources, *Phys. Rev. X* **6**, 021043 (2016).

[14] T. Peng, A. W. Harrow, M. Ozols, and X. Wu, Simulating large quantum circuits on a small quantum computer, *Phys. Rev. Lett.* **125**, 150504 (2020).

[15] A. Eddins, M. Motta, T. P. Gujarati, S. Bravyi, A. Mezzacapo, C. Hadfield, and S. Sheldon, Doubling the size of quantum simulators by entanglement forging, *PRX Quantum* **3**, 010309 (2022).

[16] K. Fujii, K. Mizuta, H. Ueda, K. Mitarai, W. Mizukami, and Y. O. Nakagawa, Deep variational quantum eigensolver: A divide-and-conquer method for solving a larger problem with smaller size quantum computers, *PRX Quantum* **3**, 010346 (2022).

[17] X. Yuan, J. Sun, J. Liu, Q. Zhao, and Y. Zhou, Quantum simulation with hybrid tensor networks, *Phys. Rev. Lett.* **127**, 040501 (2021).

[18] T. L. Scholten, C. J. Williams, D. Moody, M. Mosca, W. Hurley, W. J. Zeng, M. Troyer, and J. M. Gambetta, Assessing the benefits and risks of quantum computers (2024), [arXiv:2401.16317 \[quant-ph\]](https://arxiv.org/abs/2401.16317).

[19] A. Lowe, M. Medvidović, A. Hayes, L. J. O'Riordan, T. R. Bromley, J. M. Arrazola, and N. Killoran, Fast quantum circuit cutting with randomized measurements, *Quantum* **7**, 934 (2023).

[20] L. Brenner, C. Piveteau, and D. Sutter, Optimal wire cutting with classical communication, *IEEE Transactions on Information Theory* **71**, 7742 (2025).

[21] H. Harada, K. Wada, and N. Yamamoto, Doubly optimal parallel wire cutting without ancilla qubits, *PRX Quantum* **5**, 040308 (2024).

[22] E. Pednault, An alternative approach to optimal wire cutting without ancilla qubits (2023), [arXiv:2303.08287 \[quant-ph\]](https://arxiv.org/abs/2303.08287).

[23] A. W. Harrow and A. Lowe, Optimal quantum circuit cuts with application to clustered hamiltonian simulation, *PRX Quantum* **6**, 010316 (2025).

[24] K. Mitarai and K. Fujii, Constructing a virtual two-qubit gate by sampling single-qubit operations, *New Journal of Physics* **23**, 023021 (2021).

[25] K. Mitarai and K. Fujii, Overhead for simulating a non-local channel with local channels by quasiprobability sampling, *Quantum* **5**, 388 (2021).

[26] C. Piveteau and D. Sutter, Circuit knitting with classical communication, *IEEE Transactions on Information Theory* **1** (2023).

[27] C. Ufrecht, M. Periyasamy, S. Rietsch, D. D. Scherer, A. Plinge, and C. Mutschler, Cutting multi-control quantum gates with ZX calculus, *Quantum* **7**, 1147 (2023).

[28] L. Schmitt, C. Piveteau, and D. Sutter, Cutting circuits with multiple two-qubit unitaries, *Quantum* **9**, 1634 (2025).

[29] S. Endo, S. C. Benjamin, and Y. Li, Practical quantum error mitigation for near-future applications, *Phys. Rev. X* **8**, 031027 (2018).

[30] H. Pashayan, J. J. Wallman, and S. D. Bartlett, Estimating outcome probabilities of quantum circuits using quasiprobabilities, *Phys. Rev. Lett.* **115**, 070501 (2015).

[31] K. Temme, S. Bravyi, and J. M. Gambetta, Error mitigation for short-depth quantum circuits, *Phys. Rev. Lett.* **119**, 180509 (2017).

[32] M. Bechtold, J. Barzen, F. Leymann, A. Mandl, J. Obst, F. Truger, and B. Weder, Investigating the effect of circuit cutting in qaoa for the maxcut problem on nisq devices, *Quantum Science and Technology* **8**, 045022 (2023).

[33] C. Ying, B. Cheng, Y. Zhao, H.-L. Huang, Y.-N. Zhang, M. Gong, Y. Wu, S. Wang, F. Liang, J. Lin, Y. Xu, H. Deng, H. Rong, C.-Z. Peng, M.-H. Yung, X. Zhu, and J.-W. Pan, Experimental simulation of larger quantum circuits with fewer superconducting qubits, *Phys. Rev. Lett.* **130**, 110601 (2023).

[34] A. Carrera Vazquez, C. Tornow, D. Riste, S. Woerner, M. Takita, and D. J. Egger, Combining quantum processors with real-time classical communication, *Nature* **636**, 75 (2024).

[35] W. Tang, T. Tomesh, M. Suchara, J. Larson, and M. Martonosi, Cutqc: Using small quantum computers for large quantum circuit evaluations, in *Proceedings of the 26th ACM International Conference on Architectural Support for Programming Languages and Operating Systems*, ASPLOS '21 (Association for Computing Machinery, New York, NY, USA, 2021) p. 473–486.

[36] T. Tomesh, Z. H. Saleem, M. A. Perlin, P. Gokhale,

M. Suchara, and M. Martonosi, Divide and Conquer for Combinatorial Optimization and Distributed Quantum Computation , in *2023 IEEE International Conference on Quantum Computing and Engineering (QCE)* (IEEE Computer Society, Los Alamitos, CA, USA, 2023) pp. 1–12.

[37] S. Brandhofer, I. Polian, and K. Krsulich, Optimal partitioning of quantum circuits using gate cuts and wire cuts, *IEEE Transactions on Quantum Engineering* **5**, 1 (2024).

[38] X. Yuan, Y. Liu, Q. Zhao, B. Regula, J. Thompson, and M. Gu, Universal and operational benchmarking of quantum memories, *npj Quantum Information* **7**, 108 (2021).

[39] J. Schuhmacher, M. Ballarin, A. Baiardi, G. Magnifico, F. Tacchino, S. Montangero, and I. Tavernelli, Hybrid tree tensor networks for quantum simulation, *PRX Quantum* **6**, 010320 (2025).

[40] H. Harada, Y. Suzuki, B. Yang, Y. Tokunaga, and S. Endo, Density matrix representation of hybrid tensor networks for noisy quantum devices, *Quantum* **9**, 1823 (2025).

[41] S. Kanno, H. Nakamura, T. Kobayashi, S. Gocho, M. Hatanaka, N. Yamamoto, and Q. Gao, Quantum computing quantum monte carlo with hybrid tensor network for electronic structure calculations, *npj Quantum Information* **10**, 56 (2024).

[42] K. Mizuta, M. Fujii, S. Fujii, K. Ichikawa, Y. Imamura, Y. Okuno, and Y. O. Nakagawa, Deep variational quantum eigensolver for excited states and its application to quantum chemistry calculation of periodic materials, *Phys. Rev. Res.* **3**, 043121 (2021).

[43] P. Huembeli, G. Carleo, and A. Mezzacapo, Entanglement forging with generative neural network models (2022), [arXiv:2205.00933 \[quant-ph\]](https://arxiv.org/abs/2205.00933).

[44] S. C. Marshall, J. Tura, and V. Dunjko, All this for one qubit? bounds on local circuit cutting schemes (2023), [arXiv:2303.13422 \[quant-ph\]](https://arxiv.org/abs/2303.13422).

[45] J. Huang, Y. Tang, and X. Yuan, Estimating local observables via cluster-level light-cone decomposition (2025), [arXiv:2512.02377 \[quant-ph\]](https://arxiv.org/abs/2512.02377).

[46] M. DeCross, E. Chertkov, M. Kohagen, and M. Foss-Feig, Qubit-reuse compilation with mid-circuit measurement and reset, *Phys. Rev. X* **13**, 041057 (2023).

[47] Z. Cai, R. Babbush, S. C. Benjamin, S. Endo, W. J. Huggins, Y. Li, J. R. McClean, and T. E. O’Brien, Quantum error mitigation, *Rev. Mod. Phys.* **95**, 045005 (2023).

[48] M. Howard and E. Campbell, Application of a resource theory for magic states to fault-tolerant quantum computing, *Phys. Rev. Lett.* **118**, 090501 (2017).

[49] J. R. Seddon and E. T. Campbell, Quantifying magic for multi-qubit operations, *Proceedings of the Royal Society A: Mathematical, Physical and Engineering Sciences* **475**, 20190251 (2019).

[50] J. R. Seddon, B. Regula, H. Pashayan, Y. Ouyang, and E. T. Campbell, Quantifying quantum speedups: Improved classical simulation from tighter magic monotones, *PRX Quantum* **2**, 010345 (2021).

[51] M. Horodecki, P. W. Shor, and M. B. Ruskai, Entanglement breaking channels, *Reviews in Mathematical Physics* **15**, 629 (2003).

[52] W. Hoeffding, Probability inequalities for sums of bounded random variables, *Journal of the American Statistical Association* **58**, 13 (1963).

[53] J. J. Vartiainen, M. Möttönen, and M. M. Salomaa, Efficient decomposition of quantum gates, *Phys. Rev. Lett.* **92**, 177902 (2004).

[54] A. M. Krol, A. Sarkar, I. Ashraf, Z. Al-Ars, and K. Bertels, Efficient decomposition of unitary matrices in quantum circuit compilers, *Applied Sciences* **12**, 10.3390/app12020759 (2022).

[55] M. Gută, J. Kahn, R. Kueng, and J. A. Tropp, Fast state tomography with optimal error bounds, *Journal of Physics A: Mathematical and Theoretical* **53**, 204001 (2020).

[56] L. Zambrano, S. Ramos-Calderer, and R. Kueng, Fast quantum measurement tomography with dimension-optimal error bounds (2025), [arXiv:2507.04500 \[quant-ph\]](https://arxiv.org/abs/2507.04500).

[57] J. A. Tropp, An introduction to matrix concentration inequalities, *Foundations and Trends® in Machine Learning* **8**, 1 (2015).

[58] Z. Webb, The clifford group forms a unitary 3-design, *Quantum Info. Comput.* **16**, 1379–1400 (2016).

[59] H.-Y. Huang, R. Kueng, and J. Preskill, Predicting many properties of a quantum system from very few measurements, *Nature Physics* **16**, 1050 (2020).

[60] D. Grier, H. Pashayan, and L. Schaeffer, Sample-optimal classical shadows for pure states, *Quantum* **8**, 1373 (2024).

[61] L. K. Grover, *Quantum telecomputation* (1997), [arXiv:quant-ph/9704012 \[quant-ph\]](https://arxiv.org/abs/quant-ph/9704012).

[62] R. Cleve and H. Buhrman, Substituting quantum entanglement for communication, *Physical Review A* **56**, 1201–1204 (1997).

[63] J. I. Cirac, A. K. Ekert, S. F. Huelga, and C. Macchiavello, Distributed quantum computation over noisy channels, *Phys. Rev. A* **59**, 4249 (1999).

[64] D. Barral, F. J. Cardama, G. Díaz-Camacho, D. Fañde, I. F. Llovo, M. Mussa-Juane, J. Vázquez-Pérez, J. Villasuso, C. Piñeiro, N. Costas, J. C. Pichel, T. F. Pena, and A. Gómez, Review of distributed quantum computing: From single qpu to high performance quantum computing, *Computer Science Review* **57**, 100747 (2025).

[65] J. Cotler, S. Choi, A. Lukin, H. Gharibyan, T. Grover, M. E. Tai, M. Rispoli, R. Schittko, P. M. Preiss, A. M. Kaufman, M. Greiner, H. Pichler, and P. Hayden, Quantum virtual cooling, *Phys. Rev. X* **9**, 031013 (2019).

[66] X. Yuan, B. Regula, R. Takagi, and M. Gu, Virtual quantum resource distillation, *Phys. Rev. Lett.* **132**, 050203 (2024).

[67] R. Takagi, X. Yuan, B. Regula, and M. Gu, Virtual quantum resource distillation: General framework and applications, *Phys. Rev. A* **109**, 022403 (2024).

[68] H. Yao, X. Liu, C. Zhu, and X. Wang, Optimal unilocal virtual quantum broadcasting, *Physical Review A* **110**, 012458 (2024).

[69] A. J. Parzygnat, J. Fullwood, F. Buscemi, and G. Chiribella, Virtual quantum broadcasting, *Phys. Rev. Lett.* **132**, 110203 (2024).

[70] K. Yamamoto, Y. Matsuzaki, Y. Suzuki, Y. Tokunaga, and S. Endo, Virtual entanglement purification via noisy entanglement (2024), [arXiv:2411.10024 \[quant-ph\]](https://arxiv.org/abs/2411.10024).

[71] K. Wada, J. Kato, H. Harada, and N. Yamamoto, State-to-hamiltonian conversion with a few copies (2025), [arXiv:2509.14791 \[quant-ph\]](https://arxiv.org/abs/2509.14791).

[72] S. Endo, Z. Cai, S. C. Benjamin, and X. Yuan, Hybrid quantum-classical algorithms and quantum error mitigation, *Journal of the Physical Society of Japan* **90**, 032001 (2021).

[73] J. Emerson, R. Alicki, and K. Życzkowski, Scalable noise estimation with random unitary operators, *Journal of Optics B: Quantum and Semiclassical Optics* **7**, S347 (2005).

[74] E. Knill, D. Leibfried, R. Reichle, J. Britton, R. B. Blakestad, J. D. Jost, C. Langer, R. Ozeri, S. Seidelin, and D. J. Wineland, Randomized benchmarking of quantum gates, *Phys. Rev. A* **77**, 012307 (2008).

[75] E. Magesan, J. M. Gambetta, and J. Emerson, Scalable and robust randomized benchmarking of quantum processes, *Phys. Rev. Lett.* **106**, 180504 (2011).

[76] A. Elben, R. Kueng, H.-Y. R. Huang, R. van Bijnen, C. Kokail, M. Dalmonte, P. Calabrese, B. Kraus, J. Preskill, P. Zoller, and B. Vermersch, Mixed-state entanglement from local randomized measurements, *Phys. Rev. Lett.* **125**, 200501 (2020).

[77] Z. Ji, Y.-K. Liu, and F. Song, Pseudorandom quantum states, in *Advances in Cryptology – CRYPTO 2018: 38th Annual International Cryptology Conference, Santa Barbara, CA, USA, August 19–23, 2018, Proceedings, Part III* (Springer-Verlag, Berlin, Heidelberg, 2018) p. 126–152.

[78] P. Ananth, L. Qian, and H. Yuen, Cryptography from pseudorandom quantum states, in *Annual International Cryptology Conference* (Springer, 2022) pp. 208–236.

[79] F. Ma and H.-Y. Huang, How to construct random unitaries, in *Proceedings of the 57th Annual ACM Symposium on Theory of Computing* (2025) pp. 806–809.

[80] M. A. Nielsen and I. L. Chuang, *Quantum Computation and Quantum Information: 10th Anniversary Edition* (Cambridge University Press, 2010).

[81] V. V. Shende, I. L. Markov, and S. S. Bullock, Minimal universal two-qubit controlled-not-based circuits, *Phys. Rev. A* **69**, 062321 (2004).

[82] F. G. Brandão, W. Chemissany, N. Hunter-Jones, R. Kueng, and J. Preskill, Models of quantum complexity growth, *PRX Quantum* **2**, 030316 (2021).

[83] C. Dankert, Efficient simulation of random quantum states and operators (2005), [arXiv:quant-ph/0512217 \[quant-ph\]](https://arxiv.org/abs/quant-ph/0512217).

[84] C. Dankert, R. Cleve, J. Emerson, and E. Livine, Exact and approximate unitary 2-designs and their application to fidelity estimation, *Phys. Rev. A* **80**, 012304 (2009).

[85] D. Gross, K. Audenaert, and J. Eisert, Evenly distributed unitaries: On the structure of unitary designs, *Journal of mathematical physics* **48**, <https://doi.org/10.1063/1.2716992> (2007).

[86] A. Ambainis and J. Emerson, Quantum t-designs: t-wise independence in the quantum world, in *Twenty-Second Annual IEEE Conference on Computational Complexity (CCC'07)* (2007) pp. 129–140.

[87] S. Hoggard, t-designs in projective spaces, *European Journal of Combinatorics* **3**, 233 (1982).

[88] P. DELSARTE, J. GOETHALS, and J. SEIDEL, Spherical codes and designs, in *Geometry and Combinatorics*, edited by D. Corneil and R. Mathon (Academic Press, 1991) pp. 68–93.

[89] D. Gottesman, *Stabilizer codes and quantum error correction* (California Institute of Technology, 1997).

[90] R. Kueng and D. Gross, Qubit stabilizer states are complex projective 3-designs (2015), [arXiv:1510.02767 \[quant-ph\]](https://arxiv.org/abs/1510.02767).

[91] Z. Webb, The clifford group forms a unitary 3-design, *Quantum Info. Comput.* **16**, 1379–1400 (2016).

[92] H. Zhu, Multiqubit clifford groups are unitary 3-designs, *Phys. Rev. A* **96**, 062336 (2017).

[93] H. Zhu, R. Kueng, M. Grassl, and D. Gross, The clifford group fails gracefully to be a unitary 4-design (2016), [arXiv:1609.08172 \[quant-ph\]](https://arxiv.org/abs/1609.08172).

[94] E. Van Den Berg, A simple method for sampling random clifford operators, in *2021 IEEE International Conference on Quantum Computing and Engineering (QCE)* (2021) pp. 54–59.

[95] R. Koenig and J. A. Smolin, How to efficiently select an arbitrary clifford group element, *Journal of Mathematical Physics* **55**, 122202 (2014).

[96] S. Aaronson and D. Gottesman, Improved simulation of stabilizer circuits, *Phys. Rev. A* **70**, 052328 (2004).

[97] W. K. Wootters and B. D. Fields, Optimal state-determination by mutually unbiased measurements, *Annals of Physics* **191**, 363 (1989).

[98] J. Lawrence, Č. Brukner, and A. Zeilinger, Mutually unbiased binary observable sets on n qubits, *Phys. Rev. A* **65**, 032320 (2002).

[99] U. Seyfarth, Cyclic mutually unbiased bases and quantum public-key encryption (2019), [arXiv:1907.02726 \[quant-ph\]](https://arxiv.org/abs/1907.02726).

[100] P. Gokhale, O. Angiuli, Y. Ding, K. Gui, T. Tomesh, M. Suchara, M. Martonosi, and F. T. Chong, $o(n^3)$ measurement cost for variational quantum eigensolver on molecular hamiltonians, *IEEE Transactions on Quantum Engineering* **1**, 1 (2020).

[101] J. M. Renes, R. Blume-Kohout, A. J. Scott, and C. M. Caves, Symmetric informationally complete quantum measurements, *Journal of Mathematical Physics* **45**, 2171 (2004).

[102] I. D. Ivanovic, Geometrical description of quantal state determination, *Journal of Physics A: Mathematical and General* **14**, 3241 (1981).

[103] A. Klappenecker and M. Rötteler, Mutually unbiased bases are complex projective 2-designs, in *Proceedings. International Symposium on Information Theory, 2005. ISIT 2005.* (2005) pp. 1740–1744.

[104] O. Crawford, B. v. Straaten, D. Wang, T. Parks, E. Campbell, and S. Brierley, Efficient quantum measurement of Pauli operators in the presence of finite sampling error, *Quantum* **5**, 385 (2021).

[105] Q. Zhang, Q. Liu, and Y. Zhou, Minimal-clifford shadow estimation by mutually unbiased bases, *Phys. Rev. Appl.* **21**, 064001 (2024).

[106] Y. Wang and W. Cui, Classical shadow tomography with mutually unbiased bases, *Phys. Rev. A* **109**, 062406 (2024).

[107] A. A. Mele, Introduction to Haar Measure Tools in Quantum Information: A Beginner’s Tutorial, *Quantum* **8**, 1340 (2024).

[108] A. W. Harrow, The church of the symmetric subspace (2013), [arXiv:1308.6595 \[quant-ph\]](https://arxiv.org/abs/1308.6595).

[109] R. I. Oliveira, Concentration of the adjacency matrix and of the laplacian in random graphs with independent edges (2010), [arXiv:0911.0600 \[math.CO\]](https://arxiv.org/abs/0911.0600).

[110] J. A. Tropp, User-friendly tail bounds for sums of random matrices, *Foundations of computational mathe-*

ematics **12**, 389 (2012).

[111] Y. A. Rozanov, *Probability theory: a concise course* (Courier Corporation, 2013).

[112] R. Nagai, S. Kanno, Y. Sato, and N. Yamamoto, Quantum channel decomposition with preselection and post-selection, *Phys. Rev. A* **108**, 022615 (2023).

[113] G. Uchehara, T. M. Aamodt, and O. D. Matteo, Rotation-inspired circuit cut optimization, in *2022 IEEE/ACM Third International Workshop on Quantum Computing Software (QCS)* (IEEE Computer Society, Los Alamitos, CA, USA, 2022) pp. 50–56.

[114] D. T. Chen, E. H. Hansen, X. Li, V. Kulkarni, V. Chaudhary, B. Ren, Q. Guan, S. Kuppannagari, J. Liu, and S. Xu, Efficient quantum circuit cutting by neglecting basis elements, in *2023 IEEE International Parallel and Distributed Processing Symposium Workshops (IPDPSW)* (2023) pp. 517–523.

[115] D. T. Chen, E. H. Hansen, X. Li, A. Orenstein, V. Kulkarni, V. Chaudhary, Q. Guan, J. Liu, Y. Zhang, and S. Xu, Online detection of golden circuit cutting points, in *2023 IEEE International Conference on Quantum Computing and Engineering (QCE)*, Vol. 01 (2023) pp. 26–31.

Appendices

CONTENTS

S1. Quasiprobability simulation	23
S2. Existence of a rescaling-free wire cut	24
1. Proof of Theorem 1	24
2. Proof of Theorem 2	25
3. Proof of Theorem 3	25
S3. Learning Heisenberg-evolved observables under unknown quantum channels	26
1. Background	26
a. Useful tricks with the SWAP operator	26
b. Unitary and state designs	27
c. Symmetric subspace	27
2. Construction of the unbiased estimators	29
a. 2-design ensemble	29
b. Tensor-product single qubit stabilizer states	30
c. n -qubit Pauli operator	31
3. Rigorous performance guarantees (Proof of Theorem 4)	32
a. 2-design ensemble	33
b. Tensor-product single-qubit stabilizer states	34
c. n -qubit Pauli operator	36
S4. Cluster simulation of tree-structured quantum circuits	37
1. Technical lemmas	37
2. Proof of Theorem 5	38
3. Proof of Theorem 6	42
4. Proof of Remark 1	47
S5. Exponential separation in the number of cuts compared to conventional wire-cutting methods (Proof of Theorem 7)	49
S6. Relation to existing quantum circuit-cutting methods	52
1. Developing quasiprobability decompositions with smaller sampling overhead	53
2. Reduction of sampling overhead via structure-aware methods	54

We outline the structure of the appendices. In Appendix S1, we provide a brief review of the quasiprobability simulation framework underlying quantum circuit cutting methods. In Appendix S2, we present the proofs of Theorems 1-3 on the rescaling-free wire cut introduced in the main text. In Appendix S3, we first introduce useful tools and concepts for deriving tomography methods for observables evolved under an unknown quantum channel. Using these tools, we formulate learning procedures and provide their rigorous performance guarantees. In Appendix S4, we analyze the sample complexity upper bound of simulating tree-structured quantum circuits on local devices using our learning-based protocols. In Appendix S5, we focus on two-layer tree-structured quantum circuits and perform an information-theoretic analysis that proves an exponential in the number of cuts between our learning-based cluster simulation method and the conventional quasiprobability-based wire-cutting method. In Appendix S6, we discuss the relationship between Theorem 1 and conventional wire-cutting methods.

Appendix S1: Quasiprobability simulation

Quasiprobability simulation provides a general framework for classically reproducing the outcome statistics of a quantum process that cannot be directly implemented, using only the available operations on a given device. This simulation scheme has been extensively employed across a wide range of quantum information and computation tasks, including quantum error mitigation [29, 31, 47], classical simulation of quantum systems [30, 48–50], and quantum

circuit cutting. For instance, in the context of classical simulation of quantum systems, a non-Clifford gate is regarded as the desired operation to be replaced, and it is typically simulated by stabilizer operations.

The key technical idea of the quasiprobability simulation is to express the target operation as a linear combination of implementable ones, referred to as a quasiprobability decomposition (QPD). Suppose that, due to physical limitations or experimental costs, the available set of quantum operations is restricted to a family F , while the desired operation \mathcal{T} lies outside this set. Then, we represent \mathcal{T} as a linear combination of operations $\{\mathcal{E}_i\}_i \subseteq F$:

$$\mathcal{T} = \sum_i a_i \mathcal{E}_i, \quad (\text{S11})$$

where the coefficients a_i are real numbers that may take negative values. Building on this decomposition, quasiprobability simulation effectively reproduces the action of \mathcal{T} by randomly sampling \mathcal{E}_i with the probabilities $|a_i|/\gamma$ and weighting outcomes by $\gamma \text{sgn}(a_i)$, where $\gamma := \sum_i |a_i|$.

To illustrate this idea, let us consider the task of estimating the expectation value of an observable O with $\|O\|_\infty \leq 1$ for the state obtained by applying \mathcal{T} to an initial state ρ . Using Eq. (S11), the desired quantity can be rewritten as

$$\text{tr}[O\mathcal{T}(\rho)] = \sum_i \frac{|a_i|}{\gamma} \gamma \text{sgn}(a_i) \text{tr}[O\mathcal{E}_i(\rho)]. \quad (\text{S12})$$

where $\gamma := \sum_i |a_i|$ and $\text{sgn}(\cdot)$ denotes the sign function. Since $|a_i|/\gamma$ defines a normalized probability over the implementable operations, Eq. (S12) provides a natural Monte-Carlo sampling scheme: for each shot, select an index i according to the probability $|a_i|/\gamma$, apply the corresponding operation \mathcal{E}_i to ρ , measure the observable O , and weight the measurement outcome by $\gamma \text{sgn}(a_i)$. By averaging these weighted outcomes over the total number of shots N , we obtain the desired expectation value $\text{tr}[O\mathcal{T}(\rho)]$.

Appendix S2: Existence of a rescaling-free wire cut

1. Proof of Theorem 1

Theorem 1 (Existence of a rescaling-free wire cut). *Let $\Phi : \mathcal{L}(\mathbb{C}^{d_{\text{in}}}) \rightarrow \mathcal{L}(\mathbb{C}^{d_{\text{out}}})$ be a CPTP map, and let $O \in \mathcal{H}(\mathbb{C}^{d_{\text{out}}})$ be a Hermitian operator. Then there exists a MP channel $\mathcal{M}_{\text{id}} : \mathcal{L}(\mathbb{C}^{d_{\text{in}}}) \rightarrow \mathcal{L}(\mathbb{C}^{d_{\text{in}}})$ such that, for any $X \in \mathcal{L}(\mathbb{C}^{d_{\text{in}}})$,*

$$\text{tr}[O\Phi(X)] = \text{tr}[O\Phi \circ \mathcal{M}_{\text{id}}(X)]. \quad (\text{S21})$$

An explicit construction of \mathcal{M}_{id} is given by

$$\mathcal{M}_{\text{id}}(X) = \sum_j \text{tr}[V|j\rangle\langle j|V^\dagger X] V|j\rangle\langle j|V^\dagger, \quad (\text{S22})$$

where $\{|j\rangle\}$ denotes the computational basis, and V is a unitary that diagonalizes $O_\Phi := \Phi^\dagger(O)$, i.e.,

$$O_\Phi := \Phi^\dagger(O) = VDV^\dagger. \quad (\text{S23})$$

Proof of Theorem 1. Let $D := \sum_j \lambda_j |j\rangle\langle j|$ with the computational basis $\{|j\rangle\}$. By the definition of \mathcal{M}_{id} in Eq. (S22), it is straightforward to see

$$\mathcal{M}_{\text{id}}(O_\Phi) = \sum_j \langle j|V^\dagger O_\Phi V|j\rangle V|j\rangle\langle j|V^\dagger \quad (\text{S24})$$

$$= \sum_j \lambda_j V|j\rangle\langle j|V^\dagger \quad (\text{S25})$$

$$= O_\Phi, \quad (\text{S26})$$

which implies O_Φ is a fixed point of \mathcal{M} . Thus, we have

$$\text{tr}[O\Phi \circ \mathcal{M}_{\text{id}}(X)] = \text{tr}[\mathcal{M}_{\text{id}}^\dagger(O_\Phi)X] \quad (\text{S27})$$

$$= \text{tr}[\mathcal{M}_{\text{id}}(O_\Phi)X] \quad (\text{S28})$$

$$= \text{tr}[O_\Phi X] \quad (\text{S29})$$

$$= \text{tr}[O\Phi(X)]. \quad (\text{S210})$$

Here, the second equality uses the self-adjointness of \mathcal{M}_{id} with respect to the Hilbert-Schmidt inner product, the third equality uses Eq. (S26). This proves Theorem 1. \square

2. Proof of Theorem 2

Theorem 2 (Rescaling-free wire cut with an approximated unitary). *Let $\Phi : \mathcal{L}(\mathbb{C}^{d_{\text{in}}}) \rightarrow \mathcal{L}(\mathbb{C}^{d_{\text{out}}})$ be a CPTP map, and let $O \in \mathcal{H}(\mathbb{C}^{d_{\text{out}}})$ be a Hermitian operator. Denote by $O_\Phi := \Phi^\dagger(O)$ the corresponding effective observable, and let \tilde{O}_Φ be its Hermitian approximation satisfying $\|\tilde{O}_\Phi - O_\Phi\|_\infty \leq \epsilon$. Define the MP channel $\mathcal{M}_{\text{apr}} : \mathcal{L}(\mathbb{C}^{d_{\text{in}}}) \rightarrow \mathcal{L}(\mathbb{C}^{d_{\text{in}}})$ given by*

$$\mathcal{M}_{\text{apr}}(X) := \sum_j \text{tr} \left[\tilde{V} |j\rangle \langle j| \tilde{V}^\dagger X \right] \tilde{V} |j\rangle \langle j| \tilde{V}^\dagger, \quad (\text{S211})$$

where $\{|j\rangle\}$ denotes the computational basis, and \tilde{V} is a unitary that diagonalizes \tilde{O}_Φ (i.e., $\tilde{O}_\Phi = \tilde{V} \tilde{D} \tilde{V}^\dagger$). Then for any $X \in \mathcal{L}(\mathbb{C}^{d_{\text{in}}})$,

$$\left| \text{tr}[O\Phi \circ \mathcal{M}_{\text{apr}}(X)] - \text{tr}[O\Phi(X)] \right| \leq 2\epsilon \|X\|_1. \quad (\text{S212})$$

Proof of Theorem 2. Using the definition of $O_\Phi := \Phi^\dagger(O)$ and the self-adjointness of \mathcal{M}_{apr} , the difference between the expectation value with and without cut can be rewritten as

$$\text{tr}[O\Phi \circ \mathcal{M}_{\text{apr}}(X)] - \text{tr}[O\Phi(X)] = \text{tr}[(\mathcal{M}_{\text{apr}}(O_\Phi) - O_\Phi) X]. \quad (\text{S213})$$

Here, Hölder's inequality, $|\text{tr}[AB]| \leq \|A\|_\infty \|B\|_1$, yields

$$\left| \text{tr}[(\mathcal{M}_{\text{apr}}(O_\Phi) - O_\Phi) X] \right| \leq \|\mathcal{M}_{\text{apr}}(O_\Phi) - O_\Phi\|_\infty \|X\|_1. \quad (\text{S214})$$

Since \tilde{O}_Φ is a fixed point of \mathcal{M}_{apr} , i.e., $\mathcal{M}_{\text{apr}}(\tilde{O}_\Phi) = \tilde{O}_\Phi$, we obtain

$$\mathcal{M}_{\text{apr}}(O_\Phi) - O_\Phi = \mathcal{M}_{\text{apr}}(O_\Phi - \tilde{O}_\Phi) - (O_\Phi - \tilde{O}_\Phi). \quad (\text{S215})$$

With the triangle inequality, the operator norm of this difference can be bounded as

$$\|\mathcal{M}_{\text{apr}}(O_\Phi) - O_\Phi\|_\infty \leq \|\mathcal{M}_{\text{apr}}(O_\Phi - \tilde{O}_\Phi)\|_\infty + \|O_\Phi - \tilde{O}_\Phi\|_\infty \quad (\text{S216})$$

$$\leq 2\|O_\Phi - \tilde{O}_\Phi\|_\infty \quad (\text{S217})$$

$$\leq 2\epsilon, \quad (\text{S218})$$

where the second inequality follows from the contractivity of the MP channel, i.e., $\|\mathcal{M}_{\text{apr}}(A)\|_\infty \leq \|A\|_\infty, \forall A$, which are guaranteed by its construction as a unital pinching map. Substituting this bound into Eq. (S214), we arrive at

$$\left| \text{tr}[O\Phi \circ \mathcal{M}_{\text{apr}}(X)] - \text{tr}[O\Phi(X)] \right| \leq 2\epsilon \|X\|_1, \quad (\text{S219})$$

which completes the proof. \square

3. Proof of Theorem 3

Theorem 3. *Let $\Phi : \mathcal{L}(\mathbb{C}^{d_{\text{in}}}) \rightarrow \mathcal{L}(\mathbb{C}^{d_{\text{out}}})$ be a CPTP map, and let $O \in \mathcal{H}(\mathbb{C}^{d_{\text{out}}})$ be a Hermitian operator. Denote by $O_\Phi := \Phi^\dagger(O)$ the corresponding effective observable, and let \tilde{O}_Φ be its Hermitian approximation satisfying $\|\tilde{O}_\Phi - O_\Phi\|_\infty \leq \epsilon$. Define the classical post-processing function*

$$\mathcal{C}_{\text{apr}}(X) := \sum_j \text{tr} \left[\tilde{V} |j\rangle \langle j| \tilde{V}^\dagger X \right] \tilde{\lambda}_j, \quad (\text{S220})$$

where $\{|j\rangle\}$ denotes the computational basis, \tilde{V} is a unitary that diagonalizes \tilde{O}_Φ (i.e., $\tilde{O}_\Phi = \tilde{V} \tilde{D} \tilde{V}^\dagger$), and $\tilde{D} := \sum_j \tilde{\lambda}_j |j\rangle \langle j|$. Then, for any $X \in \mathcal{L}(\mathbb{C}^{d_{\text{in}}})$,

$$\left| \mathcal{C}_{\text{apr}}(X) - \text{tr}[O\Phi(X)] \right| \leq \epsilon \|X\|_1, \quad (\text{S221})$$

$$\max_j |\tilde{\lambda}_j| \leq \|O\|_\infty + \epsilon. \quad (\text{S222})$$

Proof of Theorem 3. By the definition of \tilde{D} , it is straightforward to rewrite Eq. (S220) as

$$\mathcal{C}_{\text{apr}}(X) = \text{tr}[\tilde{O}_\Phi X]. \quad (\text{S223})$$

Hence, using Hölder's inequality,

$$|\mathcal{C}_{\text{apr}}(X) - \text{tr}[O \Phi(X)]| \leq \|\tilde{O}_\Phi - O_\Phi\|_\infty \|X\|_1 \leq \epsilon \|X\|_1. \quad (\text{S224})$$

For Eq. (S222), since O is Hermitian we have $O \leq \|O\|_\infty I$. Since the adjoint map of the CPTP map is unital and positive, we have

$$\Phi^\dagger(O) \leq \|O\|_\infty \Phi^\dagger(I) = \|O\|_\infty I. \quad (\text{S225})$$

Thus,

$$\max_j |\lambda_j| = \|\tilde{O}_\Phi\|_\infty \quad (\text{S226})$$

$$\leq \|O_\Phi\|_\infty + \|\tilde{O}_\Phi - O_\Phi\|_\infty \quad (\text{S227})$$

$$\leq \|O\|_\infty + \epsilon, \quad (\text{S228})$$

which completes the proof. \square

Appendix S3: Learning Heisenberg-evolved observables under unknown quantum channels

1. Background

a. Useful tricks with the SWAP operator

In the following, we present formulas for the SWAP operator, which will be used, especially, to introduce a protocol for learning local observables; see Sec. IV. We denote by SWAP_n the operator that swaps two copies of an n -qubit system, defined as

$$\text{SWAP}_n := \sum_{i,j \in \{0,1\}^n} |i\rangle\langle j| \otimes |j\rangle\langle i|, \quad (\text{S31})$$

where $\{|i\rangle\}_{i \in \{0,1\}^n}$ denotes the computational basis of \mathbb{C}^d with $d = 2^n$. First, we introduce a well-known decomposition of SWAP_n with the tensor products of two n -qubit Pauli observables.

Lemma 1. *The $2n$ -qubit SWAP operator can be expressed as a uniform sum of tensor products of identical n -qubit Pauli operators:*

$$\text{SWAP}_n = \frac{1}{2^n} \sum_{P \in \{I, X, Y, Z\}^{\otimes n}} P \otimes P. \quad (\text{S32})$$

Proof of Lemma 1. It is straightforward to verify that the two-qubit SWAP operator can be decomposed with the single-qubit Pauli basis as $\text{SWAP}_1 = \sum_{P \in \{I, X, Y, Z\}} P \otimes P$. Since $\text{SWAP}_n = \text{SWAP}_1^{\otimes n}$, Eq. (S32) follows immediately, which complete the proof. \square

Next, we introduce a useful identity known as the (partial) SWAP-trick.

Lemma 2 (Partial-swap-trick). *For all operators $A, B \in \mathcal{L}(\mathbb{C}^d)$ with $d := 2^n$, we have*

$$\text{tr}_1 [\text{SWAP}_n(A \otimes B)] = AB. \quad (\text{S33})$$

Proof of Lemma 2. By definition of SWAP_n in Eq. (S31), it follows that

$$\text{tr}_1 [\text{SWAP}_n(A_1 \otimes B_1)] = \sum_{i,j} \text{tr}_1 [|i\rangle\langle j| \otimes |j\rangle\langle i| (A \otimes B)] = \sum_{i,j} (\langle j|A|i\rangle |j\rangle\langle i|) B = AB. \quad (\text{S34})$$

\square

b. Unitary and state designs

Haar random unitaries and pure states underlie many primitives in various quantum information processing, such as randomized benchmarking [73–76], quantum tomography [55, 56, 59], and quantum cryptography [77–79]. However, the exact implementation of Haar random objects is generally infeasible, since typical unitaries require circuit depth exponential in the number of qubits [80–82]. Fortunately, many applications do not require full Haar randomness: reproducing only the first few statistical moments of the Haar measure often suffices. This motivates the notion of *unitary t -designs* [83–85] and *state t -designs* [86]) (a.k.a., *complex projective t -design* [87] or *spherical t -designs* [88]), which formalize the ensembles that approximate the Haar distribution up to the t -th moment. We briefly recall their definitions below.

Definition 1 (Unitary t -design). A probability distribution $\{p_i, U_i\}$ over $U(\mathbb{C}^d)$ is a *unitary t -design* if and only if, for all $A \in L((\mathbb{C}^d)^{\otimes t})$,

$$\sum_i p_i U_i^{\otimes t} A(U_i^\dagger)^{\otimes t} = \int_{U(\mathbb{C}^d)} d\mu_H U_i^{\otimes t} A(U_i^\dagger)^{\otimes t}, \quad (\text{S35})$$

where $d\mu_H$ denotes the normalized Haar measure on $U(\mathbb{C}^d)$.

Definition 2 (State t -design). A probability distribution $\{p_i, |\psi_i\rangle\}$ over pure states in \mathbb{C}^d is a *state t -design* (or *complex projective t -design*) if and only if

$$\sum_i p_i (|\psi_i\rangle \langle \psi_i|)^{\otimes t} = \int_{\phi} d\phi (|\phi\rangle \langle \phi|)^{\otimes t}, \quad (\text{S36})$$

where the integral is taken with respect to the normalized Haar measure on the unit sphere of \mathbb{C}^d .

Our randomized protocol discussed in Sec. IV B requires ensembles that form a unitary or state 2-design. A representative example is given by the uniform distribution over the n -qubit Clifford group $Cl(2^n)$ [89], which is known to form a unitary 3-design [90–92] but not a 4-design [93]. The n -qubit Clifford circuits have been extensively studied, and importantly, they are considered to be particularly suitable for implementation for the following two reasons: (i) there exist efficient algorithms for uniform sampling from $Cl(2^n)$ [94, 95] and (ii) Clifford circuits can be implemented with at most $\mathcal{O}(n^2/\log n)$ elementary gates (CNOT, Hadamard, and phase gates) [96].

Other prominent examples of state ensembles forming a 2-design are provided by mutually unbiased bases (MUBs) [97–100] and symmetric informationally complete positive operator-valued measures (SIC-POVMs) [101]. Here, we focus on MUBs in particular, which are defined as follows.

Definition 3 (Mutually unbiased bases). Let $\{\mathcal{B}_k\}_{k=1}^m$ be orthonormal bases of \mathbb{C}^d , where $\mathcal{B}_k = \{|\phi_i^{(k)}\rangle\}_{i=1}^d$. The bases are said to be mutually unbiased if and only if, for all $k \neq k'$ and all $i, j \in \{1, \dots, d\}$,

$$|\langle \phi_i^{(k)} | \phi_j^{(k')} \rangle|^2 = \frac{1}{d}. \quad (\text{S37})$$

A set of MUBs is called *maximal* if $m = d + 1$. In prime-power dimensions, including $d = 2^n$, the maximal sets of $d + 1$ MUBs exists [97, 102], and the uniform distribution over $\bigcup_{k=1}^{d+1} \mathcal{B}_k$ constitutes a state 2-design [103]. For qubits ($d = 2^n$), there are efficient constructions of circuits that prepare MUB states or implement the corresponding unitaries, e.g., methods via the stabilizer formalism [100, 104]. A practical advantage of MUBs is the compactness of the ensemble that involves only $2^n + 1$ states, in stark contrast to sampling from the n -qubit Clifford group, whose size is $2^{n^2+2n} \prod_{j=1}^n (4^j - 1)$. This compactness helps reduce classical overhead, especially in scenarios where many random samples are required (e.g., when the number of required random circuits is on the order of 2^n or larger) [21, 105, 106]. For example, if n is relatively small, one can make the lookup tables for the associated state-preparation circuits and reuse them during the sampling stage [21].

c. Symmetric subspace

To derive our randomized protocols in Sec. IV B, we need to employ moment calculations with respect to Haar random states. To provide the necessary tools for such calculations (Appendices S32 and S33), we here present a brief review of the symmetric subspace. For further details, see Refs. [107, 108].

Definition 4 (Permutation operator). Let S_k denote the symmetric group on k elements. For any $\pi \in S_k$, define the permutation operator $P_d(\pi)$ on the k -fold tensor product $(\mathbb{C}^d)^{\otimes k}$ by

$$P_d(\pi) |\psi_1\rangle \otimes \cdots \otimes |\psi_k\rangle = |\psi_{\pi^{-1}(1)}\rangle \otimes \cdots \otimes |\psi_{\pi^{-1}(k)}\rangle, \quad (\text{S38})$$

for all $|\psi_1\rangle, \dots, |\psi_k\rangle \in \mathbb{C}^d$. Equivalently, it can be expressed as

$$P_d(\pi) = \sum_{i_1, \dots, i_k \in [d]} |i_{\pi^{-1}(1)}, \dots, i_{\pi^{-1}(k)}\rangle \langle i_1, \dots, i_k|. \quad (\text{S39})$$

Definition 5 (Symmetric subspace). The symmetric subspace of $(\mathbb{C}^d)^{\otimes k}$, denoted by $\vee^k \mathbb{C}^d$, is defined as

$$\vee^k \mathbb{C}^d := \{|\psi\rangle \in (\mathbb{C}^d)^{\otimes k} : P_d(\pi) |\psi\rangle = |\psi\rangle \text{ for all } \pi \in S_k\}. \quad (\text{S310})$$

We now present two fundamental facts about the symmetric subspace: the orthogonal projector and its dimension. We omit the proofs of these results here, but the detailed arguments can be found in Refs. [107, 108].

Fact 1 (Orthogonal projector onto $\vee^k \mathbb{C}^d$). Define

$$P_{\text{sym}}^{d,k} := \frac{1}{k!} \sum_{\pi \in S_k} P_d(\pi). \quad (\text{S311})$$

Then, $P_{\text{sym}}^{d,k}$ is the orthogonal projector onto $\vee^k \mathbb{C}^d$.

Fact 2 (Dimension of $\vee^k \mathbb{C}^d$).

$$\dim(\vee^k \mathbb{C}^d) = \text{tr}(P_{\text{sym}}^{d,k}) = \binom{d+k-1}{k}. \quad (\text{S312})$$

We conclude this subsection by introducing a useful identity that will be employed in the subsequent analysis. Define the tensor product state

$$\rho_{k\text{-sym}} := \int_{\phi} d\phi (|\phi\rangle \langle \phi|)^{\otimes k}, \quad (\text{S313})$$

where the integral is taken over the pure states $|\phi\rangle \in \mathbb{C}^d$ from the Haar measure. By unitary invariance, it follows that $\rho_{k\text{-sym}}$ commutes with $U^{\otimes k}$ for any unitary U . Moreover, it is known that $\vee^k \mathbb{C}^d$ affords the irreducible representation arising from the action $U \mapsto U^{\otimes k}$. Therefore, by Schur's lemma, $\rho_{k\text{-sym}}$ is proportional to the orthogonal projection onto the symmetric subspace. Combining this with Facts 1 and 2, we obtain the following characterization of tensor powers of Haar-random pure states.

Lemma 3. Let $d\phi$ denote the normalized Haar measure on pure states of \mathbb{C}^d . For any $k \in \mathbb{N}$,

$$\int d\phi (|\phi\rangle \langle \phi|)^{\otimes k} = \frac{P_{\text{sym}}^{d,k}}{\text{tr}(P_{\text{sym}}^{d,k})} \quad (\text{S314})$$

$$= \frac{1}{d(d+1)\cdots(d+k-1)} \sum_{\pi \in S_k} P_d(\pi). \quad (\text{S315})$$

This lemma is useful for deriving closed-form expressions for randomized protocol schemes and for evaluating their efficiency. In our calculations in Appendices S3.2 and S3.3, we frequently use the cases $k = 1$ and $k = 2$, so we present the corresponding formulas explicitly below.

Corollary 1. Let $d\phi$ denote the normalized Haar measure on pure states of \mathbb{C}^d with $d := 2^n$. Then,

$$\int d\phi (|\phi\rangle \langle \phi|) = \frac{I_d}{d}, \quad (\text{S316})$$

$$\int d\phi (|\phi\rangle \langle \phi|)^{\otimes 2} = \frac{1}{d(d+1)} (I_{d^2} + \text{SWAP}_n). \quad (\text{S317})$$

2. Construction of the unbiased estimators

In this section, we explain how we derive the unbiased estimators introduced in Sec. IV B. To obtain \hat{O}_Φ satisfying $\|\hat{O}_\Phi - O_\Phi\|_\infty \leq \epsilon$, we need to collect informative data from the measurements of the circuit composed of an unknown CPTP map $\Phi : \mathcal{L}(\mathbb{C}^{d_{\text{in}}}) \rightarrow \mathcal{L}(\mathbb{C}^{d_{\text{out}}})$ and a known Hermitian operator $O \in \mathcal{H}(\mathbb{C}^{d_{\text{out}}})$, probed with an appropriately chosen ensemble of input states $\mathcal{S} := \{(p_i, |\psi_i\rangle\langle\psi_i|)\}$. We thus consider the following randomized protocol, which performs measurements on random inputs and stores the corresponding data:

Step 1 (Random sampling): Sample a state $|\psi_i\rangle\langle\psi_i|$ according to the probability distribution p_i .

Step 2 (Measurement): Prepare the corresponding quantum state $|\psi_i\rangle\langle\psi_i|$, evolve it under the CPTP map Φ , and measure with the observable O (i.e., apply a unitary rotation W^\dagger immediately before measurement in the computational basis $\{|j\rangle\}$). Denote the measurement outcome by j

Step 3 (Data storage): Store the weighted state $\nu_j |\psi_i\rangle\langle\psi_i|$ in classical memory.

For the above process (**Step 1-3**), we define the mapping $\mathcal{M} : \mathcal{H}(\mathbb{C}^{d_{\text{in}}}) \rightarrow \mathcal{H}(\mathbb{C}^{d_{\text{in}}})$ from O_Φ to its classical description $\mathbb{E}_{i,j}[\nu_j |\psi_i\rangle\langle\psi_i|]$ that average over the choice of quantum states and measurement outcomes. Explicitly,

$$\begin{aligned} \mathcal{M}(O_\Phi) &= \sum_i p_i \sum_j \text{tr} [|j\rangle\langle j| W^\dagger \Phi(|\psi_i\rangle\langle\psi_i|) W] \nu_j |\psi_i\rangle\langle\psi_i| \\ &= \sum_i p_i \text{tr} [O_\Phi |\psi_i\rangle\langle\psi_i|] |\psi_i\rangle\langle\psi_i|. \end{aligned} \quad (\text{S318})$$

By choosing the ensemble \mathcal{S} appropriately, the map \mathcal{M} can be made to carry substantial information about O_Φ . Representative examples of such a choice of \mathcal{S} are an ensemble forming a 2-design or the tensor product of single-qubit stabilizer states. In Appendices S3 2 a and S3 2 b, we provide detailed discussions of these two cases, respectively. Moreover, by introducing an additional weighting in Step 3, we can also formulate a protocol based on Pauli operators. This is discussed in detail in Appendix S3 2 c.

a. 2-design ensemble

Let $\mathcal{S}_{2\text{-dgn}} = \{(p_i, |\psi_i\rangle\langle\psi_i|)\}$ be an ensemble forming a state 2-design. By definition,

$$\sum_i p_i (|\psi_i\rangle\langle\psi_i|)^{\otimes 2} = \int_{\phi} (|\phi\rangle\langle\phi|)^{\otimes 2} d\phi, \quad (\text{S319})$$

where the integral is over pure states with respect to the Haar measure; see Definition 2. A standard result states that the Haar integral in Eq. (S319) yields an operator $P_{\text{sym}}^{d_{\text{in}},2}$ proportional to the projector onto the symmetric subspace (see Corollary 1), namely,

$$\sum_i p_i (|\psi_i\rangle\langle\psi_i|)^{\otimes 2} = \frac{P_{\text{sym}}^{d_{\text{in}},2}}{\binom{d_{\text{in}}+1}{2}} = \frac{1}{d_{\text{in}}(d_{\text{in}}+1)} \left(\text{SWAP}_n + I_{d_{\text{in}}^2} \right), \quad (\text{S320})$$

where $I_{d_{\text{in}}^2}$ is the identity on the two-copy space, and SWAP_n is the swap operator. Substituting Eq. (S320) in Eq. (S318), the map \mathcal{M} acting on an operator O_Φ can be rewritten as

$$\mathcal{M}(O_\Phi) = \sum_i p_i \text{tr}_1 [(O_\Phi \otimes I_{d_{\text{in}}})(|\psi_i\rangle\langle\psi_i|)^{\otimes 2}] \quad (\text{S321})$$

$$= \frac{1}{d_{\text{in}}(d_{\text{in}}+1)} \text{tr}_1 [(O_\Phi \otimes I_{d_{\text{in}}})(\text{SWAP}_n + I_{d_{\text{in}}^2})] \quad (\text{S322})$$

$$= \frac{1}{d_{\text{in}}(d_{\text{in}}+1)} (O_\Phi + \text{tr}(O_\Phi) I_{d_{\text{in}}}). \quad (\text{S323})$$

This expression shows that the randomized map \mathcal{M} carries substantial information about the target operator O_Φ , in the form of both the trace and operator content. From Eq. (S323), the information about O_Φ can be recovered by applying the classical post-processing to the output

$$\mathcal{M}(O_\Phi) \rightarrow d_{\text{in}}(d_{\text{in}}+1) \mathcal{M}(O_\Phi) - \text{tr}(O_\Phi) I_{d_{\text{in}}}. \quad (\text{S324})$$

Here, noting that the following equality holds

$$\mathrm{tr}(O_\Phi)I_{d_{\mathrm{in}}} = \sum_i p_i \sum_j \nu_j \mathrm{tr} [|j\rangle \langle j| W^\dagger \Phi(|\psi_i\rangle \langle \psi_i|) W] \times d_{\mathrm{in}} I_{d_{\mathrm{in}}}, \quad (\mathrm{S325})$$

the above equality together with Eq. (S318) readily implies that

$$O_\Phi = \sum_i p_i \sum_j \mathrm{tr} [|j\rangle \langle j| W^\dagger \Phi(|\psi_i\rangle \langle \psi_i|) W] \nu_j (d_{\mathrm{in}}(d_{\mathrm{in}} + 1) |\psi_i\rangle \langle \psi_i| - d_{\mathrm{in}} I_{d_{\mathrm{in}}}). \quad (\mathrm{S326})$$

Thus, we can reconstruct the classical description of O_Φ in practice, by modifying **Step 3** as follows.

For $k = 1, \dots, N$, we sample an input $|\psi_i\rangle$ with the probability p_i , evolve it under Φ , perform the measurement in the basis $\{W|j\rangle\}$, obtain the outcome j (**Step 1** and **Step 2**), and store the single-shot estimator as

$$\hat{\omega}_{2-\mathrm{dgn}}^{(k)} := \nu_{j_k} (d_{\mathrm{in}}(d_{\mathrm{in}} + 1) |\psi_{i_k}\rangle \langle \psi_{i_k}| - d_{\mathrm{in}} I_{d_{\mathrm{in}}}). \quad (\mathrm{S327})$$

Then, by averaging the data as

$$\hat{O}_{\Phi,2-\mathrm{dgn}} := \frac{1}{N} \sum_{k=1}^N \hat{\omega}_{2-\mathrm{dgn}}^{(k)} \quad (\mathrm{S328})$$

$$= \frac{1}{N} \sum_{k=1}^N \nu_{j_k} (d_{\mathrm{in}}(d_{\mathrm{in}} + 1) |\psi_{i_k}\rangle \langle \psi_{i_k}| - d_{\mathrm{in}} I_{d_{\mathrm{in}}}), \quad (\mathrm{S329})$$

we obtain an unbiased estimator of O_Φ , i.e., $\mathbb{E}[\hat{O}_{\Phi,2-\mathrm{dgn}}] = O_\Phi$.

Finally, we provide some supplementary explanations regarding the above protocol. First, in the above discussion, the estimator \hat{O}_Φ was obtained by modifying the map \mathcal{M} , as demonstrated in Eq. (S324), so that only the terms of O_Φ appearing in the expansion (S323) of $\mathcal{M}(O_\Phi)$ are extracted. The resulting estimator corresponds to a linear inversion estimator for O_Φ , where the linear inversion technique is sometimes employed in quantum state/measurement tomography [55, 56] and classical shadow tomography [59].

b. Tensor-product single qubit stabilizer states

We focus on the case where the input ensemble $\mathcal{S}_{\mathrm{stab}}$ is chosen as the set of all n -fold tensor products of the single-qubit stabilizer states

$$\mathcal{Q}_{\mathrm{stab}} := \{|0\rangle, |1\rangle, |+\rangle, |-\rangle, |+i\rangle, |-i\rangle\}, \quad (\mathrm{S330})$$

sampled uniformly with probability $p_i = 1/6^n$. Formally,

$$\mathcal{S}_{\mathrm{stab}} := \left\{ \left(\frac{1}{6^n}, \bigotimes_{s=1}^n |u^s\rangle \right) : |u^s\rangle \in \mathcal{Q}_{\mathrm{stab}} \right\}. \quad (\mathrm{S331})$$

Before turning to general n , it is convenient to verify the single-qubit case ($n = 1$). Let

$$\mathcal{Q}_x = \{|\pm\rangle\}, \quad \mathcal{Q}_y = \{|\pm i\rangle\}, \quad \mathcal{Q}_z = \{|0\rangle, |1\rangle\}, \quad (\mathrm{S332})$$

the eigenstate sets of the Pauli operators X, Y, Z, respectively, and define $\mathcal{Q}_{\mathrm{stab}} := \mathcal{Q}_x \cup \mathcal{Q}_y \cup \mathcal{Q}_z$. The three bases $\mathcal{Q}_x, \mathcal{Q}_y, \mathcal{Q}_z$ form a maximal set of mutually unbiased bases (MUBs) in dimension $d_{\mathrm{in}} = 2$, and the uniform ensemble over $\mathcal{Q}_{\mathrm{stab}}$ is shown to be a complex-projective 2-design [103]. Equivalently,

$$\frac{1}{6} \sum_{|u\rangle \in \mathcal{Q}_{\mathrm{stab}}} (|u\rangle \langle u|)^{\otimes 2} = \frac{1}{6} (\mathrm{SWAP} + I). \quad (\mathrm{S333})$$

Using Eq. (S333) (equivalently, inserting $d_{\mathrm{in}} = 2$ into Eq. (S326)), we obtain

$$\sum_{|u\rangle \in \mathcal{Q}_{\mathrm{stab}}} \frac{1}{6} \mathrm{tr}[A|u\rangle \langle u|] (6|u\rangle \langle u| - 2I) = A, \quad \forall A \in \mathsf{H}(\mathbb{C}^2). \quad (\mathrm{S334})$$

We now extend the discussion above to the multiple-qubit case. Taking the n -fold tensor products of both sides of Eq. (S334), for any product operator $A = \bigotimes_{s=1}^n A^s$ with $A^s \in \mathbb{H}(\mathbb{C}^2)$, we have

$$\bigotimes_{s=1}^n \sum_{|u^s\rangle \in \mathcal{Q}_{\text{stab}}} \frac{1}{6} \text{tr}[A^s |u^s\rangle \langle u^s|] (6|u^s\rangle \langle u^s| - 2I) = \sum_{\substack{|u^1\rangle, \dots, |u^n\rangle \\ \in \mathcal{Q}_{\text{stab}}}} \frac{1}{6^n} \prod_{s=1}^n \text{tr}[A^s |u^s\rangle \langle u^s|] \bigotimes_{s=1}^n (6|u^s\rangle \langle u^s| - 2I). \quad (\text{S335})$$

Using $\prod_{s=1}^n \text{tr}[A^s |u^s\rangle \langle u^s|] = \text{tr}[A |u\rangle \langle u|]$ for $|u\rangle := |u^1 u^2 \dots u^n\rangle$, we can rewrite this as

$$A = \sum_{|u\rangle \in \mathcal{Q}_{\text{stab}}^{\otimes n}} \frac{1}{6^n} \text{tr}[A |u\rangle \langle u|] \bigotimes_{s=1}^n (6|u^s\rangle \langle u^s| - 2I). \quad (\text{S336})$$

By linearity, Eq. (S336) also holds for any $A \in \mathbb{H}(\mathbb{C}^{2^n})$. Hence, for the uniform product-stabilizer ensemble $\mathcal{S}_{\text{stab}}$, we can express

$$O_\Phi = \sum_{|u\rangle \in \mathcal{Q}_{\text{stab}}^{\otimes n}} \frac{1}{6^n} \sum_j \text{tr}[|j\rangle \langle j| W^\dagger \Phi(|u\rangle \langle u|) W] \nu_j \bigotimes_{s=1}^n (6|u^s\rangle \langle u^s| - 2I). \quad (\text{S337})$$

Thus, to obtain the classical description of O_Φ in this case, we repeat the following randomized protocol independently for $k = 1, \dots, N$. At the k -th round, we sample inputs $|u_k\rangle \in \mathcal{Q}_{\text{stab}}^{\otimes n}$ uniformly, applies Φ , measuring in the basis $\{W|j\rangle\}$ and obtaining outcome j_k , and records the single-shot estimator

$$\hat{\omega}_{\text{stab}}^{(k)} := \nu_{j_k} \bigotimes_{s=1}^n (6|u_k^s\rangle \langle u_k^s| - 2I). \quad (\text{S338})$$

Finally, the empirical estimator is obtained as the sample average

$$\hat{O}_{\Phi, \text{stab}} := \frac{1}{N} \sum_{k=1}^N \hat{\omega}_{\text{stab}}^{(k)} \quad (\text{S339})$$

$$= \frac{1}{N} \sum_{k=1}^N \nu_{j_k} \bigotimes_{s=1}^n (6|u_k^s\rangle \langle u_k^s| - 2I). \quad (\text{S340})$$

By construction and Eq. (S337), this is an unbiased estimator of O_Φ .

c. n -qubit Pauli operator

To make the discussion self-contained, we recall the definitions of the single-qubit Pauli operators and their eigenvalue decompositions in the main text:

$$P_i = \sum_{e \in [2]} c_{i,e} |v_{i,e}\rangle \langle v_{i,e}|, \quad i \in \{1, 2, 3, 4\} = [4], \quad (\text{S341})$$

where P_1, P_2, P_3 , and P_4 correspond to the identity and the Pauli operators X, Y, and Z, respectively. The eigenstates and their associated eigenvalues are summarized as

$$\begin{aligned} |v_{1,1}\rangle &= |0\rangle, & c_{1,1} &= +1, & |v_{1,2}\rangle &= |1\rangle, & c_{1,2} &= +1, \\ |v_{2,1}\rangle &= |+\rangle, & c_{2,1} &= +1, & |v_{2,2}\rangle &= |-\rangle, & c_{2,2} &= -1, \\ |v_{3,1}\rangle &= |+i\rangle, & c_{3,1} &= +1, & |v_{3,2}\rangle &= |-i\rangle, & c_{3,2} &= -1, \\ |v_{4,1}\rangle &= |0\rangle, & c_{4,1} &= +1, & |v_{4,2}\rangle &= |1\rangle, & c_{4,2} &= -1. \end{aligned} \quad (\text{S342})$$

Building upon these single-qubit definitions, we can naturally extend them to the n -qubit setting by defining the Pauli ensemble

$$\mathcal{S}_{\text{Paulis}} := \left\{ \left(\frac{1}{4^n}, P_i := \bigotimes_{s=1}^n P_{i_s} \right) : i \in [4]^n \right\}, \quad (\text{S343})$$

where $\mathbf{i} = (i_1, \dots, i_n)$. Each operator in this ensemble can be expressed via its eigenvalue decomposition as

$$P_{\mathbf{i}} = \sum_{\mathbf{e} \in [2]^n} c_{\mathbf{i}, \mathbf{e}} |v_{\mathbf{i}, \mathbf{e}}\rangle \langle v_{\mathbf{i}, \mathbf{e}}|, \quad c_{\mathbf{i}, \mathbf{e}} := \prod_{s=1}^n c_{i_s, e_s}, \quad |v_{\mathbf{i}, \mathbf{e}}\rangle := \bigotimes_{s=1}^n |v_{i_s, e_s}\rangle. \quad (\text{S344})$$

With these definitions, we can describe the sampling process as follows: for each trial, a Pauli operator $P_{\mathbf{i}}$ is drawn uniformly at random from $\mathcal{S}_{\text{Pauli}}$, and one of its eigenstates $|v_{\mathbf{i}, \mathbf{e}}\rangle$ is selected uniformly to serve as the probe state.

1. **Random sampling:** Sample a Pauli operator and its eigenstates $(P_{\mathbf{i}}, |v_{\mathbf{i}, \mathbf{e}}\rangle)$ uniformly at random.
2. **Measurement:** Prepare the corresponding quantum state $|v_{\mathbf{i}, \mathbf{e}}\rangle$, evolve it under the map Φ , and measure with the observable O . Denote the measurement outcome by j .
3. **Data storage:** Store the weighted Pauli operator $\nu_j c_{\mathbf{i}, \mathbf{e}} P_{\mathbf{i}}$ in classical memory.

As in the previous discussions, we show that the output of this procedure contains a large amount of information of O_{Φ} in expectation. To this end, we define the mapping $\mathcal{M} : \mathbb{H}(\mathbb{C}^{d_{\text{in}}}) \rightarrow \mathbb{H}(\mathbb{C}^{d_{\text{in}}})$, which map the observable O_{Φ} to its classical description $\mathbb{E}_{\mathbf{i}, \mathbf{j}, \mathbf{e}}[\nu_j c_{\mathbf{i}, \mathbf{e}} P_{\mathbf{i}}]$, obtained by averaging over the labels (\mathbf{i}, \mathbf{e}) and measurement outcomes j . Explicitly,

$$\mathcal{M}(O_{\Phi}) = \sum_{\mathbf{i} \in [4]^n, \mathbf{e} \in [2]^n} \frac{1}{8^n} \sum_j \text{tr} [|j\rangle \langle j| W^{\dagger} \Phi(|v_{\mathbf{i}, \mathbf{e}}\rangle \langle v_{\mathbf{i}, \mathbf{e}}|) W] \nu_j c_{\mathbf{i}, \mathbf{e}} P_{\mathbf{i}} \quad (\text{S345})$$

$$= \sum_{\mathbf{i} \in [4]^n} \frac{1}{8^n} \text{tr}[O_{\Phi} P_{\mathbf{i}}] P_{\mathbf{i}}, \quad (\text{S346})$$

where we have used the eigenvalue decomposition of O_{Φ} and $P_{\mathbf{i}}$ in Eqs. (23) and (S344), respectively. Here, the decomposition formula of swap operators in Lemma 1 enables a further simplification of the above equality as

$$\mathcal{M}(O_{\Phi}) = \frac{1}{4^n} O_{\Phi} \left(= \frac{1}{4^n} \text{tr}_1 \left[(O_{\Phi} \otimes I) \left(\frac{1}{2^n} \sum_{\mathbf{i} \in [4]^n} P_{\mathbf{i}} \otimes P_{\mathbf{i}} \right) \right] \right). \quad (\text{S347})$$

Hence, to obtain the classical description of O_{Φ} , we repeat the following randomized protocol independently for $k = 1, \dots, N$. At the k -th round, we uniformly sample the labels of a Pauli operator and its eigenstate $(\mathbf{i}_k, \mathbf{e}_k)$, prepare the input state $|v_{\mathbf{i}_k, \mathbf{e}_k}\rangle$, apply Φ , rotate the state by W , measure in the computational basis $\{|j\rangle\}$, obtain outcome j_k , and records the single-shot estimator as

$$\hat{\omega}_{\text{pauli}}^{(k)} := 4^n \nu_{j_k} c_{\mathbf{i}_k, \mathbf{e}_k} P_{\mathbf{i}_k} \quad (\text{S348})$$

in classical memory. Finally, the empirical estimator is obtained as the sample average

$$\hat{O}_{\Phi, \text{pauli}} := \frac{1}{N} \sum_{k=1}^N \hat{\omega}_{\text{pauli}}^{(k)} \quad (\text{S349})$$

$$= \frac{1}{N} \sum_{k=1}^N 4^n \nu_{j_k} c_{\mathbf{i}_k, \mathbf{e}_k} P_{\mathbf{i}_k}. \quad (\text{S350})$$

By construction and Eq. (S347), this is an unbiased estimator of O_{Φ} .

3. Rigorous performance guarantees (Proof of Theorem 4)

In the main text, we provide the following performance guarantee for the estimator $\hat{O}_{\Phi, x}$ with each $x \in \{2\text{-dgn, stab, pauli}\}$.

Theorem 4 (Performance guarantee for $\hat{O}_{\Phi, x}$). *Let $\Phi : \mathbb{L}(\mathbb{C}^{d_{\text{in}}}) \rightarrow \mathbb{L}(\mathbb{C}^{d_{\text{out}}})$ be an unknown CPTP map, and let $O \in \mathbb{H}(\mathbb{C}^{d_{\text{out}}})$ be a known Hermitian operator. Denote by $O_{\Phi} := \Phi^{\dagger}(O)$ the corresponding effective observable. Fix a probability distribution over sets of quantum states or Pauli operators associated with $x \in \{2\text{-dgn, stab, pauli}\}$.*

Then the following number of iterations suffices to ensure that the learning protocol defined in Sec. IV B produces an estimate $\hat{O}_{\Phi,x}$ satisfying $\|\hat{O}_{\Phi,x} - O_\Phi\|_\infty \leq \epsilon$ with probability at least $1 - \delta$, for any $\epsilon > 0$:

$$\begin{aligned} [2\text{-dgn}] \quad & \frac{2 \max\{1, \|O\|_\infty^2\} (d_{\text{in}}^2 + 1) (d_{\text{in}} + 1 + \epsilon/3)}{\epsilon^2} \ln\left(\frac{d_{\text{in}}}{\delta}\right), \\ [\text{stab}] \quad & \frac{2 \max\{1, \|O\|_\infty^2\} (d_{\text{in}}^{3.33} + (\epsilon/3)(d_{\text{in}}^2 + 1))}{\epsilon^2} \ln\left(\frac{d_{\text{in}}}{\delta}\right), \\ [\text{pauli}] \quad & \frac{2 \max\{1, \|O\|_\infty^2\} (d_{\text{in}}^4 + 1 + (\epsilon/3)(d_{\text{in}}^2 + 1))}{\epsilon^2} \ln\left(\frac{d_{\text{in}}}{\delta}\right). \end{aligned}$$

In the following subsections, we provide the proof of Theorem 4 for each $x \in \{2\text{-dgn, stab, pauli}\}$. Now, we outline the basic proof strategy below. For each choice of x , the estimator $\hat{O}_{\Phi,x}$ of O_Φ , generated by the algorithm described in Sec. IV is obtained as the average of independently sampled random operators $\hat{\omega}_x^{(k)}$; see Sec. IV B or Appendix S3.2. Since $\hat{\omega}_x^{(k)}$ is an unbiased estimator of O_Φ , for each $k \in [N]$,

$$X^{(k)} = \frac{1}{N} (\hat{\omega}_x^{(k)} - O_\Phi), \quad (\text{S351})$$

is the centered random matrices which satisfy $\mathbb{E}[X^{(k)}] = 0$. Moreover, each $X^{(k)}$ is independent, random, self-adjoint, and bounded as

$$\|X^{(k)}\|_\infty = \frac{1}{N} \|\hat{\omega}_x^{(k)} - O_\Phi\|_\infty \quad (\text{S352})$$

$$\leq \frac{1}{N} \left\{ \|\hat{\omega}_x^{(k)}\|_\infty + \|O_\Phi\|_\infty \right\}. \quad (\text{S353})$$

Then, for such independent random matrices, to analyze the deviation $\hat{O}_{\Phi,x} - O_\Phi = \sum_{k=1}^N X^{(k)}$, we employ the matrix extension of Bernstein's inequality developed independently in Refs. [109, 110].

Lemma 4 (Matrix Bernstein inequality: Hermitian case [57]). *Consider a finite sequence $X^{(1)}, \dots, X^{(N)}$ of independent, random, Hermitian matrices with dimension d . Assume that each random matrix satisfies $\mathbb{E}[X^{(k)}] = 0$ and $\|X^{(k)}\|_\infty \leq \alpha$ almost surely for all k . Then, for all $\epsilon \geq 0$,*

$$\Pr \left[\left\| \sum_{k=1}^N X^{(k)} \right\|_\infty \geq \epsilon \right] \leq d \exp \left(\frac{-\epsilon^2/2}{\sigma^2 + \alpha\epsilon/3} \right) \quad (\text{S354})$$

where $\sigma^2 = \|\sum_{k=1}^N \mathbb{E}[(X^{(k)})^2]\|_\infty$.

Hence, we complete the proof of Theorem 4 by evaluating α and σ^2 for each choice of x .

a. 2-design ensemble

Proof. The algorithm described in Sec. IV B produces an estimator of observable O_Φ as

$$\hat{O}_{\Phi,2\text{-dgn}} := \frac{1}{N} \sum_{k=1}^N \hat{\omega}_{2\text{-dgn}}^{(k)} \quad (\text{S355})$$

$$= \frac{1}{N} \sum_{k=1}^N \nu_{j_k} (d_{\text{in}}(d_{\text{in}} + 1) |\psi_{i_k}\rangle \langle \psi_{i_k}| - d_{\text{in}} I_{d_{\text{in}}}), \quad (\text{S356})$$

where each $\hat{\omega}_{2\text{-dgn}}^{(k)}$ is an i.i.d. copy of a random matrix $\omega_{2\text{-dgn}} \in \mathsf{H}(\mathbb{C}^{d_{\text{in}}})$ taking the value

$$\nu_j (d_{\text{in}}(d_{\text{in}} + 1) |\psi_i\rangle \langle \psi_i| - d_{\text{in}} I_{d_{\text{in}}}) \quad (\text{S357})$$

with probability $p_i \langle j | W^\dagger \Phi(|\psi_i\rangle \langle \psi_i|) W | j \rangle$ for all $k \in \{1, \dots, N\}$. Since the estimator is unbiased, i.e., $\mathbb{E}[\hat{O}_\Phi] = O_\Phi$, the deviation $\hat{O}_{\Phi,2\text{-dgn}} - O_\Phi$ can be written as a sum of N independent, centered random matrices of the form $X_{2\text{-dgn}}^{(k)} := (\omega_{2\text{-dgn}}^{(k)} - O_\Phi)/N$. These matrices obey

$$\frac{1}{N} \|X_{2\text{-dgn}}^{(k)}\|_\infty \leq \frac{1}{N} \left\{ \|\omega_{2\text{-dgn}}^{(k)}\|_\infty + \|O_\Phi\|_\infty \right\} \quad (\text{S358})$$

$$\leq \frac{1}{N} \left\{ \max_{|\psi_i\rangle, \nu_j} |\nu_j| \|d_{\text{in}}(d_{\text{in}} + 1) |\psi_i\rangle \langle \psi_i| - d_{\text{in}} I_{d_{\text{in}}} \|_{\infty} + \|O_{\Phi}\|_{\infty} \right\} \quad (\text{S359})$$

$$\leq \frac{(d_{\text{in}}^2 + 1) \|O\|_{\infty}}{N} := \alpha. \quad (\text{S360})$$

where the last inequality follows from the fact that Φ is CPTP, which implies that $\Phi^{\dagger}(I_{d_{\text{in}}}) \leq I_{d_{\text{in}}}$, and from the bound $O \leq \|O\|_{\infty} I$. Also, the random matrix $\omega_{2\text{-dgn}}$ obeys

$$\mathbb{E}[(\omega_{2\text{-dgn}} - \mathbb{E}[\omega_{2\text{-dgn}}])^2] = \mathbb{E}[\omega_{2\text{-dgn}}^2] - (\mathbb{E}[\omega_{2\text{-dgn}}])^2 \quad (\text{S361})$$

$$= \mathbb{E}[\omega_{2\text{-dgn}}^2] - O_{\Phi}^2 \quad (\text{S362})$$

and we have

$$\mathbb{E}[\omega_{2\text{-dgn}}^2] = \sum_i p_i \sum_j \text{tr} [|j\rangle \langle j| W^{\dagger} \Phi(|\psi_i\rangle \langle \psi_i|) W] \nu_j^2 (d_{\text{in}}(d_{\text{in}} + 1) |\psi_i\rangle \langle \psi_i| - d_{\text{in}} I_{d_{\text{in}}})^2 \quad (\text{S363})$$

$$= \sum_i p_i \sum_j \text{tr} [\Phi^{\dagger}(O^2) |\psi_i\rangle \langle \psi_i|] (d_{\text{in}}^2(d_{\text{in}}^2 - 1) |\psi_i\rangle \langle \psi_i| + d_{\text{in}}^2 I_{d_{\text{in}}}) \quad (\text{S364})$$

$$= d_{\text{in}}^2(d_{\text{in}}^2 - 1) \sum_i p_i \sum_j \text{tr} [\Phi^{\dagger}(O^2) |\psi_i\rangle \langle \psi_i|] |\psi_i\rangle \langle \psi_i| + d_{\text{in}}^2 \sum_i p_i \text{tr} [\Phi^{\dagger}(O^2) |\psi_i\rangle \langle \psi_i|] I_{d_{\text{in}}} \quad (\text{S365})$$

$$= d_{\text{in}}^2(d_{\text{in}}^2 - 1) \text{tr}_1 \left[(\Phi^{\dagger}(O^2) \otimes I) \frac{\text{SWAP}_n + I_{d_{\text{in}}^2}}{d_{\text{in}}(d_{\text{in}} + 1)} \right] + d_{\text{in}} \text{tr} [\Phi^{\dagger}(O^2)] I_{d_{\text{in}}} \quad (\text{S366})$$

$$= d_{\text{in}}(d_{\text{in}} - 1) \Phi^{\dagger}(O^2) + d_{\text{in}}^2 \text{tr} [\Phi^{\dagger}(O^2)] I_{d_{\text{in}}}, \quad (\text{S367})$$

where in the second equality we use the eigenvalue decomposition of O in Eq. (23) together with the adjoint map Φ^{\dagger} of Φ ; in the fourth equality we apply the Corollary 1, which follows from the fact that the probability distribution $\mathcal{S}_{2\text{-dgn}}$ forms a state 2-design. Finally, in the last line, we employ the partial-swap-trick from Lemma (2).

Hence, the variance σ^2 can be upper bounded by

$$\left\| \sum_{k=1}^N \mathbb{E} \left[\left(\frac{\omega_{2\text{-dgn}}^{(k)} - O_{\Phi}}{N} \right)^2 \right] \right\|_{\infty} = \frac{1}{N} \|d_{\text{in}}(d_{\text{in}} - 1) \Phi^{\dagger}(O^2) + d_{\text{in}}^2 \text{tr} [\Phi^{\dagger}(O^2)] I_{d_{\text{in}}} - O_{\Phi}^2\|_{\infty} \quad (\text{S368})$$

$$\leq \frac{1}{N} \{ d_{\text{in}}(d_{\text{in}} - 1) \|\Phi^{\dagger}(O^2)\|_{\infty} + d_{\text{in}}^2 \text{tr} [\Phi^{\dagger}(O^2)] + \|O_{\Phi}^2\|_{\infty} \} \quad (\text{S369})$$

$$\leq \frac{1}{N} \{ d_{\text{in}}(d_{\text{in}} - 1) \|O\|_{\infty}^2 + d_{\text{in}}^3 \|O\|_{\infty}^2 + \|O_{\Phi}\|_{\infty}^2 \} \quad (\text{S370})$$

$$\leq \frac{\|O\|_{\infty}^2 (d_{\text{in}}^2 + 1)(d_{\text{in}} + 1)}{N} := \sigma^2, \quad (\text{S371})$$

where the third inequality follows from the fact that Φ is CPTP, which implies that $\Phi^{\dagger}(I_{d_{\text{in}}}) \leq I_{d_{\text{in}}}$, and from the bound $O \leq \|O\|_{\infty} I_{d_{\text{in}}}$. Substituting Eqs. (S360) and (S371) into Eq. (S354) yields

$$\Pr \left[\left\| \hat{O}_{\Phi,2\text{-dgn}} - O_{\Phi} \right\|_{\infty} \geq \epsilon \right] \leq d_{\text{in}} \exp \left(\frac{-N\epsilon^2/2}{\|O\|_{\infty}^2 (d_{\text{in}}^2 + 1)(d_{\text{in}} + 1) + \|O\|_{\infty} (d_{\text{in}}^2 + 1)\epsilon/3} \right). \quad (\text{S372})$$

Thus, it can be concluded that

$$N \geq \frac{2 \max\{1, \|O\|_{\infty}^2\} (d_{\text{in}}^2 + 1)(d_{\text{in}} + 1 + \epsilon/3)}{\epsilon^2} \ln \left(\frac{d_{\text{in}}}{\delta} \right) \quad (\text{S373})$$

suffices to guarantee that $\|\hat{O}_{\Phi,2\text{-dgn}} - O_{\Phi}\|_{\infty} \leq \epsilon$ with probability at least $1 - \delta$. \square

b. Tensor-product single-qubit stabilizer states

Proof. Similar to the previous discussion, since the estimator $\hat{O}_{\Phi,\text{stab}}$ has the explicit representation $\hat{O}_{\Phi,\text{stab}} = \frac{1}{N} \sum_{i=1}^N \hat{\omega}_{\text{stab}}^{(k)}$ in Eq. (33), it follows that

$$\hat{O}_{\Phi,\text{stab}} - O_{\Phi} = \sum_{k=1}^N \frac{1}{N} \left\{ \hat{\omega}_{\text{stab}}^{(k)} - O_{\Phi} \right\}. \quad (\text{S374})$$

Here, each $\hat{\omega}_{\text{stab}}^{(k)}$ is an i.i.d. copy of a random matrix $\omega_{\text{stab}} = \nu_j \bigotimes_{s=1}^n (6|u^s\rangle\langle u^s| - 2I)$, which occurs with probability $(1/6^n) \langle j| W^\dagger \Phi(|u\rangle\langle u|) W |j\rangle$, where $|u\rangle = \bigotimes_{s=1}^n |u^s\rangle$. Combining this with the unbiasedness of $\hat{O}_{\Phi, \text{stab}}$ shown in Appendix S32b implies that $\hat{O}_{\Phi, \text{stab}} - O_\Phi$ is a sum of centered random matrices $X_{\text{stab}}^{(k)} := (\hat{\omega}_{\text{stab}}^{(k)} - O_\Phi)/N$. The operator norm of each random matrix $X_{\text{stab}}^{(k)}$ can be upper bounded as

$$\|X_{\text{stab}}^{(k)}\|_\infty \leq \frac{1}{N} \left\{ \|\omega_{\text{stab}}^{(k)}\|_\infty + \|O_\Phi\|_\infty \right\} \quad (\text{S375})$$

$$\leq \frac{1}{N} \left\{ \max_{|u\rangle, \nu_j} |\nu_j| \prod_{s=1}^n \|6|u^s\rangle\langle u^s| - 2I\|_\infty + \|O_\Phi\|_\infty \right\} \quad (\text{S376})$$

$$\leq \frac{(4^n + 1)\|O\|_\infty}{N} := \alpha. \quad (\text{S377})$$

Since $\mathbb{E}[(X_{\text{stab}}^{(k)})^2] = (\mathbb{E}[\omega_{\text{stab}}^2] - O_\Phi^2)/N^2$, it suffices to calculate $\mathbb{E}[\omega_{\text{stab}}^2]$ to evaluate the variance parameter:

$$\mathbb{E}[\omega_{\text{stab}}^2] = \mathbb{E}_u \sum_j \text{tr} \left[|j\rangle\langle j| W^\dagger \Phi(|u\rangle\langle u|) W \right] \nu_j^2 \left(\bigotimes_{s=1}^n (6|u^s\rangle\langle u^s| - 2I) \right)^2 \quad (\text{S378})$$

$$= \frac{1}{6^n} \sum_{|u\rangle \in \mathcal{Q}_{\text{stab}}^{\otimes n}} \text{tr} \left[\Phi^\dagger(O^2) \bigotimes_{s=1}^n |u^s\rangle\langle u^s| \right] \left(4^n \bigotimes_{s=1}^n (3|u^s\rangle\langle u^s| + I) \right). \quad (\text{S379})$$

Here, to proceed with the above calculation, we first examine the case where the input is a product operator $A := \bigotimes_{s=1}^n A^s$ with $A^s \in \mathcal{H}(\mathbb{C}^2)$, instead of $\Phi^\dagger(O^2)$.

$$\sum_{|u\rangle \in \mathcal{Q}_{\text{stab}}^{\otimes n}} \text{tr} \left[A \bigotimes_{s=1}^n |u^s\rangle\langle u^s| \right] \left(\bigotimes_{s=1}^n (3|u^s\rangle\langle u^s| + I) \right) = \bigotimes_{s=1}^n \left(\sum_{|u^s\rangle \in \mathcal{Q}_{\text{stab}}} \text{tr} [A^s |u^s\rangle\langle u^s|] (3|u^s\rangle\langle u^s| + I) \right) \quad (\text{S380})$$

$$= 3^n \bigotimes_{s=1}^n (2\text{tr}(A^s)I + A^s) \quad (\text{S381})$$

$$= 3^n \sum_{\alpha \subseteq [n]} 2^{|\alpha|} \left(\text{tr}_\alpha [A] \otimes \bigotimes_{s \in \alpha} I_s \right), \quad (\text{S382})$$

where the second equality uses $\sum_{|u^s\rangle \in \mathcal{Q}_{\text{stab}}} \text{tr} [A^s |u^s\rangle\langle u^s|] (3|u^s\rangle\langle u^s| + I) = 3(2\text{tr}(A^s)I + A^s)$ for all $s \in [n]$, which follows from the fact that uniform distribution over the set $\mathcal{Q}_{\text{stab}}$ forms a state 2-design. By linear extension of such product operators A , the result can be applied to $\Phi^\dagger(O^2)$. Therefore, the operator norm of $\mathbb{E}[\omega_{\text{stab}}^2]$ can be upper bounded as

$$\|\mathbb{E}[\omega_{\text{stab}}^2]\|_\infty = \left\| 2^n \sum_{\alpha \subseteq [n]} 2^{|\alpha|} \left(\text{tr}_\alpha [\Phi^\dagger(O^2)] \otimes \bigotimes_{s \in \alpha} I_s \right) \right\|_\infty \quad (\text{S383})$$

$$\leq 2^n \sum_{\alpha \subseteq [n]} 2^{|\alpha|} \left\| \text{tr}_\alpha [\Phi^\dagger(O^2)] \right\|_\infty \left\| \bigotimes_{s \in \alpha} I_s \right\|_\infty \quad (\text{S384})$$

$$\leq 2^n \|O\|_\infty^2 \sum_{\alpha \subseteq [n]} 2^{|\alpha|} \cdot 2^{|\alpha|} \quad (\text{S385})$$

$$\leq 2^n \|O\|_\infty^2 \sum_{j=0}^n \binom{n}{j} 4^j \quad (\text{S386})$$

$$\leq 2^n \|O\|_\infty^2 (4+1)^n \leq 10^n \|O\|_\infty^2, \quad (\text{S387})$$

where the second-to-third line comes from the fact that $O^2 \leq \|O\|_\infty^2 I^{\otimes n}$ and $\Phi^\dagger(I^{\otimes n}) \leq I^{\otimes n}$. Hence, the variance σ^2 can be upper bounded by

$$\left\| \sum_{i=1}^N \mathbb{E} \left[\left(\frac{\omega_{\text{stab}}^{(k)} - O_\Phi}{N} \right)^2 \right] \right\|_\infty \leq \frac{1}{N} \left\{ \|\mathbb{E}[(\omega_{\text{stab}}^{(k)})^2]\|_\infty + \|O_\Phi^2\|_\infty \right\} \quad (\text{S388})$$

$$\leq \frac{\|O\|_\infty^2(10^n + 1)}{N} := \sigma^2. \quad (\text{S389})$$

Thus, Matrix Bernstein inequality in Lemma 4 implies that

$$N \geq \frac{2 \max\{1, \|O\|_\infty^2\}(10^n + 1 + (\epsilon/3)(4^n + 1))}{\epsilon^2} \ln\left(\frac{2^n}{\delta}\right) \quad (\text{S390})$$

is sufficient to ensure that $\|\hat{O}_{\Phi, \text{stab}} - O_\Phi\|_\infty \leq \epsilon$ with probability at least $1 - \delta$. \square

c. *n-qubit Pauli operator*

Proof. From the unbiasedness of $\hat{O}_{\Phi, \text{pauli}}$ together with Eq. (40), we have

$$\hat{O}_{\Phi, \text{pauli}} - O_\Phi = \sum_{k=1}^N \frac{1}{N} \left\{ \omega_{\text{pauli}}^{(k)} - O_\Phi \right\} := \sum_{k=1}^N X_{\text{pauli}}^{(k)}, \quad (\text{S391})$$

which is a sum of independent centered random matrices. For each random matrix $X_{\text{pauli}}^{(k)}$, we have the upper bound as

$$\|X_{\text{pauli}}^{(k)}\|_\infty \leq \frac{1}{N} \left\{ \left\| \omega_{\text{pauli}}^{(k)} \right\|_\infty + \|O_\Phi\|_\infty \right\} \quad (\text{S392})$$

$$\leq \frac{1}{N} \left\{ \max_{j, \mathbf{i}, \mathbf{e}} \|4^n \nu_j c_{\mathbf{i}, \mathbf{e}} P_{\mathbf{i}}\|_\infty + \|O_\Phi\|_\infty \right\} \quad (\text{S393})$$

$$= \frac{(4^n + 1)\|O\|_\infty}{N} := \alpha. \quad (\text{S394})$$

Here, $\mathbb{E}[\omega_{\text{pauli}}^2]$ can be evaluated as

$$\mathbb{E}[\omega_{\text{pauli}}^2] = \sum_{\mathbf{i}, \mathbf{e}} \frac{1}{8^n} \sum_j \text{tr} \left[|j\rangle \langle j| W^\dagger \Phi(|v_{\mathbf{i}, \mathbf{e}}\rangle \langle v_{\mathbf{i}, \mathbf{e}}|) W \right] (\nu_j 4^n c_{\mathbf{i}, \mathbf{e}} P_{\mathbf{i}})^2 \quad (\text{S395})$$

$$= \frac{1}{8^n} \sum_{\mathbf{i}, \mathbf{e}} \text{tr} \left[\Phi^\dagger(O^2) |v_{\mathbf{i}, \mathbf{e}}\rangle \langle v_{\mathbf{i}, \mathbf{e}}| \right] 16^n I^{\otimes n} \quad (\text{S396})$$

$$= 2^n \sum_{\mathbf{i} \in [4]^n} \text{tr} \left[\Phi^\dagger(O^2) \right] I^{\otimes n} \quad (\text{S397})$$

$$= 8^n \text{tr} \left[\Phi^\dagger(O^2) \right] I^{\otimes n}, \quad (\text{S398})$$

where in the second-to-third line, we employ the fact that $\sum_{\mathbf{e}} |v_{\mathbf{i}, \mathbf{e}}\rangle \langle v_{\mathbf{i}, \mathbf{e}}| = I^{\otimes n}$ for all $\mathbf{i} \in [4]^n$. Hence, we arrive at the following upper bound of the variance parameter:

$$\left\| \sum_{i=1}^N \mathbb{E} \left[\left(\frac{\omega_{\text{pauli}}^{(k)} - O_\Phi}{N} \right)^2 \right] \right\|_\infty \leq \frac{1}{N} \left\{ \left\| \mathbb{E}[(\omega_{\text{pauli}}^{(k)})^2] \right\|_\infty + \|O_\Phi^2\|_\infty \right\} \quad (\text{S399})$$

$$\leq \frac{\|O\|_\infty^2(16^n + 1)}{N} := \sigma^2, \quad (\text{S3100})$$

where in the second-to-last line, we use $O^2 \leq \|O\|_\infty^2 I^{\otimes n}$ and $\text{tr}[\Phi(I^{\otimes n})] \leq 2^n$.

Like the preceding discussion, the Matrix Bernstein inequality shows that the number of iterations

$$N \geq \frac{2 \max\{1, \|O\|_\infty^2\}(d_{\text{in}}^4 + 1 + (\epsilon/3)(d_{\text{in}}^2 + 1))}{\epsilon^2} \ln\left(\frac{d_{\text{in}}}{\delta}\right) \quad (\text{S3101})$$

suffices to ensure that $\|\hat{O}_{\Phi, \text{pauli}} - O_\Phi\|_\infty \leq \epsilon$ with probability at least $1 - \delta$. \square

Appendix S4: Cluster simulation of tree-structured quantum circuits

1. Technical lemmas

In this subsection, we present several technical lemmas that will be used for the complexity analysis in the following subsections. First, the following two lemmas are useful for bounding the norms of tensor products of local operators generated through statistical estimation procedures, and their deviation from the true value.

Lemma 5 (See, e.g., Ref. [14]). *Let $r \in \mathbb{N}$ and x be a real number satisfying $0 \leq x \leq 1/r$. Then, the following inequality holds:*

$$(1+x)^r \leq 1 + (e-1)rx. \quad (\text{S41})$$

Proof of Lemma 5. Since $\ln(1+x) \leq x$ for all $x > -1$, we obtain $(1+x)^r = \exp(r \ln(1+x)) \leq e^{rx}$. Now we consider the exponential function $f(t) = e^t$. Since $f(t)$ is convex, for $t \in [0, 1]$ its graph lies below the line segment connecting the points $(0, 1)$ and $(1, e)$, i.e., $e^t \leq (e-1)t+1$. Applying this with $t = rx$ and noting that $0 \leq rx \leq 1$ by assumption, we have

$$(1+x)^r \leq e^{rx} \leq 1 + (e-1)rx, \quad (\text{S42})$$

which concludes the proof. \square

Lemma 6. *Let $\{A_i\}_{i=1}^r$ and $\{B_i\}_{i=1}^r$ be sets of matrices such that $\|A_i - B_i\|_\infty \leq \epsilon_i$ for all $i = 1, \dots, r$ where $\epsilon_i \in (0, 1]$. Then the following inequality holds:*

$$\left\| \bigotimes_{i=1}^r A_i - \bigotimes_{i=1}^r B_i \right\|_\infty \leq \sum_{i=1}^r \epsilon_i \prod_{j \neq i} \max\{\|A_j\|_\infty, \|B_j\|_\infty\}. \quad (\text{S43})$$

Proof of Lemma 6. By the telescoping identity, we have

$$\bigotimes_{i=1}^r A_i - \bigotimes_{i=1}^r B_i = \sum_{i=1}^r \left(\bigotimes_{j < i} B_j \right) \otimes (A_i - B_i) \otimes \left(\bigotimes_{j > i} A_j \right). \quad (\text{S44})$$

Since $\|A \otimes B\|_\infty = \|A\|_\infty \|B\|_\infty$ and triangle inequality, it follows that

$$\left\| \bigotimes_{i=1}^r A_i - \bigotimes_{i=1}^r B_i \right\|_\infty \leq \sum_{i=1}^r \|A_i - B_i\|_\infty \prod_{j < i} \|B_j\|_\infty \prod_{j > i} \|A_j\|_\infty \quad (\text{S45})$$

$$\leq \sum_{i=1}^r \epsilon_i \prod_{j \neq i} \max\{\|A_j\|_\infty, \|B_j\|_\infty\}, \quad (\text{S46})$$

where the last inequality uses the assumption $\|A_i - B_i\|_\infty \leq \epsilon_i$. \square

Lemma 7 (Union bound; see, e.g., Ref. [111]). *Given a finite set $\{E_i\}_{i=1}^L$ of events, the following inequality holds:*

$$\Pr \left[\bigcup_{i=1}^L E_i \right] \leq \sum_{i=1}^L \Pr(E_i). \quad (\text{S47})$$

In our analysis, we often use the following equivalent inequality obtained by applying De Morgan's law:

$$1 - \sum_{i=1}^L \Pr[E_i^c] \leq \Pr \left[\bigcap_{i=1}^L E_i \right]. \quad (\text{S48})$$

Therefore, to ensure that all events E_1, \dots, E_L occurs simultaneously with probability at least $1 - \delta$, it suffices to require that

$$\sum_{i=1}^L \Pr[E_i^c] \leq \delta. \quad (\text{S49})$$

In other words, if the individual failure probabilities $\Pr[E_i^c]$ are chosen such that their sum does not exceed δ , then the probability that all events occur is at least $1 - \delta$. As a simple example, it suffices to assign equal bounds $\Pr[E_i^c] \leq \delta/L$ for all i for the desired overall confidence.

2. Proof of Theorem 5

Theorem 5 (Two-layer tree circuits). *Both the protocol based on Theorem 2 and the protocol based on Theorem 3 estimate $\langle O \rangle_{\rho_{\text{tree}}}$ up to additive error $\epsilon \in (0, 1]$ with probability at least $1 - \delta$, provided that the numbers of measurements satisfy, for $k = 1, \dots, R$,*

$$\begin{aligned} N_{a,k} = N_{b,k} &= \mathcal{O} \left(\frac{d^3 R^2}{\epsilon^2} \ln \left(\frac{(R+1)d}{\delta} \right) \right), \\ N_{a,0} = N_{b,0} &= \mathcal{O} \left(\frac{1}{\epsilon^2} \ln \left(\frac{R+1}{\delta} \right) \right). \end{aligned} \quad (\text{S410})$$

Consequently, the total numbers of measurements scale as

$$N_{a,\text{tot}} = N_{b,\text{tot}} = \mathcal{O} \left(\frac{d^3 R^3}{\epsilon^2} \ln \left(\frac{(R+1)d}{\delta} \right) \right). \quad (\text{S411})$$

Proof of Theorem 5. We first provide the complexity analysis for the protocol based on Theorem 2.

Proof of Theorem 5 (protocol (a))

Assume that the operator-norm error of each effective estimated effective observable \tilde{M}_k in Step (a-1) is upper bounded by η , i.e.,

$$\left\| \tilde{M}_k - M_k \right\|_{\infty} \leq \eta, \quad k = 1, \dots, R. \quad (\text{S412})$$

Define the approximate target mean of Step (a-3) as

$$\mu_a := \text{tr} \left[O \left(\bigotimes_{k=1}^R \Phi_k \circ \mathcal{M}_{\text{apr}}^{(k)} \right) (\rho) \right]. \quad (\text{S413})$$

Under this assumption, our first goal is to relate the individual errors η to the total bias in Step (a-3). To this end, we express the bias,

$$\text{Bias}_a := \left| \mu_a - \langle O \rangle_{\rho_{\text{tree}}} \right|, \quad (\text{S414})$$

solely in terms of the quantity η . Using Eq. (49), this can be rewritten and bounded as

$$\text{Bias}_a = \left| \text{tr} \left[\left(\bigotimes_{k=1}^R \mathcal{M}_{\text{apr}}^{(k)} (M_k) \right) \rho \right] - \text{tr} \left[\left(\bigotimes_{k=1}^R M_k \right) \rho \right] \right| \quad (\text{S415})$$

$$\leq \left\| \bigotimes_{k=1}^R \mathcal{M}_{\text{apr}}^{(k)} (M_k) - \bigotimes_{k=1}^R M_k \right\|_{\infty}, \quad (\text{S416})$$

where the inequality follows from Hölder's inequality, $|\text{tr}[AB]| \leq \|A\|_{\infty} \|B\|_1$. Applying the telescoping identity (see Lemma 6), we obtain

$$\text{Bias}_a \leq \sum_{k=1}^R \left\| \mathcal{M}_{\text{apr}}^{(k)} (M_k) - M_k \right\|_{\infty} \prod_{l \neq k} \max \left\{ \left\| \mathcal{M}_{\text{apr}}^{(l)} (M_l) \right\|_{\infty}, \|M_l\|_{\infty} \right\}. \quad (\text{S417})$$

Since each MP channel $\mathcal{M}_{\text{apr}}^{(k)}$ is a unital pinching map, it is contractive in operator norm, $\|\mathcal{M}_{\text{apr}}^{(k)}(A)\|_{\infty} \leq \|A\|_{\infty}$ for any Hermitian operator A . Moreover, $\mathcal{M}_{\text{apr}}^{(k)}(\tilde{M}_k) = \tilde{M}_k$ by construction; see Appendix S2.1. Hence,

$$\left\| \mathcal{M}_{\text{apr}}^{(k)} (M_k) - M_k \right\|_{\infty} \leq \left\| \mathcal{M}_{\text{apr}}^{(k)} (M_k - \tilde{M}_k) \right\|_{\infty} + \left\| \tilde{M}_k - M_k \right\|_{\infty} \quad (\text{S418})$$

$$\leq 2 \left\| \tilde{M}_k - M_k \right\|_{\infty} \leq 2\eta. \quad (\text{S419})$$

Similarly, since Φ_l is CPTP, Φ_l^\dagger is completely positive and unital. As positive unital maps are contractive in the operator norm, we have $\|M_l\|_\infty = \|\Phi_l^\dagger(O_l)\|_\infty \leq \|O_l\|_\infty$. Using $\|\mathcal{M}_{\text{apr}}^{(l)}(M_l)\|_\infty \leq \|M_l\|_\infty$ and Eq. (S419) in Eq. (S417) yields

$$\text{Bias}_a \leq \sum_{k=1}^R 2\eta \prod_{l \neq k} \|M_l\|_\infty \leq 2R\eta. \quad (\text{S420})$$

Hence, by choosing

$$\eta = \frac{\epsilon}{4R}, \quad (\text{S421})$$

the Bias_a is upper bounded by $\epsilon/2$.

Next, we consider the statistical error in Step (a-3). Let $\hat{\mu}_a$ be the empirical mean from $N_{a,0}$ shots in Step (a-3). Define the statistical event

$$E_0^a := \left\{ |\hat{\mu}_a - \mu_a| \leq \frac{\epsilon}{2} \right\}, \quad (\text{S422})$$

where μ_a is defined in Eq. (S413).

Here, μ_a depends on the outputs $\{\tilde{M}_k\}$ derived from the randomized learning procedure, as it includes the MP channels $\{\mathcal{M}_{\text{apr}}^{(k)}\}$. Conditioned on fixed $\{\tilde{M}_k\}$, the Step (a-3) performs $N_{a,0}$ i.i.d. repetitions whose single-shot outcome corresponds to measuring the Hermitian observables $O = \bigotimes_{k=1}^R O_k$ with $\|O_k\|_\infty \leq 1$. Thus, each outcome is bounded in $[-1, 1]$. Hoeffding's inequality yields, for any fixed $\{\tilde{M}_k\}$,

$$\Pr \left[(E_0^a)^c \mid \tilde{M}_1, \dots, \tilde{M}_R \right] \leq 2 \exp \left(-\frac{N_{a,0}\epsilon^2}{8} \right). \quad (\text{S423})$$

Since the right-hand side is uniform in $\{\tilde{M}_k\}$, taking expectation over $\{\tilde{M}_k\}$ gives the unconditional bound

$$\Pr [(E_0^a)^c] \leq 2 \exp \left(-\frac{N_{a,0}\epsilon^2}{8} \right). \quad (\text{S424})$$

Thus, it suffices to choose

$$N_{a,0} = \mathcal{O} \left(\frac{1}{\epsilon^2} \ln \left(\frac{R+1}{\delta} \right) \right), \quad (\text{S425})$$

so that $\Pr [(E_0^a)^c] \leq \delta/(R+1)$.

For each $k = 1, \dots, R$, define

$$E_k^a := \left\{ \|\tilde{M}_k - M_k\|_\infty \leq \eta \right\}, \quad (\text{S426})$$

with η chosen as in Eq. (S421). By Theorem 4, it suffices to take

$$N_{a,k} = \mathcal{O} \left(\frac{d^3 R^2}{\epsilon^2} \ln \frac{(R+1)d}{\delta} \right) \quad (\text{S427})$$

to ensure $\Pr [(E_k^a)^c] \leq \delta/(R+1)$.

On the event $\bigcap_{k=1}^R E_k^a$, we have $\text{Bias}_a \leq \epsilon/2$, and $|\hat{\mu}_a - \mu_a| \leq \epsilon/2$. Hence on $\bigcap_{k=0}^R E_k^a$, the triangle inequality gives

$$|\hat{\mu}_a - \langle O \rangle_{\rho_{\text{tree}}}| \leq \text{Bias}_a + |\hat{\mu}_a - \mu_a| \leq \epsilon. \quad (\text{S428})$$

Finally, by the union bound,

$$\Pr \left[\bigcap_{k=0}^R E_k^a \right] \geq 1 - \sum_{k=0}^R \Pr [(E_k^a)^c] \geq 1 - (R+1) \cdot \frac{\delta}{R+1} = 1 - \delta. \quad (\text{S429})$$

Combining Eqs. (S425) and (S427) proves the theorem statement for protocol (a).

Proof of Theorem 5 (protocol (b))

Assume that each estimated effective observable \tilde{M}_k in Step **(b-1)** satisfies

$$\left\| \tilde{M}_k - M_k \right\|_{\infty} \leq \xi, \quad k = 1, \dots, R. \quad (\text{S430})$$

Define the approximate target mean of Step **(b-3)** as

$$\mu_b := \text{tr} \left[\left(\bigotimes_{k=1}^R \tilde{M}_k \right) \rho \right], \quad (\text{S431})$$

where the equality follows from the definition of $\mathcal{C}_{\text{apr}}^{(k)}$.

Under this assumption of Eq. (S430), we first analyze the relationship between the individual errors ξ and the total bias

$$\text{Bias}_b := \left| \mu_b - \langle O \rangle_{\rho_{\text{tree}}} \right| \quad (\text{S432})$$

for Step **(b-3)**. Now, the total bias can be bounded as

$$\text{Bias}_b = \left| \text{tr} \left[\left(\bigotimes_{k=1}^R \tilde{M}_k - \bigotimes_{k=1}^R M_k \right) \rho \right] \right| \leq \left\| \bigotimes_{k=1}^R \tilde{M}_k - \bigotimes_{k=1}^R M_k \right\|_{\infty}, \quad (\text{S433})$$

where we used Hölder's inequality, $|\text{tr}[AB]| \leq \|A\|_{\infty} \|B\|_1$. Using the telescoping identity in Lemma 6, we obtain

$$\text{Bias}_b \leq \sum_{k=1}^R \left\| \tilde{M}_k - M_k \right\|_{\infty} \prod_{l \neq k} \max \left\{ \|M_l\|_{\infty}, \|\tilde{M}_l\|_{\infty} \right\} \quad (\text{S434})$$

$$\leq \sum_{k=1}^R \left\| \tilde{M}_k - M_k \right\|_{\infty} \prod_{l \neq k} \max \left\{ \|M_l\|_{\infty}, \|M_l\|_{\infty} + \left\| \tilde{M}_l - M_l \right\|_{\infty} \right\} \quad (\text{S435})$$

$$\leq R\xi(1+\xi)^{R-1}, \quad (\text{S436})$$

where in the last inequality we used $\|M_l\|_{\infty} \leq 1$ and $\left\| \tilde{M}_l - M_l \right\|_{\infty} \leq \xi$ for all l .

We now derive an explicit upper bound on the total bias Bias_b in terms of the estimation errors ξ . We further simplify the derived expression using the following fact (see Lemma 5):

$$(1+x)^r \leq 1 + (e-1)rx, \quad (0 \leq x \leq 1/r). \quad (\text{S437})$$

In particular, we set $\xi = \epsilon/[2R(e-1)]$ for $k = 1, \dots, R$. Substituting this into Eq. (S436) yields

$$\text{Bias}_b \leq R \times \frac{\epsilon}{2R(e-1)} \times \left(1 + \frac{\epsilon}{2R(e-1)} \right)^{R-1} \quad (\text{S438})$$

$$\leq R \times \frac{\epsilon}{2R(e-1)} \times \left(1 + \frac{\epsilon}{2} \right) \quad (\text{S439})$$

$$\leq \frac{\epsilon}{2} \times \frac{1.5}{e-1} \leq \frac{\epsilon}{2}, \quad (\text{S440})$$

where in the last two inequalities we use $\epsilon \leq 1$ and the fact that $1.5/(e-1) \leq 1$. Hence, by choosing

$$\xi = \frac{\epsilon}{2R(e-1)}, \quad (\text{S441})$$

the Bias_b is upper bounded by $\epsilon/2$.

In Step **(b-3)**, each run outputs a classical random variable Y such that $\mathbb{E}[Y | \tilde{M}_1, \dots, \tilde{M}_R] = \mu_b$. Moreover, conditioned on fixed $\{\tilde{M}_k\}$, the output is upper bounded by

$$|Y| \leq \gamma(\tilde{M}) := \left\| \bigotimes_{k=1}^R \tilde{M}_k \right\|_{\infty} \leq \prod_{k=1}^R \left\| \tilde{M}_k \right\|_{\infty}. \quad (\text{S442})$$

On the good-tomography event in Eq. (S445) below, we will show that $\gamma(\tilde{M}) \leq 3/2$.

Next, we consider the statistical error in Step **(b-3)**. Let $\hat{\mu}_b$ be the empirical mean from $N_{b,0}$ shots. Define the statistical event

$$E_0^b := \left\{ |\hat{\mu}_b - \mu_b| \leq \frac{\epsilon}{2} \right\}, \quad (\text{S443})$$

where μ_b is defined in Eq. (S431).

Conditioned on fixed $\{\tilde{M}_k\}$, the $N_{b,0}$ samples are i.i.d. and bounded in $[-\gamma(\tilde{M}), \gamma(\tilde{M})]$. Hence, Hoeffding's inequality gives

$$\Pr \left[(E_0^b)^c \mid \tilde{M}_1, \dots, \tilde{M}_R \right] \leq 2 \exp \left(-\frac{N_{b,0}\epsilon^2}{8\gamma(\tilde{M})^2} \right). \quad (\text{S444})$$

Here, let T be the good-tomography event where the tomography errors are within the desired value as in Eq. (S441)

$$T := \bigcap_{k=1}^R E_k^b = \bigcap_{k=1}^R \left\{ \left\| \tilde{M}_k - M_k \right\|_\infty \leq \xi \right\}. \quad (\text{S445})$$

On the event T , we have

$$\gamma(\tilde{M}) = \left\| \bigotimes_{k=1}^R \tilde{M}_k \right\|_\infty \leq \prod_{k=1}^R \left\| \tilde{M}_k \right\|_\infty \leq (1 + \xi)^R, \quad (\text{S446})$$

where we used the triangle inequality, $\|\tilde{M}_k\|_\infty \leq \|M_k\|_\infty + \|M_k - \tilde{M}_k\|_\infty \leq 1 + \xi$. With $\xi = \epsilon/[2R(e-1)] \leq 1/R$ chosen as in Eq. (S441), Lemma 5 yields

$$(1 + \xi)^R \leq 1 + \frac{\epsilon}{2} \leq \frac{3}{2}, \quad (\text{S447})$$

so $\gamma(\tilde{M}) \leq 3/2$ holds on the good-tomography event T . Consequently, for any realization with T ,

$$\Pr \left[(E_0^b)^c \mid \tilde{M}_1, \dots, \tilde{M}_R \right] \leq 2 \exp \left(-\frac{N_{b,0}\epsilon^2}{18} \right). \quad (\text{S448})$$

Therefore, by the tower property and the fact that the above conditional bound holds whenever T occurs, we have

$$\Pr \left[(E_0^b)^c \cap T \right] = \mathbb{E} \left[\mathbf{1}_T \Pr \left[(E_0^b)^c \mid \tilde{M}_1, \dots, \tilde{M}_R \right] \right] \leq 2 \exp \left(-\frac{N_{b,0}\epsilon^2}{18} \right), \quad (\text{S449})$$

where $\mathbf{1}_T$ is the indicator function about T .

Thus, it is sufficient to choose

$$N_{b,0} = \mathcal{O} \left(\frac{1}{\epsilon^2} \ln \left(\frac{R+1}{\delta} \right) \right), \quad (\text{S450})$$

so that $\Pr[(E_0^b)^c \cap T] \leq \delta/(R+1)$.

Then, on $T \cap E_0^b$, we have $\text{Bias}_b \leq \epsilon/2$ and $|\hat{\mu}_b - \mu_b| \leq \epsilon/2$. The triangle inequality yields

$$\left| \hat{\mu}_b - \langle O \rangle_{\rho_{\text{tree}}} \right| \leq \text{Bias}_b + |\hat{\mu}_b - \mu_b| \leq \epsilon. \quad (\text{S451})$$

Finally, by the union bound applied to the R good-tomography events and the statistical failure on T , the failure probability can be upper-bounded as

$$\Pr \left[(T \cap E_0^b)^c \right] \leq \Pr[T^c] + \Pr[(E_0^b)^c \cap T] \leq \sum_{k=1}^R \Pr[(E_k^b)^c] + \Pr[(E_0^b)^c \cap T]. \quad (\text{S452})$$

By putting everything together, Theorem 4 implies that it suffices to take

$$N_{b,k} = \mathcal{O} \left(\frac{d^3 R^2}{\epsilon^2} \ln \left(\frac{(R+1)d}{\delta} \right) \right), \quad (\text{S453})$$

so that $\Pr[(E_k^b)^c] \leq \delta/(R+1)$ for each k . Together with Eqs. (S450) and (S452), we obtain

$$\Pr \left[(T \cap E_0^b)^c \right] \leq R \cdot \frac{\delta}{R+1} + \frac{\delta}{R+1} = \delta, \quad (\text{S454})$$

i.e., $\Pr[T \cap E_0^b] \geq 1 - \delta$. This proves the theorem statement for protocol (b). \square

Algorithm 2: Cluster simulation of tree circuit with $R \geq 2$

Input: Unknown CPTP maps $\{\Phi_{(i_1, \dots, i_l)}\}$ for $l = 1, \dots, L$; an unknown quantum state ρ ; and known observables $O_{(i_1, \dots, i_L)}$ with $\|O_{(i_1, \dots, i_L)}\|_\infty \leq 1$; accuracy ϵ

Output: Estimate $\hat{\mu}$ of $\text{tr}(O\rho_{\text{tree}})$

```

 $\tilde{M}_{(i_1, \dots, i_L, 1)} \leftarrow O_{(i_1, \dots, i_L)};$ 
for  $l = L, L-1, \dots, 1$  do
  for  $\mathbf{i} = (i_1, \dots, i_l) \in [R]^l$  do
    Estimate  $\tilde{M}_{\mathbf{i}}$  using the learning protocols in Sec. IV, with inputs  $\{\tilde{M}_{(\mathbf{i}, a)}\}_a$  and  $\Phi_{\mathbf{i}}$  from shots  $N_{\mathbf{i}}$ ;
    Diagonalize  $\tilde{M}_{\mathbf{i}} := \tilde{V}_{\mathbf{i}} \tilde{D}_{\mathbf{i}} \tilde{V}_{\mathbf{i}}^\dagger$  with  $\tilde{D}_{\mathbf{i}} := \sum_j \tilde{\lambda}_{j, \mathbf{i}} |j\rangle \langle j|$ ;
for  $k \leftarrow 1$  to  $N_0$  do
  Measure  $\rho$  in the product basis  $\left\{ \bigotimes_{i_1=1}^R \tilde{V}_{i_1} |j_1 \dots j_R\rangle \right\}$ , obtaining  $x_k \in \{j_1, \dots, j_R\}$ ;
  Set  $\omega_{x_k} := \prod_{i_1=1}^R \tilde{\lambda}_{j_{i_1}, i_1}$  to the corresponding eigenvalue, by weighting the outcome  $x_k$  accordingly;
 $\hat{\mu} \leftarrow \frac{1}{N_0} \sum_{k=1}^{N_0} \omega_{x_k}$ ;
return  $\hat{\mu}$ ;

```

3. Proof of Theorem 6

Theorem 6 (Multi-layer tree circuits). Suppose ρ_{tree} is the quantum state generated by an (L, R, d) -tree quantum circuit with $R \geq 2$, $L \geq 1$, and $d = 2^n$, and let O be the observable defined in Eq. (46). Assume that we have access only to devices whose size is bounded by the maximal number of qubits required to represent ρ and $\Phi_{(i_1, \dots, i_l)}$ for each $l = 1, \dots, L$. Then the total number of measurements

$$\mathcal{O}\left(\frac{4^L d^3 L^2 R^{3L}}{\epsilon^2} \ln\left(\frac{R^L d}{\delta}\right)\right) \quad (\text{S455})$$

is sufficient to estimate $\langle O \rangle_{\rho_{\text{tree}}}$ within additive error $\epsilon \in (0, 1]$ with probability at least $1 - \delta$.

Proof of Theorem 6. For simplicity, we consider a complete R -ary tree-structured quantum circuit with tree depth L and the bond dimension $d = 2^n$. We show that the expectation value of O with respect to ρ_{tree} can be estimated using the total number of measurements given in Eq. (S455). Note that circuits with non-uniform branching can also be reduced to this setting by padding the missing branches with the identity channels and placing the identity operators on the corresponding leaves. While this reduction yields the same worst-case upper bound, optimizing shot allocations for the actual circuit structure can lead to a smaller measurement cost.

Our algorithm for $L \geq 1$ repeatedly constructs estimators of the effective observables $M_{(i_1, \dots, i_l)}$, denoted by $\tilde{M}_{(i_1, \dots, i_l)}$, from the leaves to the root:

$$\{\tilde{M}_{(i_1, \dots, i_L)} : (i_1, \dots, i_L) \in [R]^L\} \rightarrow \dots \rightarrow \{\tilde{M}_{i_1} : i_1 \in [R]\}. \quad (\text{S456})$$

The procedure is summarized in Algorithm 2.

To guarantee that the final estimate $\hat{\mu}$ achieves additive error $\epsilon \in (0, 1]$ with probability at least $1 - \delta$, we analyze how the statistical errors from the finite number of samples propagate across depths. We will first investigate the accuracy requirements for each estimation step so that the final estimate $\hat{\mu}$ achieves the desired accuracy. Then, we choose the number of measurements so that all these requirements hold simultaneously with probability at least $1 - \delta$.

Before delving into the detailed analysis, we introduce some notations. For each depth $l = 1, \dots, L$, define the deviation

$$\Delta M_{(i_1, \dots, i_l)} := \tilde{M}_{(i_1, \dots, i_l)} - M_{(i_1, \dots, i_l)} \quad (\text{S457})$$

and its uniform bound x_l such that

$$\|\Delta M_{(i_1, \dots, i_l)}\|_\infty \leq x_l \quad \text{for all } (i_1, \dots, i_l) \in [R]^l. \quad (\text{S458})$$

Let $N_{(i_1, \dots, i_l)}$ denote the number of measurements used to estimate $M_{(i_1, \dots, i_l)}$, and let N_0 denote the number of measurements used to estimate $\text{tr}\left[\left(\bigotimes_{i_1=1}^R \tilde{M}_{i_1}\right) \rho\right]$ in the final step.

1. Accuracy requirement analysis

(i) Learning process at depth L

We start with the learning process at depth L . Given the known observable $O_{(i_1, \dots, i_L)}$ and the unknown quantum channel $\Phi_{(i_1, \dots, i_L)}$, we estimate

$$M_{(i_1, \dots, i_L)} := \Phi_{(i_1, \dots, i_L)}^\dagger(O_{(i_1, \dots, i_L)}) \quad (\text{S459})$$

using the learning procedure introduced in Sec. IV. Let ϵ_L be an upper bound on the estimation error at depth L , i.e.,

$$\left\| \tilde{M}_{(i_1, \dots, i_L)} - M_{(i_1, \dots, i_L)} \right\|_\infty \leq \epsilon_L. \quad (\text{S460})$$

By the definition of x_L in Eq. (S458), we have

$$x_L = \epsilon_L. \quad (\text{S461})$$

(ii) Learning process at depth $l = 1, \dots, L-1$

Next, consider the learning process at depth l ($l = 1, \dots, L-1$). For a node $\mathbf{i} := (i_1, \dots, i_l)$, suppose that the child observables $\{\tilde{M}_{(i,k)}\}_{k=1}^R$ have already been obtained from the learning process at depth $l+1$. Given these known inputs and the unknown quantum channel $\Phi_{\mathbf{i}}$, we apply the learning procedure described in Sec. IV to construct an estimator $\tilde{M}_{\mathbf{i}}$ of

$$\Phi_{\mathbf{i}}^\dagger \left(\tilde{M}_{(i,1)} \otimes \dots \otimes \tilde{M}_{(i,R)} \right). \quad (\text{S462})$$

Let ϵ_l be an upper bound on the estimation error introduced at depth l , namely,

$$\left\| \tilde{M}_{\mathbf{i}} - \Phi_{\mathbf{i}}^\dagger \left(\tilde{M}_{(i,1)} \otimes \dots \otimes \tilde{M}_{(i,R)} \right) \right\|_\infty \leq \epsilon_l, \quad (\text{S463})$$

where the bound is required to hold for all $\mathbf{i} = (i_1, \dots, i_l) \in [R]^l$.

We now upper bound x_l in terms of x_{l+1} . Using the triangle inequality and Eq. (S463), we obtain

$$x_l \leq \left\| \tilde{M}_{\mathbf{i}} - \Phi_{\mathbf{i}}^\dagger \left(\bigotimes_{k=1}^R \tilde{M}_{(i,k)} \right) \right\|_\infty + \left\| \Phi_{\mathbf{i}}^\dagger \left(\bigotimes_{k=1}^R \tilde{M}_{(i,k)} \right) - M_{\mathbf{i}} \right\|_\infty \quad (\text{S464})$$

$$\leq \epsilon_l + \left\| \Phi_{\mathbf{i}}^\dagger \left(\bigotimes_{k=1}^R \tilde{M}_{(i,k)} \right) - \Phi_{\mathbf{i}}^\dagger \left(\bigotimes_{k=1}^R M_{(i,k)} \right) \right\|_\infty \quad (\text{S465})$$

$$\leq \epsilon_l + \left\| \bigotimes_{k=1}^R \tilde{M}_{(i,k)} - \bigotimes_{k=1}^R M_{(i,k)} \right\|_\infty \quad (\text{S466})$$

$$\leq \epsilon_l + \sum_{k=1}^R \left\| \tilde{M}_{(i,k)} - M_{(i,k)} \right\|_\infty \prod_{m \neq k} \max \left\{ \|M_{(i,m)}\|_\infty, \|\tilde{M}_{(i,m)}\|_\infty \right\} \quad (\text{S467})$$

$$\leq \epsilon_l + R x_{l+1} (1 + x_{l+1})^{R-1}, \quad (\text{S468})$$

where the inequality from the second to the third line uses that $\Phi_{\mathbf{i}}$ is CPTP. Hence, since $\Phi_{\mathbf{i}}^\dagger$ is unital and positive, $\Phi_{\mathbf{i}}^\dagger$ is contractive in the operator norm: $\|\Phi_{\mathbf{i}}^\dagger(A)\|_\infty \leq \|A\|_\infty$ for all Hermitian operators A . The following inequalities follow from Lemma 6 and the triangle inequality $\|\tilde{M}_{(i,m)}\|_\infty \leq \|M_{(i,m)}\|_\infty + \|\Delta M_{(i,m)}\|_\infty$.

Here, assume that x_{l+1} satisfies

$$x_{l+1} \leq \frac{1}{(e-1)R}. \quad (\text{S469})$$

Then, Lemma 5 implies that $(1 + x_{l+1})^{R-1} \leq 2$, and thus Eq. (S468) simplifies to

$$x_l \leq \epsilon_l + 2R x_{l+1}. \quad (\text{S470})$$

Combining Eq. (S461) with Eq. (S470), for $l = 1, \dots, L$, we arrive at

$$x_l \leq \sum_{k=l}^L (2R)^{k-l} \epsilon_k. \quad (\text{S471})$$

(iii) Learning process at depth 0

As the final step, we estimate $\hat{\mu}$ from $\{\tilde{M}_{i_1}\}_{i_1=1}^R$ and ρ . By the same argument as in Sec. V B, choosing x_1 such that

$$x_1 \leq \frac{\epsilon}{2R(e-1)} \quad (\text{S472})$$

implies

$$\left\| \bigotimes_{i_1=1}^R \tilde{M}_{i_1} - \bigotimes_{i_1=1}^R M_{i_1} \right\|_{\infty} \leq \frac{\epsilon}{2}. \quad (\text{S473})$$

Let ϵ_0 denote an upper bound on the estimation error at this step, i.e.,

$$\left| \hat{\mu} - \text{tr} \left[\bigotimes_{i_1=1}^R \tilde{M}_{i_1} \rho \right] \right| \leq \epsilon_0. \quad (\text{S474})$$

Similarly, it is sufficient to take

$$\epsilon_0 = \frac{\epsilon}{2}, \quad (\text{S475})$$

by the triangle inequality,

$$\left| \hat{\mu} - \text{tr} \left[\bigotimes_{i_1=1}^R M_{i_1} \rho \right] \right| \leq \left| \hat{\mu} - \text{tr} \left[\bigotimes_{i_1=1}^R \tilde{M}_{i_1} \rho \right] \right| + \left| \text{tr} \left[\bigotimes_{i_1=1}^R \tilde{M}_{i_1} \rho \right] - \text{tr} \left[\bigotimes_{i_1=1}^R M_{i_1} \rho \right] \right| \quad (\text{S476})$$

$$\leq \frac{\epsilon}{2} + \frac{\epsilon}{2} = \epsilon. \quad (\text{S477})$$

The condition on x_1 in Eq. (S472) can be satisfied by choosing

$$\epsilon_k = \frac{\epsilon}{(2R)^k (e-1)L} \quad \text{for each } k = 1, \dots, L, \quad (\text{S478})$$

which can be confirmed from Eq. (S471):

$$x_1 \leq \sum_{k=1}^L (2R)^{k-1} \frac{\epsilon}{(2R)^k (e-1)L} = \frac{\epsilon}{2R(e-1)}. \quad (\text{S479})$$

2. Shot allocation

We now choose the numbers of measurements $\{N_{(i_1, \dots, i_l)}\}_{l=1}^L$ and N_0 so that all accuracy requirements derived above hold simultaneously with probability at least $1 - \delta$. First, we summarize the good-tomography event for the learning procedure at each depth. For each depth $l = 1, \dots, L$ and each node $\mathbf{i} := (i_1, \dots, i_l) \in [R]^l$, define the local good-tomography event

$$E_{\mathbf{i}}^{(l)} := \left\{ \left\| \tilde{M}_{\mathbf{i}} - \Phi_{\mathbf{i}}^{\dagger} \left(\bigotimes_{k=1}^R \tilde{M}_{(i_k, k)} \right) \right\|_{\infty} \leq \epsilon_l \right\} \quad (l = 1, \dots, L-1). \quad (\text{S480})$$

At depth L , define

$$E_{\mathbf{i}}^{(L)} := \left\{ \left\| \tilde{M}_{\mathbf{i}} - \Phi_{\mathbf{i}}^{\dagger} (O_{\mathbf{i}}) \right\|_{\infty} \leq \epsilon_L \right\} \quad (\mathbf{i} \in [R]^L). \quad (\text{S481})$$

In addition, for $l = 1, \dots, L$, we define the good-tomography event G_l where all learning steps at depths $k = 1, \dots, L$ succeed:

$$G_l := \bigcap_{k=l}^L \bigcap_{\mathbf{j} \in [R]^k} E_{\mathbf{j}}^{(k)}. \quad (\text{S482})$$

Thus, G_1 is the global good-tomography event.

On G_{l+1} , we have $\|\Delta M_{(\mathbf{i},k)}\|_{\infty} \leq x_{l+1}$ for all (\mathbf{i},k) . Thus, for any node $\mathbf{i} \in [R]^l$, the following bound holds:

$$\left\| \bigotimes_{k=1}^R \tilde{M}_{(\mathbf{i},k)} \right\|_{\infty} \leq \prod_{k=1}^R \|\tilde{M}_{(\mathbf{i},k)}\|_{\infty} \leq \prod_{k=1}^R \left(\|M_{(\mathbf{i},k)}\|_{\infty} + \left\| M_{(\mathbf{i},k)} - \tilde{M}_{(\mathbf{i},k)} \right\|_{\infty} \right) \leq (1 + x_{l+1})^R. \quad (\text{S483})$$

With our choice of $\{\epsilon_k\}_{k=1}^L$ in Eq. (S478), we have $x_{l+1} \leq x_1 \leq 1/(e-1)R$, and Lemma 5 implies

$$\left\| \bigotimes_{k=1}^R \tilde{M}_{(\mathbf{i},k)} \right\|_{\infty} \leq (1 + x_{l+1})^R \leq 2. \quad (\text{S484})$$

Therefore, on G_{l+1} , the input observables of the learning step at depth l have operator norm at most 2.

Next, we will bound the global failure probability $\Pr[G_1^c]$. Fix $l \in \{1, \dots, L\}$ and $\mathbf{i} \in [R]^l$. Theorem 4 gives a performance guarantee of the form: for any Hermitian operator O with $\|O\|_{\infty} \leq 2$, sufficiently large $N_{\mathbf{i}}$ implies, for all realizations of past such that G_{l+1} occurs,

$$\Pr \left[(E_{\mathbf{i}}^{(l)})^c \mid \text{past} \right] \leq \delta_l, \quad (\text{S485})$$

where past denotes all random outcomes generated in the learning steps at depths $k = l+1, \dots, L$. Using the tower property, we have

$$\Pr \left[(E_{\mathbf{i}}^{(l)})^c \cap G_{l+1} \right] = \mathbb{E} \left[\mathbf{1}_{G_{l+1}} \Pr \left[(E_{\mathbf{i}}^{(l)})^c \mid \text{past} \right] \right] \leq \delta_l, \quad (\text{S486})$$

where $\mathbf{1}_{G_{l+1}}$ is the indicator function about G_{l+1} . Since $G_l = (\cap_{\mathbf{i} \in [R]^l} E_{\mathbf{i}}^{(l)}) \cap G_{l+1}$, we arrive at

$$\Pr[G_l^c] \leq \Pr[G_{l+1}^c] + \Pr \left[\left(\bigcup_{\mathbf{i} \in [R]^l} (E_{\mathbf{i}}^{(l)})^c \right) \cap G_{l+1} \right] \quad (\text{S487})$$

$$\leq \Pr[G_{l+1}^c] + \sum_{\mathbf{i} \in [R]^l} \Pr \left[(E_{\mathbf{i}}^{(l)})^c \cap G_{l+1} \right] \quad (\text{S488})$$

$$\leq \Pr[G_{l+1}^c] + R^l \delta_l, \quad (\text{S489})$$

where the last line uses Eq. (S486). Iterating Eq. (S489) from $l = L$ down to $l = 1$ yields the bound

$$\Pr[G_1^c] \leq \sum_{l=1}^L R^l \delta_l. \quad (\text{S490})$$

We then turn to consider the statistical estimation in the final step. Let

$$E_0 := \left\{ \left| \hat{\mu} - \text{tr} \left[\left(\bigotimes_{i_1=1}^R \tilde{M}_{i_1} \right) \rho \right] \right| \leq \epsilon_0 = \frac{\epsilon}{2} \right\}. \quad (\text{S491})$$

Conditioned on $\{\tilde{M}_{i_1}\}_{i_1=1}^R$, the N_0 samples are i.i.d. and bounded in $[-\gamma(\tilde{M}), \gamma(\tilde{M})]$ with $\gamma(\tilde{M}) = \left\| \bigotimes_{i_1=1}^R \tilde{M}_{i_1} \right\|_{\infty}$. On G_1 , the same argument as in Eq. (S484) gives $\gamma(\tilde{M}) \leq 2$. Hence, Hoeffding's inequality implies that on G_1 ,

$$\Pr \left[E_0^c \mid \tilde{M}_1, \dots, \tilde{M}_R \right] \leq 2 \exp \left(-\frac{N_0 \epsilon_0^2}{8} \right). \quad (\text{S492})$$

Taking expectation with the tower property gives

$$\Pr [E_0^c \cap G_1] = \mathbb{E} \left[\mathbf{1}_{G_1} \Pr \left[E_0^c \mid \tilde{M}_1, \dots, \tilde{M}_R \right] \right] \leq 2 \exp \left(-\frac{N_0 \epsilon_0^2}{8} \right). \quad (\text{S493})$$

Finally, combining Eqs. (S490) and (S493), we have

$$\Pr [(G_1 \cap E_0)^c] \leq \Pr [G_1^c] + \Pr [E_0^c \cap G_1] \leq \sum_{l=1}^L R^l \delta_l + 2 \exp \left(-\frac{N_0 \epsilon^2}{32} \right). \quad (\text{S494})$$

Choose $\{\delta_l\}$ such that $\sum_{l=1}^L R^l \delta_l \leq \delta/2$ and N_0 so that $2 \exp(-N_0 \epsilon^2/32) \leq \delta/2$. Then $\Pr[G_1 \cap E_0] \geq 1 - \delta$. On $G_1 \cap E_0$, the triangle inequality implies $|\hat{\mu} - \langle O \rangle_{\rho_{\text{tree}}}^c| \leq \epsilon$.

Building on the above analysis, we allocate the failure probability budget as

$$\delta_l := \frac{\delta}{2 \sum_{t=1}^L R^t}. \quad (\text{S495})$$

Then, $\sum_{l=1}^L R^l \delta_l \leq \delta/2$ holds by construction, and Eq. (S490) implies $\Pr[G_1^c] \leq \delta/2$.

Next, we choose N_0 so that the second term in Eq. (S494) is at most $\delta/2$. By Eq. (S493), it suffices to take

$$N_0 = \mathcal{O} \left(\frac{1}{\epsilon^2} \ln \left(\frac{R^L}{\delta} \right) \right), \quad (\text{S496})$$

which guarantees $\Pr[E_0^c \cap G_1] \leq \delta/2$.

Then, we determine the number of measurements $N_{(i_1, \dots, i_l)}$. Recalling Eq. (S484), we have the uniform bound on the input operator O as $\|O\|_\infty \leq 2$. We also remember that fixing $l \in \{1, \dots, L\}$ and $\mathbf{i} \in [R]^l$, Theorem 4 gives a performance guarantee such that for any Hermitian operator O with $\|O\|_\infty \leq 2$, sufficiently large $N_{\mathbf{i}}$ yields, for all realizations of past such that G_{l+1} occurs,

$$\Pr \left[(E_{\mathbf{i}}^{(l)})^c \mid \text{past} \right] \leq \delta_l. \quad (\text{S497})$$

Therefore, for the 2-design learning protocol, Theorem 4 with $\|O\|_\infty \leq 2$ implies that it suffices to take

$$N_{(i_1, \dots, i_l)} = \mathcal{O} \left(\frac{d^3}{\epsilon_l^2} \ln \left(\frac{d}{\delta_l} \right) \right), \quad (l = 1, \dots, L-1). \quad (\text{S498})$$

At depth L , Theorem 4 with $\|O_{(i_1, \dots, i_L)}\|_\infty \leq 1$ similarly implies

$$N_{(i_1, \dots, i_L)} = \mathcal{O} \left(\frac{d^3}{\epsilon_L^2} \ln \left(\frac{d}{\delta_L} \right) \right). \quad (\text{S499})$$

By substituting the choice of ϵ_l in Eq. (S478) and δ_l in Eq. (S495) in Eqs. (S498) and (S499), we have the sufficient number of measurements

$$N_{(i_1, \dots, i_l)} = \mathcal{O} \left(\frac{d^3 (2R)^{2l} L^2}{\epsilon^2} \ln \left(\frac{R^L d}{\delta_l} \right) \right), \quad l = 1, \dots, L, \quad (\text{S4100})$$

where we used $\sum_{l=1}^L R^l = \mathcal{O}(R^L)$ for $R \geq 2$.

Finally, the total number of measurements N_{tot} is given by

$$N_{\text{tot}} = N_0 + \sum_{l=1}^L \sum_{\mathbf{i} \in [R]^l} N_{\mathbf{i}} \quad (\text{S4101})$$

$$= \mathcal{O} \left(\frac{1}{\epsilon^2} \ln \left(\frac{R^L}{\delta} \right) \right) + \sum_{l=1}^L R^l \cdot \mathcal{O} \left(\frac{d^3 (2R)^{2l} L^2}{\epsilon^2} \ln \left(\frac{R^L d}{\delta} \right) \right) \quad (\text{S4102})$$

$$= \mathcal{O} \left(\frac{d^3 4^L L^2 R^{3L}}{\epsilon^2} \ln \left(\frac{R^L d}{\delta} \right) \right), \quad (\text{S4103})$$

which completes the proof. \square

4. Proof of Remark 1

Remark 1 ($R = 1$). Consider partitioning the quantum circuit in Fig. 7 at the wires between Φ_i and Φ_{i+1} for $i = 0, \dots, L-1$. Then the total number of measurements

$$\mathcal{O}\left(\frac{L^3d^3}{\epsilon^2} \ln\left(\frac{(L+1)d}{\delta}\right)\right) \quad (\text{S4104})$$

is sufficient to estimate the expectation value within additive error $\epsilon \in (0, 1]$ with probability at least $1 - \delta$.

Proof of Remark 1. Let $\rho := \Phi_0(|0^m\rangle\langle 0^m|)$ and define the effective observable M_l ($l = 1, \dots, L$) by

$$M_L := \Phi_L^\dagger(O_L), \quad M_l = \Phi_l^\dagger(O_l \otimes M_{l+1}) \quad (l = 1, \dots, L-1). \quad (\text{S4105})$$

Our computational strategy is to sequentially construct estimators of the effective observable M_l , denoted by \tilde{M}_l , in the order of

$$\tilde{M}_L \rightarrow \tilde{M}_{L-1} \rightarrow \dots \rightarrow \tilde{M}_1, \quad (\text{S4106})$$

and then estimate the expectation value $\mu := \text{tr}[(O_0 \otimes M_1)\rho]$. For the analysis, we define

$$x_l := \|\tilde{M}_l - M_l\|_\infty, \quad (l = 1, \dots, L). \quad (\text{S4107})$$

1. Accuracy requirement analysis

(i) Learning process at depth L

Given the known observable O_L and the unknown quantum channel Φ_L , we estimate $M_L := \Phi_L^\dagger(O_L)$ using the learning protocol in Sec. IV. Let $\epsilon_L > 0$ be an upper bound on the estimation error at depth L such that

$$\|\tilde{M}_L - \Phi_L^\dagger(O_L)\|_\infty \leq \epsilon_L. \quad (\text{S4108})$$

Thus, $x_L \leq \epsilon_L$.

(ii) Learning process at depth $l = 1, \dots, L-1$

Fix $l \in \{1, \dots, L-1\}$. Given the estimated effective observables \tilde{M}_{l+1} at depth $l+1$ and the unknown quantum channel Φ_l , we estimate $M_l = \Phi_l^\dagger(O_l \otimes M_{l+1})$ by constructing \tilde{M}_l as an estimator of $\Phi_l^\dagger(O_l \otimes \tilde{M}_{l+1})$. Let ϵ_l be an upper bound on the estimation error introduced at depth l such that

$$\|\tilde{M}_l - \Phi_l^\dagger(O_l \otimes \tilde{M}_{l+1})\|_\infty \leq \epsilon_l. \quad (\text{S4109})$$

Then, using the triangle inequality and contractivity of Φ_l^\dagger in operator norm since Φ_l is CPTP, and $\|O_l\|_\infty \leq 1$, we obtain

$$x_l = \|\tilde{M}_l - M_l\|_\infty \quad (\text{S4110})$$

$$\leq \|\tilde{M}_l - \Phi_l^\dagger(O_l \otimes \tilde{M}_{l+1})\|_\infty + \|\Phi_l^\dagger(O_l \otimes \tilde{M}_{l+1}) - \Phi_l^\dagger(O_l \otimes M_{l+1})\|_\infty \quad (\text{S4111})$$

$$\leq \epsilon_l + \|O_l \otimes (\tilde{M}_{l+1} - M_{l+1})\|_\infty \leq \epsilon_l + x_{l+1}. \quad (\text{S4112})$$

Iterating Eq. (S4112) from $l = L-1$ down to $l = 1$ and using $x_L \leq \epsilon_L$ yields

$$x_1 \leq \sum_{l=1}^L \epsilon_l. \quad (\text{S4113})$$

(iii) Learning process at depth 0

Given the estimated effective observables \tilde{M}_1 , an observable O_0 , the unknown quantum state ρ , we finally estimate $\mu = \text{tr}[(O_0 \otimes M_1)\rho]$. Here, Hölder's inequality with $\|O_0\|_\infty \leq 1$ yields

$$\left| \text{tr}[(O_0 \otimes \tilde{M}_1)\rho] - \text{tr}[(O_0 \otimes M_1)\rho] \right| \leq \|O_0 \otimes (\tilde{M}_1 - M_1)\|_\infty \leq x_1. \quad (\text{S4114})$$

Therefore, it is sufficient to ensure

$$x_1 \leq \frac{\epsilon}{2}, \quad (\text{S4115})$$

and to estimate $\text{tr}[(O_0 \otimes \tilde{M}_1)\rho]$ within $\epsilon/2$. By Eq. (S4113), it suffices to choose

$$\epsilon_l = \frac{\epsilon}{2L}, \quad (l = 1, \dots, L), \quad (\text{S4116})$$

which implies $x_1 \leq \sum_{k=1}^L \epsilon_k = \epsilon/2$.

2. Shot allocation

Define the local good-tomography events

$$E_L := \left\{ \left\| \tilde{M}_L - \Phi_L^\dagger(O_L) \right\|_\infty \leq \epsilon_L \right\}, \quad (\text{S4117})$$

$$E_l := \left\{ \left\| \tilde{M}_l - \Phi_l^\dagger(O_l \otimes \tilde{M}_{l+1}) \right\|_\infty \leq \epsilon_l \right\}, \quad (l = 1, \dots, L-1) \quad (\text{S4118})$$

and the event

$$G_l := \bigcap_{k=l}^L E_k, \quad (l = 1, \dots, L). \quad (\text{S4119})$$

Thus, G_1 is the global success event for all learning steps.

On G_{l+1} , by iterating Eq. (S4112), we obtain

$$x_{l+1} = \left\| \tilde{M}_{l+1} - M_{l+1} \right\|_\infty \leq \sum_{k=l+1}^L \epsilon_k \leq \sum_{k=1}^L \epsilon_k = \frac{\epsilon}{2}. \quad (\text{S4120})$$

Since $\|M_{l+1}\|_\infty \leq 1$ and $\|O_l\|_\infty \leq 1$, we have

$$\|O_l \otimes \tilde{M}_{l+1}\|_\infty \leq \|\tilde{M}_{l+1}\|_\infty \quad (\text{S4121})$$

$$\leq \|M_{l+1}\|_\infty + \|\tilde{M}_{l+1} - M_{l+1}\|_\infty \quad (\text{S4122})$$

$$\leq 1 + \frac{\epsilon}{2}. \quad (\text{S4123})$$

With $\epsilon \in (0, 1]$, we have $\gamma \leq 3/2$. Hence, on G_{l+1} , the learning protocol at depth l receives an input observable of operator norm at most $3/2$.

Fix $l \in \{1, \dots, L-1\}$. Conditioned on all random outcomes generated at steps $k = l+1, \dots, L$, denoted by past, the input $O_l \otimes \tilde{M}_{l+1}$ is fixed. By Theorem 4 with $\|O\|_\infty \leq 3/2$, for sufficiently large N_l , we have, for all realizations of past such that G_{l+1} occurs,

$$\Pr[E_l^c \mid \text{past}] \leq \delta_l. \quad (\text{S4124})$$

Taking expectation with the tower property yields

$$\Pr[E_l^c \cap G_{l+1}] = \mathbb{E} [\mathbf{1}_{G_{l+1}} \Pr[E_l^c \mid \text{past}]] \leq \delta_l, \quad (\text{S4125})$$

where $\mathbf{1}_{G_{l+1}}$ is the indicator function about G_{l+1} . Since $G_l = E_l \cap G_{l+1}$, we obtain

$$\Pr[G_l^c] \leq \Pr[G_{l+1}^c] + \Pr[E_l^c \cap G_{l+1}] \quad (\text{S4126})$$

$$\leq \Pr[G_{l+1}^c] + \delta_l. \quad (\text{S4127})$$

Iterating Eq. (S4127) from $l = L-1$ down to $l = 1$ and using $\Pr[G_L^c] = \Pr[E_L^c] \leq \delta_L$ gives

$$\Pr[G_1^c] \leq \sum_{l=1}^L \delta_l. \quad (\text{S4128})$$

Let $\hat{\mu}$ be the empirical mean obtained by measuring ρ in the eigenbasis of $O_0 \otimes \tilde{M}_1$ and appropriately weighting outcomes. Define

$$E_0 := \left\{ \left| \hat{\mu} - \text{tr}[(O_0 \otimes \tilde{M}_1)\rho] \right| \leq \epsilon_0 := \frac{\epsilon}{2} \right\}. \quad (\text{S4129})$$

Conditioned on \tilde{M}_1 , the samples are i.i.d. and bounded in $[-\gamma, \gamma]$ with $\gamma = \|O_0 \otimes \tilde{M}_1\|_\infty \leq \|\tilde{M}_1\|_\infty$. On G_1 , Eq. (S4123) yields $\gamma \leq 1 + x_1 \leq 3/2$. Thus, on G_1 , Hoeffding's inequality gives

$$\Pr(E_0^c \mid \tilde{M}_1) \leq 2 \exp\left(-\frac{N_0(\epsilon/2)^2}{2\gamma^2}\right) \leq 2 \exp\left(-\frac{N_0\epsilon^2}{18}\right). \quad (\text{S4130})$$

Taking expectation with the tower property yields

$$\Pr(E_0^c \cap G_1) \leq 2 \exp\left(-\frac{N_0\epsilon^2}{18}\right). \quad (\text{S4131})$$

Building on the derived results above, we will choose δ_l , N_l , and N_0 . First, we set δ_l as

$$\delta_l := \frac{\delta}{2(L+1)} \quad (l = 1, \dots, L), \quad (\text{S4132})$$

so that $\sum_{l=1}^L \delta_l \leq \delta/2$. By Eq. (S4128), we have $\Pr[G_1^c] \leq \delta/2$.

Next, we choose N_0 so that the right-hand side of Eq. (S4131) is at most $\delta/2$. Then, it suffices to take

$$N_0 = \mathcal{O}\left(\frac{1}{\epsilon^2} \ln\left(\frac{L+1}{\delta}\right)\right). \quad (\text{S4133})$$

For the learning steps, Theorem 4 yields that it suffices to take for each $l = 1, \dots, L$,

$$N_L = \mathcal{O}\left(\frac{d^3}{\epsilon_l^2} \ln\left(\frac{d}{\delta_l}\right)\right), \quad (\text{S4134})$$

$$N_l = \mathcal{O}\left(\frac{d^3}{\epsilon_l^2} \ln\left(\frac{d}{\delta_l}\right)\right) \quad (l = 1, \dots, L-1). \quad (\text{S4135})$$

Substituting Eqs. (S4116) and (S4132) into Eqs. (S4134) and (S4135) gives

$$N_l = \mathcal{O}\left(\frac{L^2 d^3}{\epsilon^2} \ln\left(\frac{(L+1)d}{\delta}\right)\right) \quad (l = 1, \dots, L). \quad (\text{S4136})$$

Therefore, the total number of measurements N_{tot} is given by

$$N_{\text{tot}} = N_0 + \sum_{l=1}^L N_l \quad (\text{S4137})$$

$$= \mathcal{O}\left(\frac{1}{\epsilon^2} \ln\left(\frac{L+1}{\delta}\right)\right) + L \cdot \mathcal{O}\left(\frac{L^2 d^3}{\epsilon^2} \ln\left(\frac{(L+1)d}{\delta}\right)\right) \quad (\text{S4138})$$

$$= \mathcal{O}\left(\frac{L^3 d^3}{\epsilon^2} \ln\left(\frac{(L+1)d}{\delta}\right)\right), \quad (\text{S4139})$$

which completes the proof. \square

Appendix S5: Exponential separation in the number of cuts compared to conventional wire-cutting methods (Proof of Theorem 7)

Theorem 7. *Consider solving Task 1 using either the learning-based approach described in Sec. V B or a conventional quasiprobability-based wire-cutting approach described in Algorithm 1.*

- Upper bound: *The learning-based approach can solve Task 1 using at most $\mathcal{O}(R^3 d^3 \ln((R+1)d) / \epsilon^2)$ total measurements, for any quantum state ρ , CPTP maps Φ_k , and observable O .*

- Lower bound: Any quasiprobability-based wire-cutting requires at least $\Omega((d+1)^R/\epsilon^2)$ measurements to solve Task 1.

Proof of Theorem 7. The upper bound can be directly derived from Theorem 5. In what follows, we establish the information-theoretic lower bound on the sample complexity for solving Task 1 using the conventional wire-cutting protocol, as described in Algorithm 1. To this end, we consider a quantum state discrimination task that utilizes Algorithm 1.

We begin by defining two d^R -dimensional quantum states as follows:

$$\tau_x := \frac{1}{d^R} (I + (-1)^x \epsilon \bar{Z}), \quad x = 0, 1 \quad (\text{S51})$$

where $\bar{Z} := \bigotimes_{r=1}^R \bar{Z}^{(r)}$ is an nR -qubit Pauli operator, and each

$$\bar{Z}^{(r)} := \bigotimes_{i=1}^n Z_i \quad (\text{S52})$$

denotes the tensor product of single-qubit Pauli-Z operators acting on the i -th qubit.

For each $r \in \{1, \dots, R\}$, we independently and randomly sample a unitary operator U_r from the Haar measure on the d -dimensional unitary group $U(\mathbb{C}^d)$. Using the tensor products of the unitaries $U := U_1 \otimes \dots \otimes U_R$ together with τ_X , we also define the following two quantum states as

$$\rho_x := U \tau_x U^\dagger = \frac{1}{d^R} (I + (-1)^x \epsilon U \bar{Z} U^\dagger), \quad x = 0, 1. \quad (\text{S53})$$

With these objects introduced above, we now consider the following discrimination task: Given a quantum state ρ_x where $x \in \{0, 1\}$ is chosen uniformly at random, we run Algorithm 1 with inputs $\rho = \rho_x$, $\Phi_r = U_r^\dagger$ and $O_r = \bar{Z}^{(r)}$. The goal is to determine the label x based on the outputs of the algorithm.

Under the above setting, the expectation value $\text{tr}(O \rho_{\text{tree}})$ satisfies

$$\text{tr}(O \rho_{\text{tree}}) = \text{tr} [\bar{Z} U^\dagger U \tau_x U^\dagger U] = (-1)^x \epsilon. \quad (\text{S54})$$

Hence, by estimating the expectation value $\text{tr}(O \rho_{\text{tree}})$ in Algorithm 1 with accuracy at least $\epsilon/3$, one can predict the label x with high probability. Let $\boldsymbol{\eta} := (\boldsymbol{\eta}_1, \dots, \boldsymbol{\eta}_N)$, $\mathbf{y} = (\mathbf{y}_1, \dots, \mathbf{y}_N)$, and $\mathbf{z} = (\mathbf{z}_1, \dots, \mathbf{z}_N)$. By Fano's inequality, this implies that

$$I(x : \boldsymbol{\eta}, \mathbf{y}, \mathbf{z}) = H(x) - H(x | \boldsymbol{\eta}, \mathbf{y}, \mathbf{z}) \geq \Omega(1), \quad (\text{S55})$$

where $I(A : B)$ denotes the mutual information, and $H(A)$ is the Shannon entropy.

On the other hand, since U and the variable $\boldsymbol{\eta}$ are independent of the variable x , we have $I(x : U, \boldsymbol{\eta}) = 0$ and hence

$$\begin{aligned} I(x : \boldsymbol{\eta}, \mathbf{y}, \mathbf{z}) &\leq I(x : \boldsymbol{\eta}, \mathbf{y}, \mathbf{z}, U) \\ &= I(x : U, \boldsymbol{\eta}) + I(x : \mathbf{y}, \mathbf{z} | U, \boldsymbol{\eta}) \\ &= I(x : \mathbf{y}, \mathbf{z} | U, \boldsymbol{\eta}) \end{aligned} \quad (\text{S56})$$

Conditioning on U and $\boldsymbol{\eta}$, the single-round variables forms a Markov chain $x \rightarrow \mathbf{y}_i \rightarrow \mathbf{z}_i$, so by the data processing inequality, $I(x : \mathbf{z} | \mathbf{y}, U, \boldsymbol{\eta}) = 0$ and thus

$$\begin{aligned} I(x : \mathbf{y}, \mathbf{z} | U, \boldsymbol{\eta}) &= I(x : \mathbf{y} | U, \boldsymbol{\eta}) + I(x : \mathbf{z} | \mathbf{y}, U, \boldsymbol{\eta}) \\ &= I(x : \mathbf{y} | U, \boldsymbol{\eta}) \end{aligned} \quad (\text{S57})$$

Then, by independence of rounds given $(x, U, \boldsymbol{\eta})$,

$$I(x : \mathbf{y} | U, \boldsymbol{\eta}) = H(\mathbf{y}_1, \dots, \mathbf{y}_N | U, \boldsymbol{\eta}) - H(\mathbf{y}_1, \dots, \mathbf{y}_N | x, U, \boldsymbol{\eta}) \quad (\text{S58})$$

$$\leq \sum_{i=1}^N (H(\mathbf{y}_i | U, \boldsymbol{\eta}) - H(\mathbf{y}_i | x, U, \boldsymbol{\eta})) \quad (\text{S59})$$

$$= \sum_{i=1}^N I(x : \mathbf{y}_i | U, \boldsymbol{\eta}) \quad (\text{S510})$$

In addition, each term can be evaluated as

$$I(x : \mathbf{y}_i | U, \boldsymbol{\eta}) = I(x : \mathbf{y}_i | U, \boldsymbol{\eta}_i) \quad (\text{S511})$$

$$= I(x : \mathbf{y}_i, \boldsymbol{\eta}_i | U) \quad (\text{S512})$$

$$\leq I(x, U : \mathbf{y}_i, \boldsymbol{\eta}_i) \quad (\text{S513})$$

where the first equality comes from the fact that $\boldsymbol{\eta}_i$ are sampled independently across rounds and are independent of (x, U) and the i -th measurement outcome depends only on $(x, U, \boldsymbol{\eta}_i)$. The last inequality uses the chain rules for the mutual information.

Now, to proceed the calculation, we use the fact that any POVM can be simulated with rank-1 POVM and classical processing. In our case, each element $M_{\boldsymbol{\eta}_i, \mathbf{y}_i}$ of the POVM $\{M_{\boldsymbol{\eta}_i, \mathbf{y}_i}\}_{\mathbf{y}_i}$ can be simulated with $\{\omega_{\boldsymbol{\eta}_i, s} d^R |v_{\boldsymbol{\eta}_i, s}\rangle \langle v_{\boldsymbol{\eta}_i, s}|\}_s$ where $|v_{\boldsymbol{\eta}_i, s}\rangle = |v_{\boldsymbol{\eta}_i, s}^1\rangle \otimes \dots \otimes |v_{\boldsymbol{\eta}_i, s}^R\rangle$ and $\sum_s \omega_{\boldsymbol{\eta}_i, s} = 1$. By the data processing inequality, we have

$$I(x, U : \mathbf{y}_i, \boldsymbol{\eta}_i) \leq I(x, U : s, \boldsymbol{\eta}_i) \quad (\text{S514})$$

Then, let us define $p_{\boldsymbol{\eta}_i, s} := p_{\boldsymbol{\eta}_i} \omega_{\boldsymbol{\eta}_i, s} d^R \langle v_{\boldsymbol{\eta}_i, s} | U \tau_x U^\dagger | v_{\boldsymbol{\eta}_i, s} \rangle$ denote the joint probability distribution of \mathbf{y}_i and $\boldsymbol{\eta}_i$ conditioned on x and U . Then, we have

$$I(x : \mathbf{y}_i | U, \boldsymbol{\eta}) \leq I(x, U : s, \boldsymbol{\eta}_i) \quad (\text{S515})$$

$$= \sum_{\boldsymbol{\eta}_i, s} \{ -(\mathbb{E}_{U, x}[p_{\boldsymbol{\eta}_i, s}]) \log(\mathbb{E}_{U, x}[p_{\boldsymbol{\eta}_i, s}]) + \mathbb{E}_{U, x}[p_{\boldsymbol{\eta}_i, s} \log(p_{\boldsymbol{\eta}_i, s})] \} \quad (\text{S516})$$

$$\leq \sum_{\boldsymbol{\eta}_i, s} \left\{ -(\mathbb{E}_{U, x}[p_{\boldsymbol{\eta}_i, s}]) \log(\mathbb{E}_{U, x}[p_{\boldsymbol{\eta}_i, s}]) + \mathbb{E}_{U, x} \left[p_{\boldsymbol{\eta}_i, s} \log(\mathbb{E}_{U, x}[p_{\boldsymbol{\eta}_i, s}]) + p_{\boldsymbol{\eta}_i, s} \frac{p_{\boldsymbol{\eta}_i, s} - \mathbb{E}_{U, x}[p_{\boldsymbol{\eta}_i, s}]}{\mathbb{E}_{U, x}[p_{\boldsymbol{\eta}_i, s}]} \right] \right\} \quad (\text{S517})$$

$$= \sum_{\boldsymbol{\eta}_i, s} \frac{\mathbb{E}_{U, x}[p_{\boldsymbol{\eta}_i, s}^2] - \mathbb{E}_{U, x}[p_{\boldsymbol{\eta}_i, s}]^2}{\mathbb{E}_{U, x}[p_{\boldsymbol{\eta}_i, s}]} \quad (\text{S518})$$

where in the second inequality, we use the fact that $\log(\bullet)$ is the concave function. Hence, it remains to evaluate the first and the second moment of $p_{\boldsymbol{\eta}_i, s}$.

Here, averaging over $x \in \{0, 1\}$ yields $\mathbb{E}_x[\tau_x] = I/d^R$, we have

$$\mathbb{E}_{U, x}[p_{\boldsymbol{\eta}_i, s}] = p_{\boldsymbol{\eta}_i} \omega_{\boldsymbol{\eta}_i, s} d^R \mathbb{E}_{U, x} [\langle v_{\boldsymbol{\eta}_i, s} | U \tau_x U^\dagger | v_{\boldsymbol{\eta}_i, s} \rangle] \quad (\text{S519})$$

$$= p_{\boldsymbol{\eta}_i} \omega_{\boldsymbol{\eta}_i, s}. \quad (\text{S520})$$

For the second moment, we have

$$\mathbb{E}_{U, x}[p_{\boldsymbol{\eta}_i, s}^2] = p_{\boldsymbol{\eta}_i}^2 \omega_{\boldsymbol{\eta}_i, s}^2 d^{2R} \text{tr} \left[\mathbb{E}_x[\tau_x^{\otimes 2}] \bigotimes_{r=1}^R \mathbb{E}_{U_r} (U_r^\dagger |v_{\boldsymbol{\eta}_i, s}^r\rangle \langle v_{\boldsymbol{\eta}_i, s}^r| U_r)^{\otimes 2} \right] \quad (\text{S521})$$

$$= p_{\boldsymbol{\eta}_i}^2 \omega_{\boldsymbol{\eta}_i, s}^2 d^{2R} \text{tr} \left[\frac{1}{d^{2R}} (I \otimes I + \epsilon^2 \bar{Z} \otimes \bar{Z}) \bigotimes_{r=1}^R \mathbb{E}_{U_r} (U_r^\dagger |v_{\boldsymbol{\eta}_i, s}^r\rangle \langle v_{\boldsymbol{\eta}_i, s}^r| U_r)^{\otimes 2} \right] \quad (\text{S522})$$

$$= p_{\boldsymbol{\eta}_i}^2 \omega_{\boldsymbol{\eta}_i, s}^2 \text{tr} \left[(I \otimes I + \epsilon^2 \bar{Z} \otimes \bar{Z}) \bigotimes_{r=1}^R \frac{I \otimes I + \text{SWAP}}{d(d+1)} \right] \quad (\text{S523})$$

$$= p_{\boldsymbol{\eta}_i}^2 \omega_{\boldsymbol{\eta}_i, s}^2 \left(\prod_{r=1}^R \text{tr} \left[\frac{I \otimes I + \text{SWAP}}{d(d+1)} \right] + \epsilon^2 \prod_{r=1}^R \text{tr} \left[\bar{Z}^{(r)} \otimes \bar{Z}^{(r)} \cdot \frac{I \otimes I + \text{SWAP}}{d(d+1)} \right] \right) \quad (\text{S524})$$

$$= p_{\boldsymbol{\eta}_i}^2 \omega_{\boldsymbol{\eta}_i, s}^2 \left(1 + \epsilon^2 \frac{1}{(d+1)^R} \right), \quad (\text{S525})$$

where in the second equality we use $\mathbb{E}_x[\tau_x^{\otimes 2}] = (I \otimes I + \bar{Z} \otimes \bar{Z})/d^{2R}$ by the definition of τ_x in Eq. (S51); in the third equality, we applied the standard Haar twirling identity for rank-1 projectors,

$$\mathbb{E}_{U_r} (U_r^\dagger |v_{\boldsymbol{\eta}_i, s}^r\rangle \langle v_{\boldsymbol{\eta}_i, s}^r| U_r)^{\otimes 2} = \frac{I \otimes I + \text{SWAP}}{d(d+1)} \quad (\text{S526})$$

valid for any fixed $|v_{\boldsymbol{\eta}_i, s}^r\rangle$ in dimension d . Inserting the calculation results Eqs. (S520) and (S525), into (S518), we have

$$I(x : \mathbf{y}_i | U, \boldsymbol{\eta}_i) \leq \sum_{\boldsymbol{\eta}_i, s} p_{\boldsymbol{\eta}_i} \omega_{\boldsymbol{\eta}_i, s} \left(1 + \epsilon^2 \frac{1}{(d+1)^R} \right) - 1 \quad (\text{S527})$$

$$= \epsilon^2 \frac{1}{(d+1)^R}. \quad (\text{S528})$$

The above result, together with the lower bound derived in Eq. (S55), yields

$$\Omega(1) \leq I(x : \boldsymbol{\eta}, \mathbf{y}, \mathbf{z}) \leq \frac{N\epsilon^2}{(d+1)^R}. \quad (\text{S529})$$

Thus, we have established the lower bound

$$N \geq \Omega\left(\frac{(d+1)^R}{\epsilon^2}\right). \quad (\text{S530})$$

□

Appendix S6: Relation to existing quantum circuit-cutting methods

We review several broad directions in prior work aimed at reducing the sampling overhead in quantum circuit cutting, and discuss how our results relate to these approaches. Quantum circuit cutting was introduced in Ref. [14] as a method for partitioning a clustered quantum system. The cutting approach employed in this work belongs to the category of wire cutting rather than gate cutting, and is based on mid-circuit Pauli measurements. Specifically, the authors use the following decomposition of the n -qubit identity channel id^n to partition a quantum circuit into subcircuits:

$$\text{id}^n(\rho) = \frac{1}{2^n} \sum_{\mathbf{i} \in [4]^n} \text{tr}[P_{\mathbf{i}}\rho] P_{\mathbf{i}} := \sum_{\mathbf{i} \in [4]^n} \mathcal{E}_{P_{\mathbf{i}}}(\rho), \quad (\text{S61})$$

where $[4] = \{1, \dots, 4\}$, $\mathbf{i} = (i_1, \dots, i_n)$, and $\{P_1, P_2, P_3, P_4\} = \{I, \text{X}, \text{Y}, \text{Z}\}$. Each term can be viewed as a process that measures the input state ρ in the Pauli observable $P_{\mathbf{i}}$ and then prepares $P_{\mathbf{i}}$ as a new input. Note that $\mathcal{E}_{P_{\mathbf{i}}}$ is a linear map and is not CPTP. Thus, in the standard wire-cutting protocol, it is implemented via randomized eigenstate preparation together with classical post-processing to form an unbiased estimator. Concretely, one rewrites the expansion into an implementable form using randomized eigenstate preparation and classical post-processing:

$$\text{id}^n = \sum_{\mathbf{i} \in [4]^n} \mathcal{E}_{P_{\mathbf{i}}}, \quad \mathcal{E}_{P_{\mathbf{i}}}(\rho) = \sum_{\mathbf{e} \in [2]^n} c_{\mathbf{i}, \mathbf{e}} \text{tr}[|v_{\mathbf{i}, \mathbf{e}}\rangle \langle v_{\mathbf{i}, \mathbf{e}}| \rho] \sum_{\mathbf{e}' \in [2]^n} p_{\mathbf{e}'} c_{\mathbf{i}, \mathbf{e}'} |v_{\mathbf{i}, \mathbf{e}'}\rangle \langle v_{\mathbf{i}, \mathbf{e}'}|, \quad (\text{S62})$$

where $p_{\mathbf{e}'} := 1/2^n$ is the probability distribution, and $c_{\mathbf{i}, \mathbf{e}} \in \{\pm 1\}$ and $|v_{\mathbf{i}, \mathbf{e}}\rangle$ denote the eigenvalue and eigenstate of $P_{\mathbf{i}}$, respectively, following the notation introduced in Appendix S3.2.c. Operationally, $\mathcal{E}_{P_{\mathbf{i}}}(\rho) = (1/2^n) \text{tr}[P_{\mathbf{i}}\rho] P_{\mathbf{i}}$ corresponds to performing a projective measurement in the eigenbasis $\{|v_{\mathbf{i}, \mathbf{e}}\rangle\}_{\mathbf{e}}$ of $P_{\mathbf{i}}$, preparing an eigenstate randomly sampled from $\{|v_{\mathbf{i}, \mathbf{e}'}\rangle\}_{\mathbf{e}'}$, and then multiplying the circuit output by $c_{\mathbf{i}, \mathbf{e}} c_{\mathbf{i}, \mathbf{e}'}$ in classical post-processing. Note that $\mathcal{E}_{P_{\mathbf{i}}}$ can also be rewritten as a probabilistic mixture of operations defined in Eq. (5). While wire cutting separates a circuit along the time direction, gate cutting was later introduced in Ref. [24] as an approach to separate a circuit along the spatial direction.

Both wire and gate cutting rely on the general framework of quasiprobability simulation (see Appendix S1). In this framework, the sampling overhead is governed by the factor $\gamma^2 := (\sum_i |a_i|)^2$ of a given quasiprobability decomposition (QPD) $\sum_{i=1}^m a_i \mathcal{E}_i$: for estimating an expectation value within a fixed additive error, a QPD with overhead γ typically increases the sufficient number of circuit shots by a factor γ^2 . If a decomposition with overhead γ_k is applied at locations $k = 1, \dots, K$, the total sampling overhead scales as $\prod_{k=1}^K \gamma_k^2$. Moreover, the number m of operations appearing in each decomposition affects the total execution time [21, 112].

To reduce this sampling overhead, many prior studies have pursued two broad approaches. The first direction focuses on minimizing the number K of cuts, using classical optimization techniques to select cutting locations so that the total number of cuts is as small as possible [35–37]. The second direction targets reducing the factor γ and has mainly employed the following two types of approaches:

1. Developing quasiprobability decompositions with smaller γ .
2. Restricting the circuit structure to eliminate certain bases from the quasiprobability decomposition.

In the following, we briefly review these two approaches and explain how our results relate to the existing methods.

Main primitive in MP channels \mathcal{M}_i	LOCC	Number of ancilla qubits	Multiplicative factor $\gamma := \sum_i a_i $	Optimality of γ
[14]	Pauli measurement	No	0	4^n
[19]	Random Clifford measurement	Yes	0	$2^{n+1} + 1$
[20]	Quantum teleportation & Virtual Bell pairs	Yes	n	$2^{n+1} - 1$
[21]	Mutually unbiased bases (MUBs)	Yes	0	$2^{n+1} - 1$
[22]	Random Clifford measurement	Yes	0	$2^{n+1} - 1$
[23]	Random diagonal unitary 2-designs	Yes	0	$2^{n+1} - 1$

TABLE S1. Comparison of existing quasiprobability decompositions for wire cuts of the form $\text{id}^n = \sum_{i=1}^m a_i \mathcal{M}_i$, where $a_i \in \mathbb{R}$ and \mathcal{M}_i represent MP channels. Here “LO” denotes local operations without classical communication, whereas “LOCC” allows classical communication.

1. Developing quasiprobability decompositions with smaller sampling overhead

One of the central directions in quantum circuit cutting is to design decompositions with small sampling overhead. In this subsection, we focus on wire cuts, which are most relevant to our work, and discuss how existing constructions relate to our results.

Review of prior works As introduced above, the first wire-cutting protocol was proposed in Ref. [14], using mid-circuit Pauli measurements as in Eq. (S62). A key feature of this protocol is that no classical communication is used inside each MP channel: the state preparation is performed independently of the measurement outcome. Subsequent works reduced the factor γ below the 4^n in Eq. (S62), by allowing classical communication within each MP channel. This line of work on wire cuts began with Ref. [19], which expressed the n -qubit identity channel as a linear combination of MP channels based on random Clifford measurements. This protocol achieves $\gamma = 2^{n+1} + 1$. Later, Ref. [20] proved the lower bound $\gamma \geq 2^{n+1} - 1$ when classical communication is allowed within each MP channel, and also provided a decomposition that achieves this bound using n additional qubits. This ancilla overhead motivated follow-up work developing alternative decompositions that preserve the optimal sampling overhead while reducing ancillary requirements [21–23]; see Table S1.

Comparison with our result Prior work has established the lower bound $\gamma \geq 2^{n+1} - 1$ for quasiprobability decompositions for wire cuts under the standard assumptions. By contrast, Theorem 1 yields a decomposition with $\gamma = 1$, which looks incompatible with the bound at first glance. This arises from a difference in the formulation of the quasiprobability decomposition. In the standard formulation adopted in earlier works [14, 19–23], one demands an exact representation of the entire target operation.

Definition 6 (Quasiprobability decomposition). Let \mathcal{T} be a target operation and let S be a set of implementable operations. A quasiprobability decomposition of \mathcal{T} over S is a representation

$$\mathcal{T} = \sum_i a_i \mathcal{E}_i, \quad (\text{S63})$$

where $a_i \in \mathbb{R}$ and $\mathcal{E}_i \in S$. We define $\gamma := \sum_i |a_i|$ and refer to γ^2 as the sampling overhead.

In contrast, our approach only requires consistency at the level of observable expectation values. That is, we consider the expectation-value-level quasiprobability decomposition, defined as follows.

Definition 7 (Expectation-value level quasiprobability decomposition). Let \mathcal{T} be a target operation and let S be a set of implementable operations. Fix a CPTP map Φ , an observable O , and a quantum state ρ . For the task of estimating $\text{tr}[O\Phi \circ \mathcal{T}(\rho)]$, we call a representation an expectation-value-level quasiprobability decomposition if it satisfies

$$\text{tr}[O\Phi \circ \mathcal{T}(\rho)] = \sum_i a_i \text{tr}[O\Phi \circ \mathcal{E}_i(\rho)], \quad (\text{S64})$$

where $a_i \in \mathbb{R}$ and $\mathcal{E}_i \in S$. For such a decomposition, we define $\gamma_{\text{eff}} := \sum_i |a_i|$ and refer to γ_{eff}^2 as the effective sampling overhead.

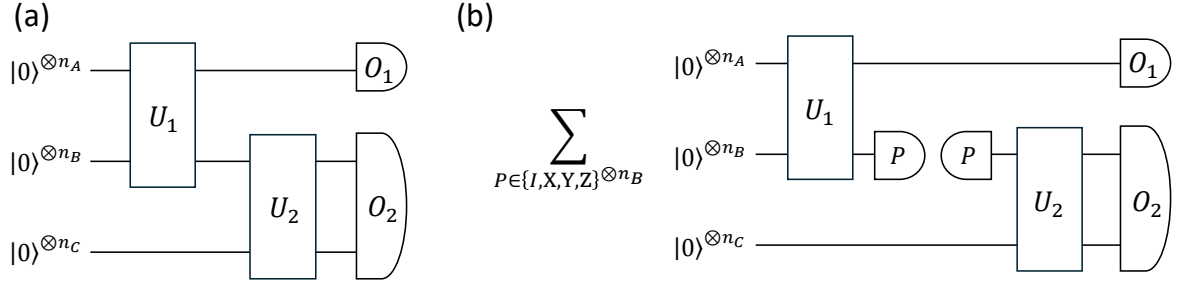


FIG. S1. (a) Quantum circuit before the decomposition. The circuit consists of the $(n_A + n_B + n_C)$ -qubit initial state $|0\rangle^{\otimes(n_A+n_B+n_C)}$, two unitary gates U_1 and U_2 , and the diagonal observable $O = O_1 \otimes O_2$ where $\|O_1\|_\infty, \|O_2\|_\infty \leq 1$. (b) Quantum circuit after the decomposition. By inserting the Pauli expansion (S61) on register B between U_1 and U_2 , the circuit is separated into two subcircuits.

We emphasize that in many settings of interest, ρ and/or Φ are not known classically. Thus, the expectation-value-level QPD should often be understood as an existence result about a decomposition that avoids the additional rescaling factor γ_{eff} in the evaluation phase. Finding such a decomposition in practice may require an additional estimation step for ρ and/or Φ , whose sample complexity is not captured by γ_{eff} .

In the context of the wire-cutting problem, previous work considers decompositions of the form

$$\text{id}^n = \sum_i a_i \mathcal{M}_i, \quad (\text{S65})$$

where $a_i \in \mathbb{R}$ and $\mathcal{M}_i \in \text{MP}$, with MP denoting the set of MP channels (with classical post-processing; see Eq. (5)). Within this standard notion of the quasiprobability decomposition (Definition 6), the ℓ_1 -norm of the coefficients a_i obey the lower bound $\gamma \geq 2^{n+1} - 1$. In contrast, Theorem 1 provides a decomposition in the sense of Definition 7:

$$\text{tr}[O\Phi \circ \text{id}^n(\rho)] = \sum_i a_i \text{tr}[O\Phi \circ \mathcal{M}_i(\rho)], \quad (\text{S66})$$

where $a_i \in \mathbb{R}$ and $\mathcal{M}_i \in \text{MP}$. The theorem shows that there exists a decomposition with $\gamma_{\text{eff}} = 1$. Here, it is important to note that, while Definition 7 fixes Φ , ρ , and O , the decomposition in Theorem 1 remains valid even for varying input states ρ , as long as Φ and O are fixed.

2. Reduction of sampling overhead via structure-aware methods

Another major line of research reduces the sampling overhead by leveraging the fact that, for certain fixed quantum circuits, many terms in the mid-circuit Pauli expansion contribute exactly zero to the target expectation value. Below, we summarize the main prior works [113–115], and show that these works can be reformulated in the language of expectation-value-level QPDs.

Review of prior works These works consider quantum circuits of the form shown in Fig. S1. The quantum circuit before the decomposition (Fig. S1(a)) starts from the $n_{\text{tot}} := (n_A + n_B + n_C)$ -qubit initial state $|0\rangle^{\otimes n_{\text{tot}}}$, followed by two unitary channels $\mathcal{U}_1(\cdot) = U_1 \cdot U_1^\dagger$ and $\mathcal{U}_2(\cdot) = U_2 \cdot U_2^\dagger$ acting on registers (A, B) and (B, C) , respectively. Measurement is performed using a diagonal observable $O := O_1 \otimes O_2$ where O_1 acts on A , O_2 acts on (B, C) , and $\|O_1\|_\infty, \|O_2\|_\infty \leq 1$. The decomposed quantum circuit (Fig. S1(b)) consists of two subcircuits obtained by inserting the Pauli expansion (S62) on register B between \mathcal{U}_1 and \mathcal{U}_2 . Using Eq. (S61) for id^{n_B} , the original expectation value $\langle O \rangle := \text{tr}[O\mathcal{U}_2 \circ \mathcal{U}_1(|0\rangle\langle 0|^{\otimes n_{\text{tot}}})]$ can be written as

$$\langle O \rangle = \frac{1}{2^{n_B}} \sum_{P \in \mathcal{P}_B} \text{tr}[(O_1 \otimes P)\mathcal{U}_1(|0\rangle\langle 0|^{\otimes(n_A+n_B)})] \text{tr}[O_2\mathcal{U}_2(P \otimes |0\rangle\langle 0|^{\otimes n_C})]. \quad (\text{S67})$$

where $\mathcal{P}_B := \{I, X, Y, Z\}^{\otimes n_B}$ is the set of n_B -qubit Pauli strings.

The key idea in Ref. [114] is to identify cut locations for which the upstream contribution vanishes for some Pauli strings:

$$\text{tr} \left[(O_1 \otimes P)\mathcal{U}_1(|0\rangle\langle 0|^{\otimes(n_A+n_B)}) \right] = 0 \quad (\text{S68})$$

for some $P \in \mathcal{P}_B$. Whenever this condition holds, the corresponding downstream term does not contribute to the final estimate, and one can omit the executions needed to estimate $\text{tr}[O_2 \mathcal{U}_2(P \otimes |0\rangle \langle 0|)^{\otimes n_C}]$. This directly reduces the total number of circuit executions. In Ref. [114], such a location is called a *golden cutting point* if Eq. (S68) holds for at least one $P \in \mathcal{P}_B$. Note that such points do not necessarily exist and are generally not unique. Moreover, one cannot know *a priori* whether a chosen cut location is a golden cutting point. Therefore, the follow-up work [115] introduces a scheme to detect such Pauli strings, if they exist, during the execution of the upstream subcircuits.

A related idea is also adopted in Ref. [113]. They consider the same circuit structure (Fig. S1), but insert unitary operators U_{rco} and U_{rco}^\dagger immediately before and after the cutting location, and then apply the Pauli expansion. By choosing U_{rco} such that the reduced operator on B becomes diagonal, the upstream contributions vanish for all Pauli strings except those in $\{I, Z\}^{\otimes n_B}$:

$$\text{tr}\left[(O_1 \otimes P)(\mathcal{U}_{\text{rco}} \circ \mathcal{U}_1)(|0\rangle \langle 0|)^{\otimes(n_A+n_B)}\right] = 0, \quad \forall P \in \mathcal{P}_B \setminus \{I, Z\}^{\otimes n_B}, \quad (\text{S69})$$

where $\mathcal{U}_{\text{rco}}(\cdot) := U_{\text{rco}} \cdot U_{\text{rco}}^\dagger$. Ref. [113] variationally optimizes such a U_{rco} and numerically demonstrates a reduction in the computational cost associated with the Pauli expansion.

Reformulation of prior works We now explain how these structure-aware approaches fit into Definition 7. Let

$$S_{\mathcal{P}_B} := \left\{ \mathcal{E}_{P_i}(\rho) = \frac{1}{2^{n_B}} \text{tr}[P_i \rho] P_i : P_i \in \mathcal{P}_B = \{I, X, Y, Z\}^{\otimes n_B} \right\} \quad (\text{S610})$$

denote the set of operations used in the mid-circuit Pauli decomposition (S61). As remarked around Eq. (S62), each \mathcal{E}_{P_i} can be implemented using a measure-and-prepare procedure with classical post-processing. Then, the decompositions considered in Refs. [114, 115] can also be understood under Definition 7 as follows.

Remark 2 (Refs. [114, 115]). Consider the quantum circuit in Fig. S1, and suppose the implementable operations are restricted to $S_{\mathcal{P}_B}$. Let $\mathcal{P}'_B \subset \mathcal{P}_B$ be a subset of n_B -qubit Pauli strings, and define $S_{\mathcal{P}'_B} := \{\mathcal{E}_P : P \in \mathcal{P}'_B\} \subset S_{\mathcal{P}_B}$. Then, Refs. [114, 115] consider decompositions that satisfy

$$\langle O \rangle = \sum_{\mathcal{M} \in S_{\mathcal{P}'_B}} \text{tr}[O \mathcal{U}_2 \circ \mathcal{M} \circ \mathcal{U}_1(|0\rangle \langle 0|)^{\otimes n_{\text{tot}}}] \quad (\text{S611})$$

Under this formulation, a golden cutting point corresponds to a cutting location for which there exists a strict subset $S_{\mathcal{P}'_B} \subsetneq S_{\mathcal{P}_B}$ satisfying Eq. (S611). At such a cutting location, $\gamma_{\text{eff}} = |S_{\mathcal{P}'_B}|$ ($1 \leq |S_{\mathcal{P}'_B}| < 4^{n_B}$) and an effective sampling overhead becomes

$$\gamma_{\text{eff}}^2 = |S_{\mathcal{P}'_B}|^2. \quad (\text{S612})$$

Similarly, the decomposition explored in Ref. [113] can be formulated under Definition 7 as follows.

Remark 3. Consider the quantum circuit shown in Fig. S1, and suppose the implementable operations are restricted to

$$S_{\mathcal{P}_B, U} := \left\{ \mathcal{E}_{U^\dagger P_i U}(\rho) := \frac{1}{2^{n_B}} \text{tr}[U^\dagger P_i U \rho] U^\dagger P_i U : P_i \in \mathcal{P}_B, U \in \mathcal{U}(\mathbb{C}^{d_B}) \right\}. \quad (\text{S613})$$

Let $\mathcal{Z} := \{I, Z\}^{\otimes n_B} \subset \mathcal{P}_B$, and let $\mathcal{P}'_B \subset \mathcal{P}_B$ be a subset of n_B -qubit Pauli strings. Then, Ref. [113] considers the decompositions that satisfy

$$\langle O \rangle = \sum_{\mathcal{M} \in S_{\mathcal{P}'_B, U}} \text{tr}[O \mathcal{U}_2 \circ \mathcal{M} \circ \mathcal{U}_1(|0\rangle \langle 0|)^{\otimes n_{\text{tot}}}] \quad (\text{S614})$$

Under this formulation, the difference between tasks in Remarks 2 and 3 can be understood as the choice of the implementable operations. The set of implementable operations in the latter case is broader than the former, since $S_{\mathcal{P}_B}$ is obtained by fixing $U = I$ in $S_{\mathcal{P}_B, U}$. Due to this broader class of implementable operations, it is guaranteed that there exists a decomposition

$$\langle O \rangle = \sum_{P_i \in \{I, Z\}^{\otimes n_B}} \text{tr}[O \mathcal{U}_2 \circ \mathcal{E}_{U^\dagger P_i U} \circ \mathcal{U}_1(|0\rangle \langle 0|)^{\otimes n_{\text{tot}}}] \quad (\text{S615})$$

We remark that the unitary operator U satisfying Eq. (S615) corresponds to U_{rco} in Eq. (S69). In this case, $\gamma_{\text{eff}} = 2^{n_B}$, and thus the effective sampling overhead becomes

$$(\gamma_{\text{eff}})^2 = 4^{n_B}. \quad (\text{S616})$$

Finally, applying Theorem 1 to the same circuit implies that, if one allows general MP channels with classical communication at the cutting location, there exist decompositions with $\gamma_{\text{eff}} = 1$:

Proposition 1. *Let $\{|j\rangle\}_{j \in \{0,1\}^{n_B}}$ denotes the computational basis on register B. Define MP channels \mathcal{M}_{in} and \mathcal{M}_{out} as*

$$\mathcal{M}_{\text{in}}(\bullet) := \sum_j \text{tr} \left[V_{\text{in}} |j\rangle \langle j| V_{\text{in}}^\dagger \bullet \right] V_{\text{in}} |j\rangle \langle j| V_{\text{in}}^\dagger, \quad (\text{S617})$$

$$\mathcal{M}_{\text{out}}(\bullet) := \sum_j \text{tr} \left[V_{\text{out}} |j\rangle \langle j| V_{\text{out}}^\dagger \bullet \right] V_{\text{out}} |j\rangle \langle j| V_{\text{out}}^\dagger. \quad (\text{S618})$$

Here, V_{in} is a unitary that diagonalizes $Q_1 := \text{tr}_A [O_1 \mathcal{U}_1 (|0\rangle \langle 0|^{\otimes(n_A+n_B)})]$ and V_{out} is a unitary that diagonalizes $Q_2 := \langle 0^{n_C} | \mathcal{U}_2^\dagger (O_2) | 0^{n_C} \rangle$, i.e., $Q_1 = V_{\text{in}} D_{\text{in}} V_{\text{in}}^\dagger$ and $Q_2 = V_{\text{out}} D_{\text{out}} V_{\text{out}}^\dagger$ with diagonal $D_{\text{in}}, D_{\text{out}}$. Then, both MP channels satisfy

$$\langle O \rangle = \text{tr} \left[O \mathcal{U}_2 \circ \mathcal{M}_{\text{in}} \circ \mathcal{U}_1 (|0\rangle \langle 0|^{\otimes n_{\text{tot}}}) \right] = \text{tr} \left[O \mathcal{U}_2 \circ \mathcal{M}_{\text{out}} \circ \mathcal{U}_1 (|0\rangle \langle 0|^{\otimes n_{\text{tot}}}) \right]. \quad (\text{S619})$$

Proof of Proposition 1. Define a CPTP map Φ from B to (B, C) by $\Phi(X) = \mathcal{U}_2(X \otimes |0\rangle \langle 0|^{\otimes n_C})$. Then, $\Phi^\dagger(O_2) = Q_2$ by definition. Theorem 1 guarantees that for any input $X \in \mathcal{L}(\mathbb{C}^{d_B})$

$$\text{tr} [O_2 \Phi(X)] = \text{tr} [O_2 \Phi \circ \mathcal{M}_{\text{out}}(X)]. \quad (\text{S620})$$

Setting $X = Q_1$ gives the second equality in Eq. (S619).

For \mathcal{M}_{in} , since it dephases in an eigenbasis of Q_1 , we have $\mathcal{M}_{\text{in}}(Q_1) = Q_1$. Therefore,

$$\text{tr} \left[O \mathcal{U}_2 \circ \mathcal{M}_{\text{in}} \mathcal{U}_1 (|0\rangle \langle 0|^{\otimes n_{\text{tot}}}) \right] = \text{tr}_{BC} \left[O_2 \mathcal{U}_2 \left(\mathcal{M}_{\text{in}}(Q_1) \otimes |0\rangle \langle 0|^{\otimes n_C} \right) \right] \quad (\text{S621})$$

$$= \text{tr}_{BC} \left[O_2 \mathcal{U}_2 \left(Q_1 \otimes |0\rangle \langle 0|^{\otimes n_C} \right) \right] = \langle O \rangle, \quad (\text{S622})$$

which completes the proof. \square

Lastly, we mention a useful connection between the previous decomposition (S615) and $\gamma_{\text{eff}} = 1$ decompositions. In the following remark, we show that the unitary operator U^\dagger in Eq. (S615) can be directly applied to construct a decomposition achieving an effective sampling overhead of unity.

Remark 4. The sum of operations $\mathcal{E}_{U^\dagger P_i U}$ in Eq. (S615) is equal to a measure-and-prepare channel, i.e.,

$$\sum_{P_i \in \{I, Z\}^{\otimes n_B}} \mathcal{E}_{U^\dagger P_i U}(\bullet) = \sum_{j \in \{0,1\}^{n_B}} \text{tr} [U^\dagger |j\rangle \langle j| U \bullet] U^\dagger |j\rangle \langle j| U. \quad (\text{S623})$$

Proof of Remark 4.

$$\sum_{P_i \in \{I, Z\}^{\otimes n_B}} \mathcal{E}_{U^\dagger P_i U}(\bullet) = \frac{1}{2^{n_B}} \sum_{P_i \in \{I, Z\}^{\otimes n_B}} \text{tr}_1 \left[(U^\dagger)^{\otimes 2} (P_i \otimes P_i) U^{\otimes 2} (\bullet \otimes I) \right] \quad (\text{S624})$$

$$= \frac{1}{2^{n_B}} \sum_{P_i \in \{I, Z\}^{\otimes n_B}} \text{tr}_1 \left[(U^\dagger)^{\otimes 2} (I_1 \otimes I_2 + Z_1 \otimes Z_2)^{\otimes n_B} U^{\otimes 2} (\bullet \otimes I) \right] \quad (\text{S625})$$

$$= \text{tr}_1 \left[(U^\dagger)^{\otimes 2} (|0\rangle \langle 0|_1 \otimes |0\rangle \langle 0|_2 + |1\rangle \langle 1|_1 \otimes |1\rangle \langle 1|_2)^{\otimes n_B} U^{\otimes 2} (\bullet \otimes I) \right] \quad (\text{S626})$$

$$= \sum_{j \in \{0,1\}^{n_B}} \text{tr}_1 \left[(U^\dagger)^{\otimes 2} (|j\rangle \langle j| \otimes |j\rangle \langle j|) U^{\otimes 2} (\bullet \otimes I) \right] \quad (\text{S627})$$

$$= \sum_{j \in \{0,1\}^{n_B}} \text{tr} [U^\dagger |j\rangle \langle j| U \bullet] U^\dagger |j\rangle \langle j| U, \quad (\text{S628})$$

which completes the proof. \square